Savannah River NUCLEAR SOLUTIONS℠
FLUOR • NEWPORT NEWS NUCLEAR • HONEYWELL

United States Department of Energy

Savannah River Site

Groundwater Flow and Solute Transport Model of the CMP Pits OU (U)

Tetra Tech, Inc. Alpharetta, GA

CERCLIS Number: 24

SRNS-TR-2017-00312

Revision 0

December 2017

Page intentionally left blank

DISCLAIMER

Printed in the United States of America

Prepared for
U.S. Department of Energy
and
Savannah River Nuclear Solutions, LLC
Aiken, South Carolina

Page intentionally left blank

EXECUTIVE SUMMARY

This report presents a numerical model of groundwater flow and solute transport for the Chemicals, Metals, and Pesticides Pits (CMP Pits) Operable Unit (OU) at the Savannah River Site (SRS). The purpose of the modeling is to estimate the extent and magnitude of future contaminant migration in groundwater and evaluate the potential for contaminant discharge to surface waters at concentrations greater than maximum contaminant levels (MCLs) or regional screening levels (RSLs). The modeling predicts how existing contaminant plumes will move in groundwater and how the remaining vadose-zone source at the CMP Pits may affect future contamination. Contamination at the site is generally moving northward in the groundwater, from beneath the CMP Pits to discharge locations along Pen Branch and one of its tributaries.

The numerical model is based on available site data that describe hydrostratigraphy, potentiometric head, groundwater flow directions, and existing contaminant concentrations. These site data have been synthesized into a hydrogeologic conceptual model (HCM) that is the basis for the numerical model. The numerical modeling is carried out using MODFLOW and MT3DMS within the Groundwater Modeling System (GMS). The model documented herein is an update of a prior 2002 model. The prior modeling did not account for source remediation that was conducted in 2001, 2005, and 2008-2009. Since the prior modeling effort source and near source concentrations have decreased substantially. In addition, new groundwater data have been collected. The current study updates the 2002 model with new groundwater data, new stratigraphic data, a representation of the remediated source, a transient calibration of solute transport, and an improved 100-year prediction of future solute transport.

Groundwater flow model calibration is achieved by adjusting initial estimates of hydraulic conductivity and boundary specifications within reasonable ranges. The calibrated model matches observed heads at observation wells and the observed baseflow into Pen Branch to pre-specified calibration criteria. Solute transport model calibration is achieved by adjusting initial estimates of chemical- and media-specific properties within reasonable ranges. In addition, further adjustment

of the groundwater flow calibration parameters was required to accurately match interpreted plume behavior.

The contaminant source from the vadose zone is used as input to the transport model. This source is estimated from data collected beneath and adjacent to the pits. The effect of the source in the current model was evaluated by comparing the future plume behavior with a continuous source based on current conditions to behavior with no source. The difference was found to be minor for both the 14-year calibration period and the 100-year predictive period. This observation suggests that accurate quantification of the source for the purpose of predicting future plume behavior is not necessary.

Four constituents of interest (COIs) are modeled for each scenario – tetrachloroethylene (PCE), trichloroethylene (TCE), lindane, and 1,4-dioxane. For PCE and TCE, predictive simulations indicate that discharge concentrations will exceed MCLs for 40 and 30 years, respectively. However, it should be noted that the wetlands adjoining the groundwater discharge locations along Pen Branch appear to provide significant degradation of PCE and TCE. Application to this site of a wetlands-specific degradation factor derived from observations of TCE degradation at an instrumented site within the C-Area of SRS, suggest that the modeled PCE and TCE discharge concentrations may be reduced by two orders of magnitude, resulting in TCE discharge concentrations currently being below MCLs and PCE discharge concentrations exceeding MCLs for approximately five years. 1,4-dioxane and lindane are unlikely to discharge to surface water at concentrations in excess of MCLs or RSLs and therefore appear to be much less important COIs than PCE and TCE at the site.

The model does have uncertainties in parameter value assignments, simplification of heterogeneous field conditions, and quantification of the processes of sorption and degradation. Despite these uncertainties, the model may be used as a tool to establish a reasonable range of future conditions, and it can be used to support the Monitored Natural Attenuation (MNA) remedial alternative for the CMP Pits OU.

TABLE OF CONTENTS

LIST OF FIGURES

LIST OF TABLES

LIST OF ACRONYMS AND ABBREVIATIONS

$\partial c/\partial x_i$	Concentration gradient
α_H	horizontal-transverse dispersivity
α_L	longitudinal dispersivity
α_T	vertical-transverse dispersivity
β	SVE mass-flux reduction efficiency
γ	soil cover mass-flux reduction efficiency
λ	decay rate
µg	micrograms
ρ_b	porous medium bulk density
θ	effective porosity
atm	atmospheres
bgs	below ground surface
c	concentration
CERCLA	Comprehensive Environmental Response, Compensation, and Liability Act
cm/s	centimeters per second
CMP	Chemical, Metals, and Pesticides
CMS/FS	Corrective Measures Study/Feasibility Study
COI	constituent of interest
CPT	cone penetrometer technology
c_s	source/sink concentration
d	day
D_{ij}	dispersion coefficient tensor
ERDMS	Environmental Restoration Data Management System
ERH	Electrical Resistance Heating
ft	feet
F_{oc}	fractional organic content
g	grams
GMS	Groundwater Modeling System
h	hydraulic head
HCM	hydrogeologic conceptual model
in	inches
K_d	sorption coefficient
kg	kilograms
K_{oc}	organic-carbon partition coefficient
K_x	horizontal (x-direction) hydraulic conductivity
K_y	horizontal (y-direction) hydraulic conductivity
K_z	vertical hydraulic conductivity
L	liters
LAZ	lower aquifer zone
LLC	Limited Liability Company
MAZ	middle aquifer zone

LIST OF ACRONYMS AND ABBREVIATIONS (*continued; end*)

MCL	maximum contaminant level
mg	milligrams
mol	moles
MNA	monitored natural attenuation
MODFLOW	Modular Three-dimensional Finite-Difference Groundwater Flow Model (code)
msl	mean sea level
MT3DMS	Modular Three-Dimensional Multispecies Transport Model (code)
NAPL	non-aqueous phase liquid
OU	Operable Unit
PCB	polychlorinated biphenyl
PCE	tetrachloroethylene
q_R	recharge (infiltration) rate
q_s	source/sink groundwater flow per unit volume
RCRA	Resource Conservation and Recovery Act
RMSE	root-mean-square error
RSL	regional screening level
SRS	Savannah River Site
SVE	soil vapor extraction
TCCZ	tan clay confining zone
TCE	trichloroethylene
TCLC	tan clay lower clay
UAZ	upper aquifer zone
USDOE	United States Department of Energy
USEPA	United States Environmental Protection Agency
UTRA	Upper Three Runs aquifer
v_i	velocity vector
VOC	volatile organic compound
WSRC	Westinghouse Savannah River Company LLC
yr	year

Page intentionally left blank

1.0 INTRODUCTION

The Chemical, Metals, and Pesticides (CMP) Pits are located about 1 mile north of L-Area, in the central part of the Savannah River Site (SRS) (Figure 1.1). There, two rows of unlined pits (Figure 1.2 and Figure 1.3) received non-radioactive waste between 1971 and 1979. The waste included organic chemicals, metals, pesticides, and lighting ballasts containing polychlorinated biphenyls (PCBs). Several environmental sampling studies identified the CMP Pits as a source of soil and groundwater contamination. In 1984, the pits were excavated, fill was added to 4 ft below grade, a liner was placed, and additional fill was added to grade. However, contamination remains in the 90-ft thick vadose zone beneath the excavated area. The CMP Pits site is a regulated waste unit under the combined Resource Conservation and Recovery Act (RCRA) and Comprehensive Environmental Response, Compensation, and Liability Act (CERCLA) program for SRS.

For this study, the fate and transport in the groundwater of four constituents of interest (COIs): tetrachloroethylene (PCE), trichloroethylene (TCE), 1-4 dioxane, and lindane, are modeled. These COIs are observed in groundwater at concentrations above their respective maximum contaminant levels (MCLs) or regional screening levels (RSLs). Other identified contaminants at the CMP Pits (e.g., PCBs) are primarily surface soil contaminants, and are not likely to lead to future groundwater contamination. Three of the COI's considered here – PCE, TCE, and 1-4 dioxane – are volatile organic compounds (VOCs). Lindane is a pesticide.

This study is based on a prior groundwater flow and transport model that was developed in 2002 (GeoTrans 2002a). The prior modeling did not account for source remediation that was conducted in 2001, 2005, and 2008-2009. Since the prior modeling effort source and near source concentrations have decreased substantially. In addition, new groundwater data have been collected. The current study updates the 2002 model with new groundwater data, new stratigraphic data, representation of a remediated source, a transient calibration of the solute transport, and an improved 100-year prediction of future solute transport of four the four COI's.

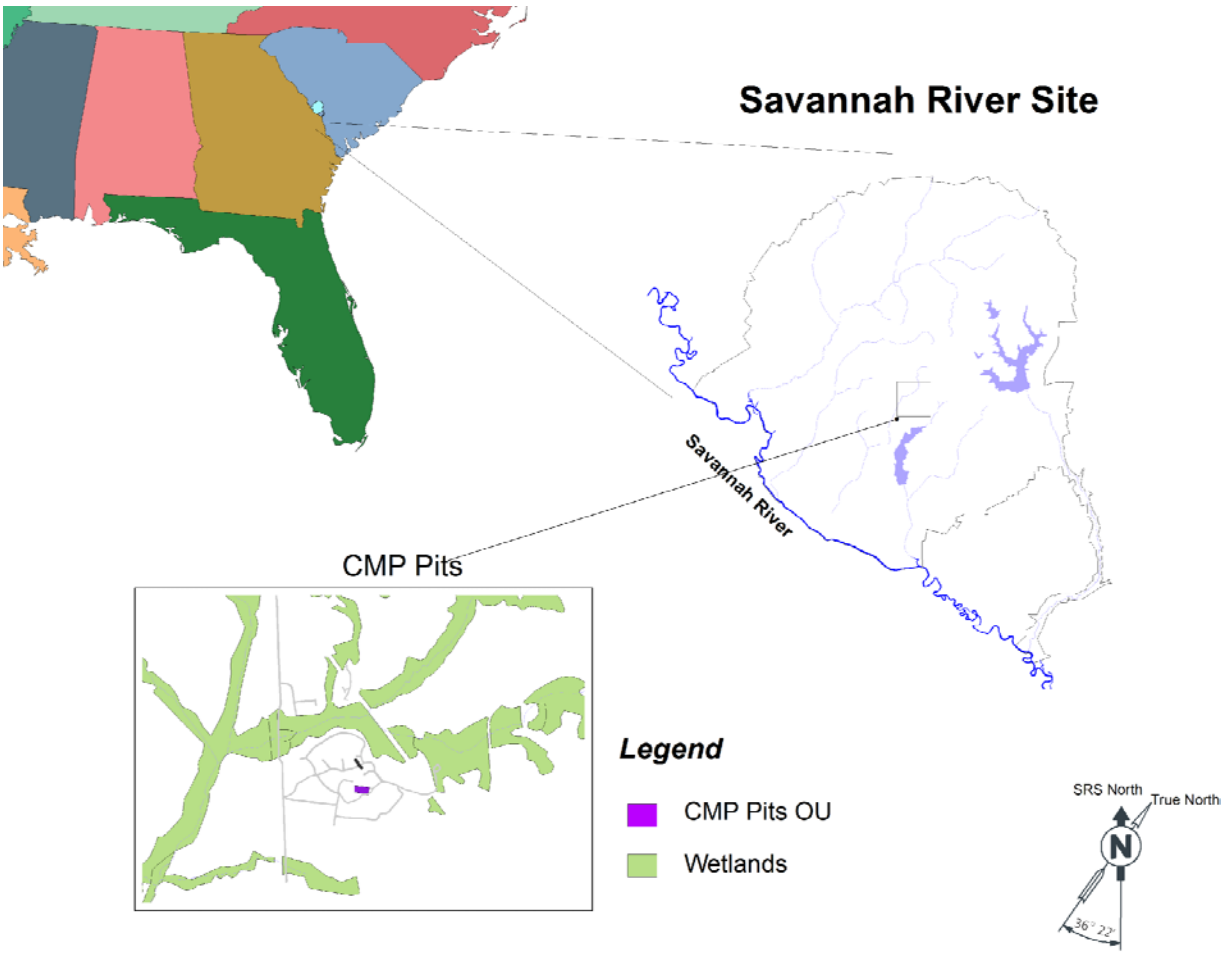

Figure 1.1 Location of the Chemicals, Metals, and Pesticides Pits

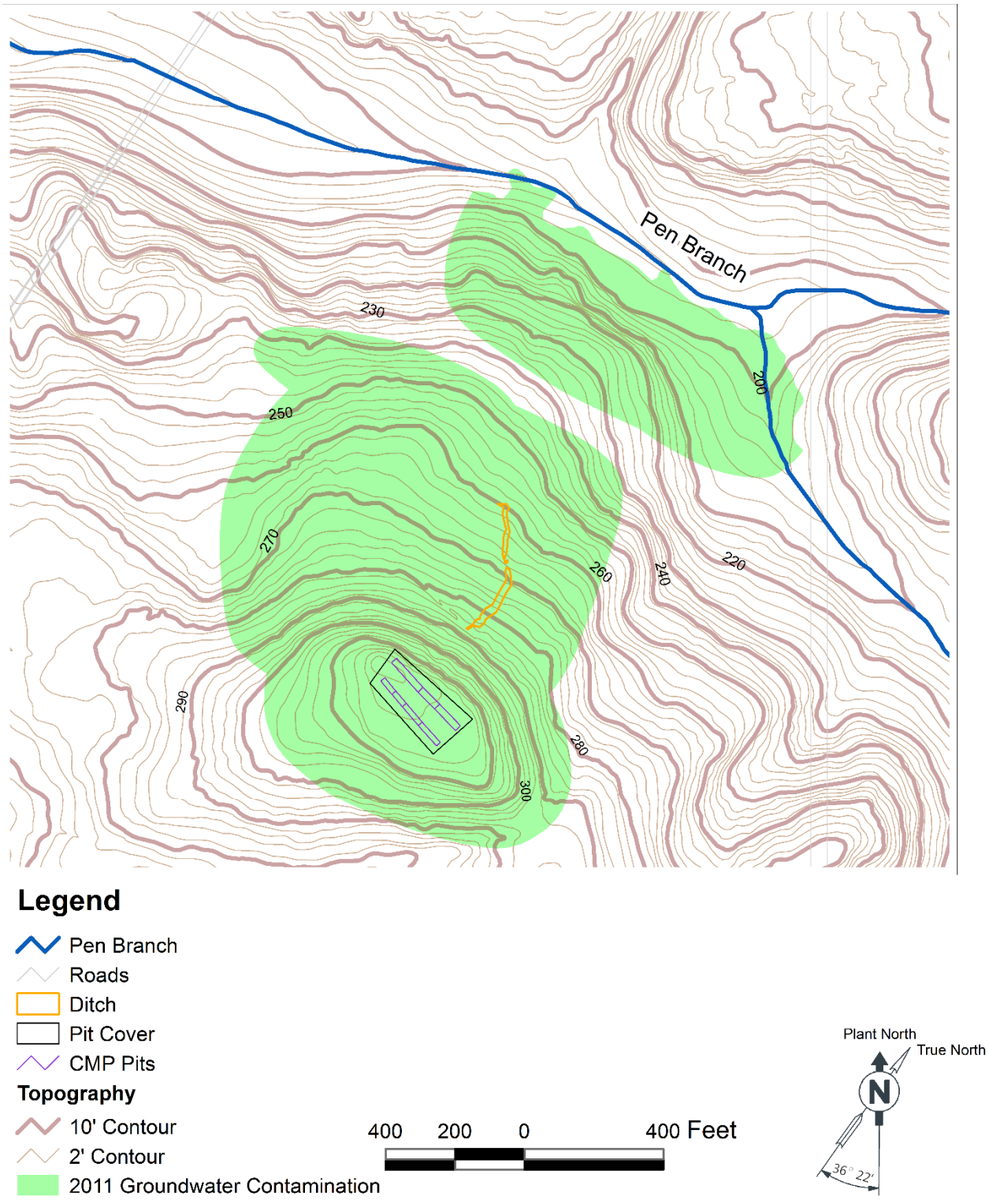

Figure 1.2 CMP Pits Site Map with Location of 2011 Groundwater Contamination

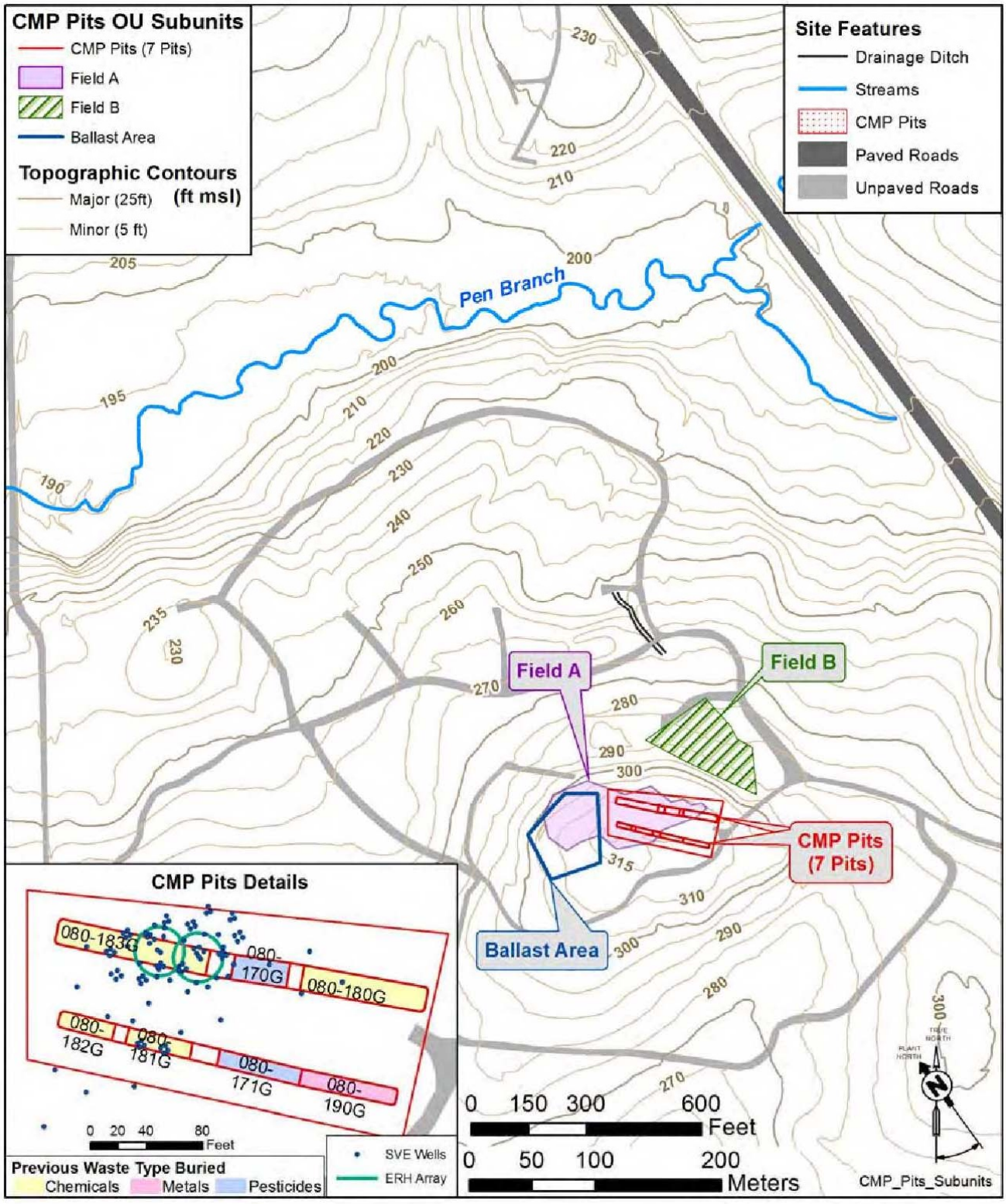

Figure 1.3 CMP Pits Subunits (SRNS 2017)

2.0 HYDROGEOLOGIC CONCEPTUAL MODEL

The first step in the modeling process is the formulation of a site-specific hydrogeologic conceptual model (HCM) of the study area. The HCM is a representation of the groundwater flow and transport system that incorporates a description of the geologic setting, hydrostratigraphic units, hydraulic properties, and system boundaries (such as streams, wells, and other sources and sinks). The HCM describes the source of contaminants, the disposition of contaminants in the subsurface, and the expected fate of contaminants. The HCM also describes the current understanding of the environmental system and defines the framework for numerical or analytical models of groundwater flow and transport.

Figure 2.1 illustrates the HCM for the CMP Pits. The original source material and surrounding soil were removed and excavated in 1984. In addition, Soil Vapor Extraction (SVE) and Electrical Resistance Heating (ERH) systems, which operated in 2008-2009, have removed much of the contamination beneath the pits. The primary contaminant source is the soil beneath the remediation systems and around the former pits outside the effective area of the remediation systems. The contaminants have moved, and continue to move, downward through the vadose zone to the water table located in the Upper Three Runs Aquifer (UTRA). Once the contamination reaches the water table, it mixes with the saturated groundwater and moves northward toward Pen Branch. The saturated groundwater plume is subject to processes of dispersion, sorption, and biological degradation. In addition to spreading horizontally toward Pen Branch, the contamination has spread vertically throughout much of the UTRA.

2.1 General Setting

The CMP Pits consist of seven 500 to 1100 ft^2 unlined pits, placed in two rows, that occupy the top of a knoll at an approximate elevation of 310 ft msl. The water table is located about 90 ft below ground surface at the pits. Saturated groundwater moves northward from the CMP Pits toward Pen Branch, which is at an elevation of about 200 ft msl approximately 1500 ft north of the pits area (Figure 1.2).

The average annual precipitation at SRS is approximately 48 inches (WSRC 2001). Some of the precipitation water evaporates at the surface, some flows overland to area water bodies, and some is taken up by vegetation. In undisturbed upland areas, about one fifth (10 in/yr) to one third (16 in/yr) of the precipitation percolates through the vadose zone and reaches the water table as groundwater recharge.

2.2 Hydrostratigraphy

The unconsolidated marine and fluvial sediments of the Atlantic Coastal Plain underlie the CMP Pits and all of SRS (Aadland and Bledsoe 1990). The sediments vary in age from Late Cretaceous to recent (Figure 2.2). They are a variably stratified, heterogeneous sequence of sand, clay, limestone, and gravel. The uppermost sediments make up the Floridan Aquifer System.

At the CMP Pits, the Floridan Aquifer System is subdivided into two aquifers: the UTRA (upper aquifer) and the Gordon Aquifer (lower aquifer). The Gordon Confining Unit – or "green clay" – separates the UTRA and the Gordon Aquifer.

Semi-continuous clay layers divide the UTRA into three different aquifer zones referred to as (from top) the transmissive zone (TZ), the middle aquifer zone (MAZ), and the lower aquifer zone (LAZ). The tan clay confining zone (TCCZ) and tan clay lower clay (TCLC) separate these aquifer zones. The confining zones, (TCCZ and TCLC) are hummocky, vary in thickness, and can be almost non-existent or leaky in areas (SRNS 2017). The contaminant plumes reside in all three aquifer zones of the UTRA.

The hydrostratigraphic surfaces used in the prior groundwater modeling study (GeoTrans 2002a) were based on cone-penetrometer test (CPT) boreholes completed prior to 2002. An additional eight wells have been installed in the model area since 2002 (Figure 2.3). Stratigraphic data from these wells were added to the existing surfaces to provide a more comprehensive representation of the hydrostratigraphy. In doing so, it became apparent that the complete set of hydrostratigraphic contact elevation data at boreholes ("picks") did not correspond to those used in the prior model. Further review indicated that the 2002 interpolation had been smoothed to reduce the irregular thicknesses caused by hummocky confining layers. This representation resulted in the MAZ being

saturated throughout and not partially saturated as shown in Figure 3 of SRNS (2017). The hydrostratigraphic data were re-evaluated and re-interpolated to be consistent with the current hydrostratigraphic picks. The current hydrostratigraphic elevations are consistent with those that have recently been presented (SRNS 2017). Figures 2.4 through 2.7 show the hydrostratigraphic elevations for the various layers.

2.3 Source Description

The CMP Pits received non-radioactive waste from 1971 to 1979 including chemicals, metals, pesticides, and fluorescent light ballasts containing PCBs. The pits are 10 to 15 ft wide, 45 to 75 ft long, and 10 to 15 ft deep (Figure 1.3). Drums and other contaminated material were excavated from the pits during a 1984 remedial action. The pits were then backfilled to approximately four feet below grade. A low-infiltration liner consisting of 80-mil high-density polyethylene was installed and covered with 3 ft of soil fill and 1 ft of topsoil. A gravel-lined ditch was installed around the liner area. The purpose of the liner is to reduce infiltration, thereby minimizing migration of residual contamination in the vadose zone. The chronology of emplacement, remediation, and transport is summarized in Figure 2.8.

Soil samples collected in 2001 and 2003 confirmed the presence of PCE in the form of a dense non-aqueous phase liquid (DNAPL) in the vadose zone beneath the CMP Pits. The maximum PCE detected was 8,800,000 µg/kg in the clay horizons beneath the pits where the 2008-2009 remedial activities would later be conducted (Figure 2.9). Outside of the pits, PCE was not detected in many locations, with a maximum measurement of 632 ug/kg (Figure 2.10). The presence of TCE and lindane was also detected in the vadose zone, but 1,4-dioxane was not detected during a 2002 characterization effort.

Remedial activities for the vadose zone and Ballast Area Soils subunits were performed in 2001 and 2005. Subsequent lindane concentrations were two to four orders of magnitude smaller than pre-remediation concentrations (from SRS data delivery). Surface soil contamination in the Ballast Area and vadose zone contamination in Field B have been successfully remediated via interim remedial actions (SRNS 2017).

Soil samples collected to the south and east of the CMP pits in 2006 resulted in a maximum PCE detection of 1.64 ug/kg and a maximum TCE detection of 1.75 ug/kg (SRNS 2017).

Electrical resistance heating (ERH) with soil vapor extraction (SVE) was selected as the remedial action for the CMP Pits vadose zone. Heat zones were created with electrodes from 25 to 45 ft bgs and 55 to 70 ft bgs. SVE wells were co-located with the electrode wells and additional SVE wells were installed throughout the CMP Pits system. ERH/SVE operation occurred from March to November 2008. SVE operation continued through March 2009, with a shut down from mid-January to early March 2009 to test rebounding. Approximately 2,300 lbs of VOCs (primarily PCE) were removed from March 2008 to March 2009. Air and soil concentration data from March 2009 indicated the SVE system had reached the point of diminishing returns and operations were discontinued in April 2009 (SRNS 2009). Monitored natural attenuation (MNA) has been selected as the follow-up remediation to the ERH/SVE implementation.

TCE concentrations after the ERH/SVE decreased by one to two orders of magnitude. Even though the ERH/SVE for PCE was successful, relatively unchanged groundwater concentration results indicate there is likely residual contamination in low permeability zones near the pits that is acting as a secondary source for groundwater contamination (SRNS 2017).

In the vadose zone, water flow is generally downward, driven only by the force of gravity. As water moves vertically downward, dissolved constituents are transported downward via advection. In the absence of other transport processes, such as dispersion and sorption, the velocity of contaminant mass in the vadose zone is the same as the velocity of the water (approximately 8 inches/yr, see GeoTrans 2002b). Vadose zone transport is represented by time varying source terms that are related to the degree of remediation (Figure 2.8).

2.4 Groundwater Contamination

The groundwater contamination near the CMP Pits has been characterized by measurements of aqueous concentration in groundwater samples from monitoring wells and CPT boreholes. Groundwater plumes for each COI in this study (PCE, TCE, lindane, and 1,4-dioxane) have been inferred based on the concentration data (plumes developed in SRNS (2017) are presented in

Section 5 as initial plumes). Figure 1.2 shows the approximate location of groundwater contamination in the CMP Pits area (the figure shows where PCE or TCE concentrations exceed the MCL of 5 μg/L in 2011). Note that there appears to be two distinct areas of contamination – one stretching northward from the CMP Pits and another northeast of the CMP Pits. It is not known whether the northeast plume emanated directly from the pits, or whether a discharge to or flow through a drainage ditch spill (Figure 1.3) created this zone of contamination. Results from a soil gas survey (WSRC 2003) show no current source at the ditch. Additional plausible reasons for the plumes include transient water tables that induce variable areas of desaturation in the TZ or upwelling of water from the MAZ into the TZ as water enters Pen Branch (SRNS 2017).

Concentrations in wells (Figure 2.11) in the distal portions of the plume have remained constant or risen slightly (CMP8 or CMP40D), while those closer to the pits have started to decrease since the remediation (CMP10D or CMB24I). Wells in the LAZ are increasing (CMP52BU and CMP54C) as the plume moves downwards (Figure 2.12 and 2.13 for PCE and TCE respectively). Cross-sections through the plume from SRNS (2017) are found in Figures 2.14 and 2.15 for PCE.

2.5 Groundwater Flow

Groundwater flow directions in the study area are determined from water-level measurements and contaminant concentration data. Near the CMP Pits source area, flow in the TZ is generally toward the north-northwest. There is a significant downward component to flow from the TZ to the MAZ, as inferred from the approximate 5 ft head drop across the TCCZ. This downward flow continues through the TCLC to the LAZ, as inferred by a head drop of approximately 10 ft across the TCLC. Like the TZ, the MAZ flow direction is to the north-northwest. Flow in the LAZ is toward the northwest. There appears to be a small amount of upward flow within the LAZ close to Pen Branch. This is seen in one well cluster, CMP064B/BU, with both wells screened within the LAZ, and CMP064B screened 30 feet below CMP064BU. The lower well has a head about 1.6 ft higher than the upper well. The phenomenon of upward hydraulic gradient in the vicinity of gaining streams is well documented. All three aquifer zones discharge to Pen Branch or the unnamed tributary feeding Pen Branch from the southeast.

Water level measurements from fall 2016 are used as targets for model calibration. This year was chosen in favor of long-term average heads due to an increase in the number of wells and measurements since the long-term average heads were developed. Water levels in the fall of 2016 are very similar to a long-term average of available data. The spatial average water level in fall 2016 is 202.9 ft, while the spatial average of long term water level data is 201.9 ft. Table 2.1 shows the average, high, low and range for water levels in Fall 2016, average over the period of record, and the difference between the period of record and the Fall 2016.

Table 2.1 Water Level (ft) Statistics for 2016 and Period of Record

	Average	High	Low	Range
Fall 2016	202.9	240.8	177.9	62.9
Period of record	201.9	236.0	178.7	57.3
Difference	1	4.8	-5.6	10.4

2.6 Solute Transport Processes

The processes of advection, diffusion, hydrodynamic dispersion, sorption, and biodegradation affect dissolved contaminants in the groundwater. Advection is the process that describes the movement of the dissolved contaminant along the groundwater flow path, and is often conceptualized as a particle trace. Diffusion is the process of random molecular motion that effectively results in mass flux from areas of high concentration to areas of lower concentration at the pore scale. A much more important process for most solute transport problems is hydrodynamic dispersion, in which a heterogeneous velocity field causes smearing (mixing) at the transport front resulting in a dilution of the contaminant concentrations. Greater velocities result in greater plume spreading. In the current analysis, as with most groundwater transport problems, diffusion is ignored but hydrodynamic dispersion is considered. Sorption is the process by which contaminant mass is adsorbed to and desorbed from soil particles, effectively retarding the movement of the plume. An equilibrium sorption process is often assumed, whereby the concentration of contaminant in groundwater is proportional to the contaminant concentration on the soil. The proportionality constant is called the sorption coefficient, or K_d, and is dependent on the organic-carbon content of the soil (for organic constituents).

Reductive dechlorination of PCE and TCE can occur in anaerobic conditions with the presence of microbes, a carbon source, and nutrients. However, rapid reduction of PCE to TCE at the CMP Pits is not apparent from available data. In the current analysis, it is assumed that the modeled COI's are undergoing a slow degradation within the groundwater system. Degradation is much more possible in the wetlands area just prior to discharge to land surface and Pen Branch. GeoTrans (2001) determined a 98.9% reduction in TCE concentration as it traversed from the ground water through wetland sediments at a highly instrumented site near Twin Lakes in C-area. Similarly, SRNS (2017) reports c-1,2 DCE detections in Pen Branch, with no PCE or TCE above MCLs. This observation is indicative of degradation occurring over a very short distance prior to entry to Pen Branch.

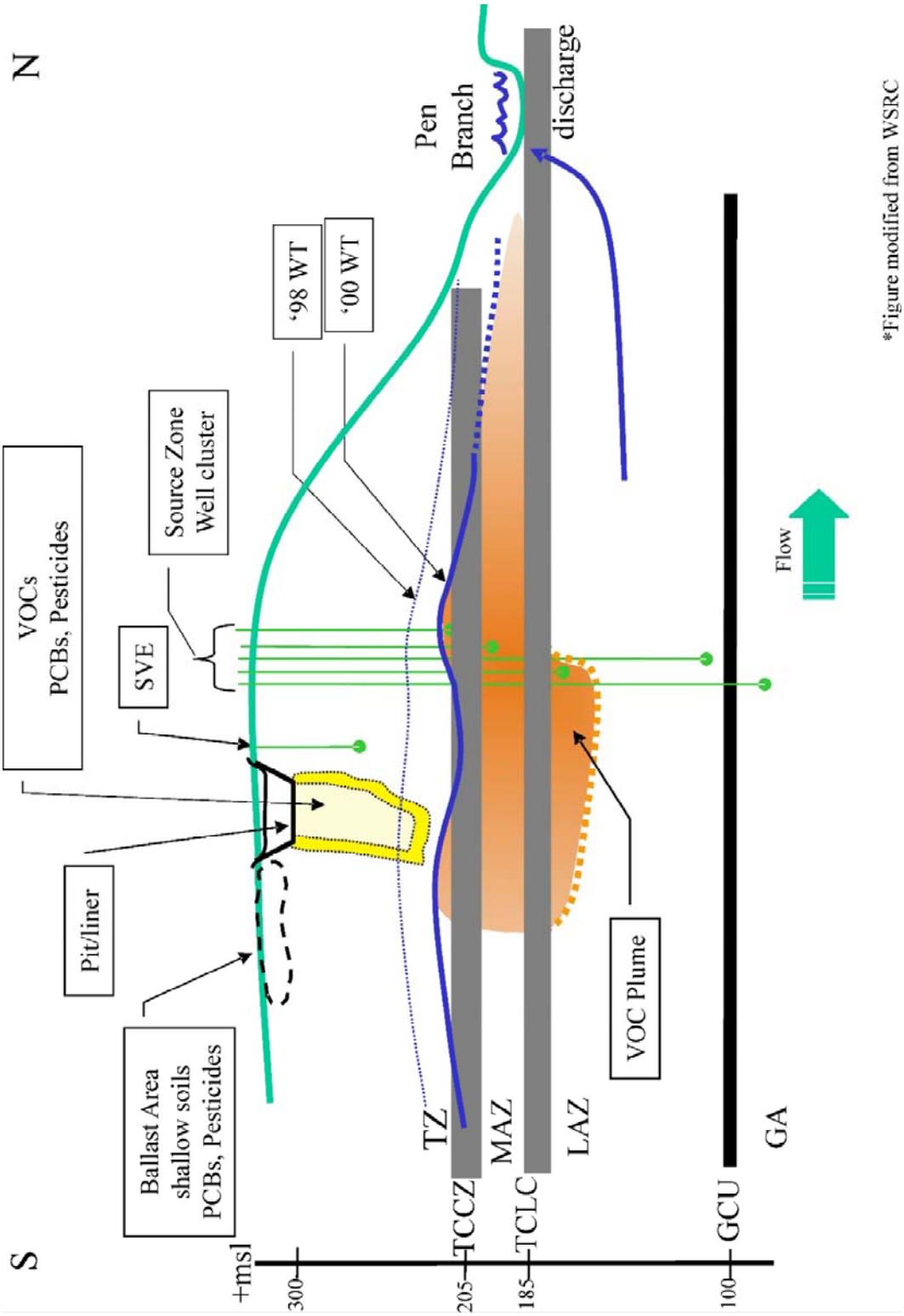

Figure 2.1 Hydrogeologic Conceptual Model for the CMP Pits Site (GeoTrans 2002a)

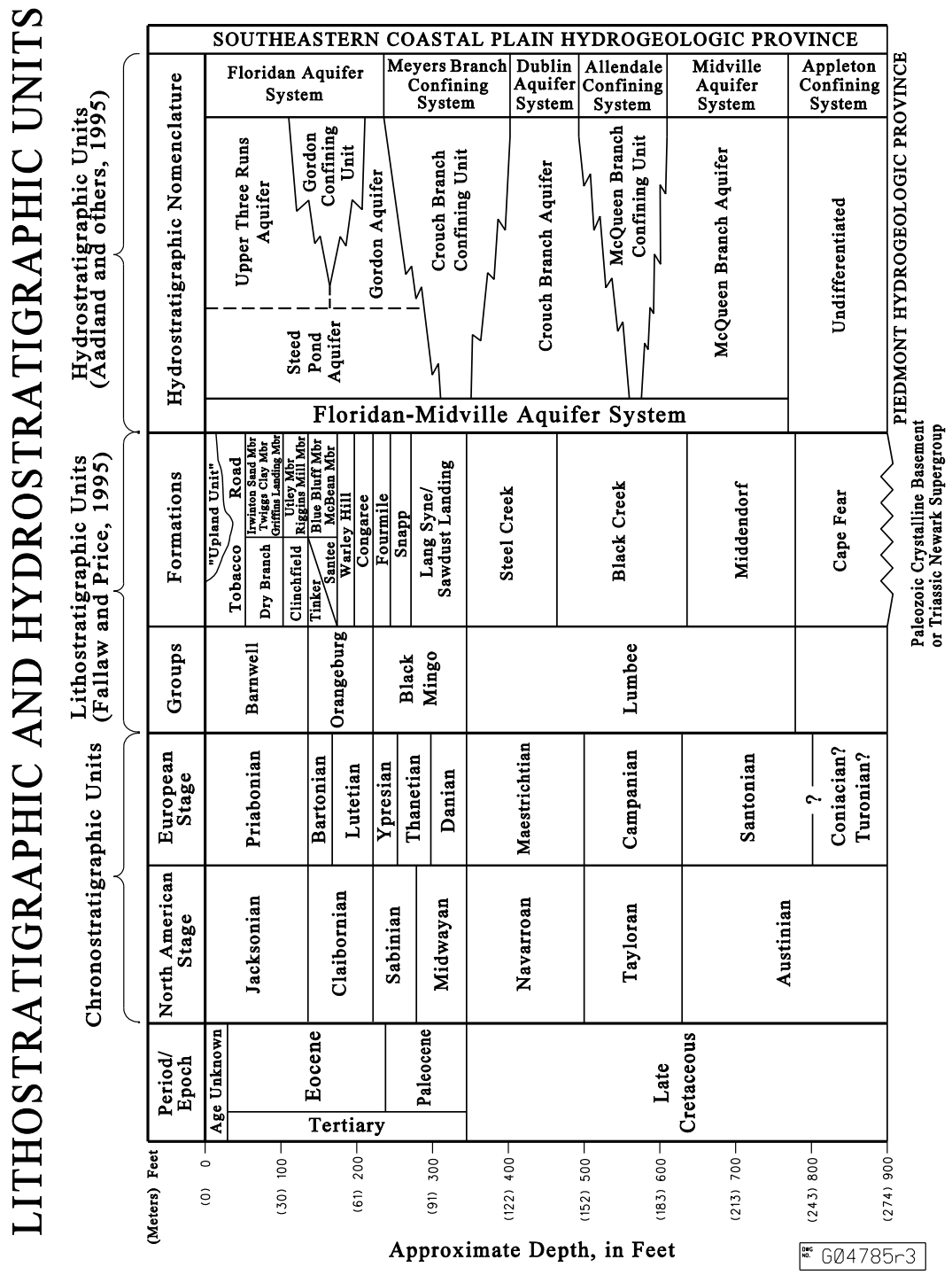

Figure 2.2 SRS Geologic Stratigraphy

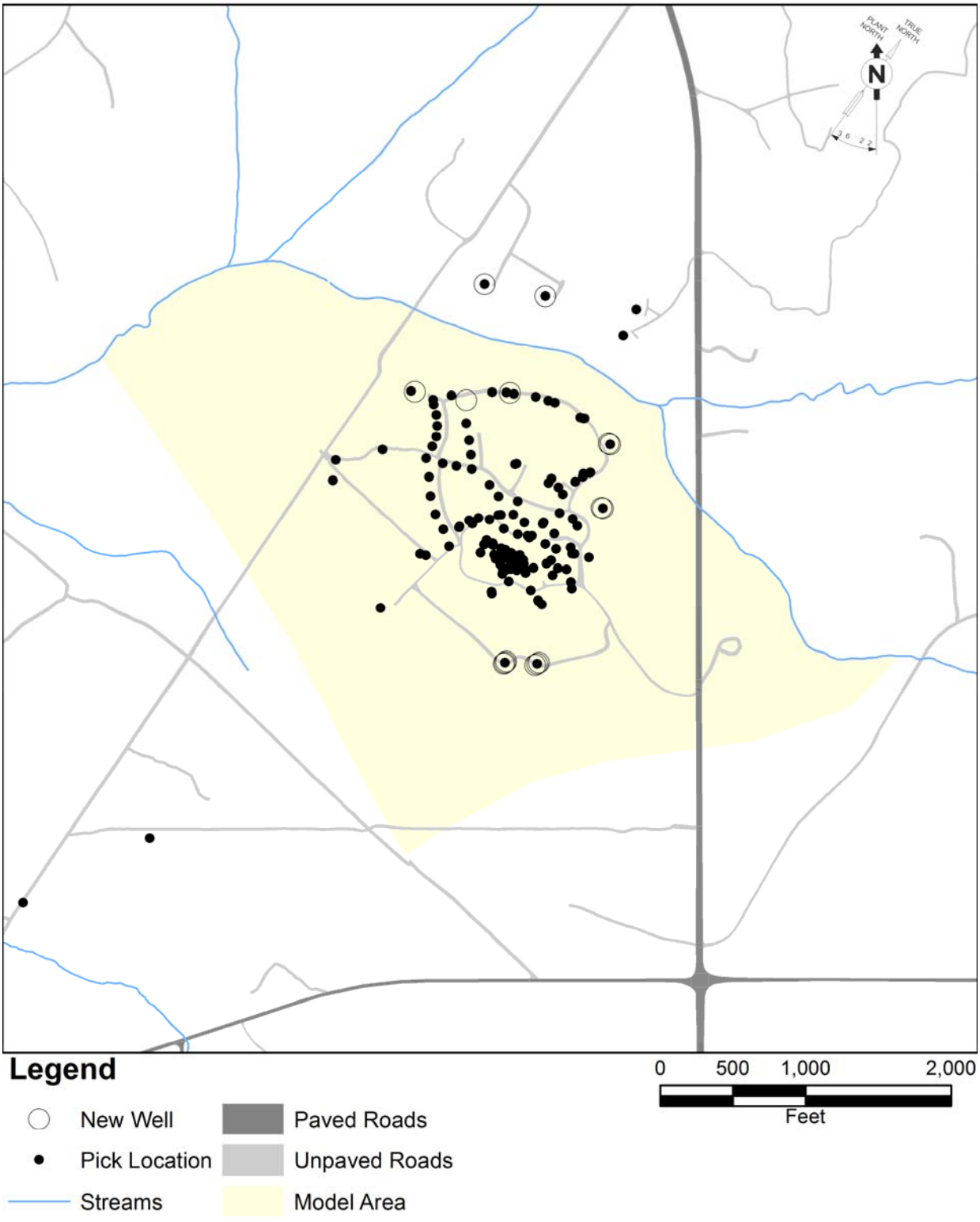

Figure 2.3 2017 Hydrostratigraphic Pick Locations

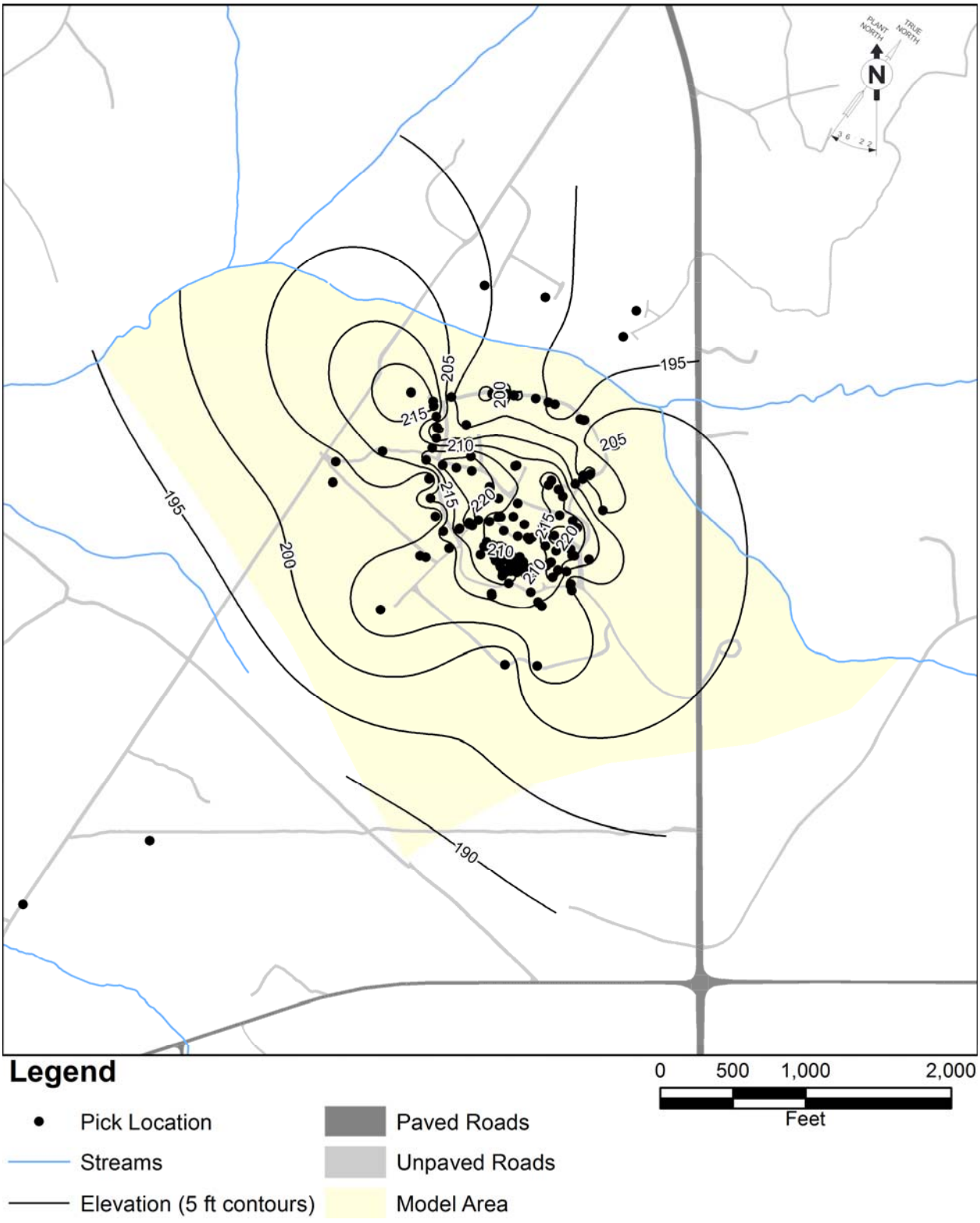

Figure 2.4 Elevation of the Top of the TCCZ

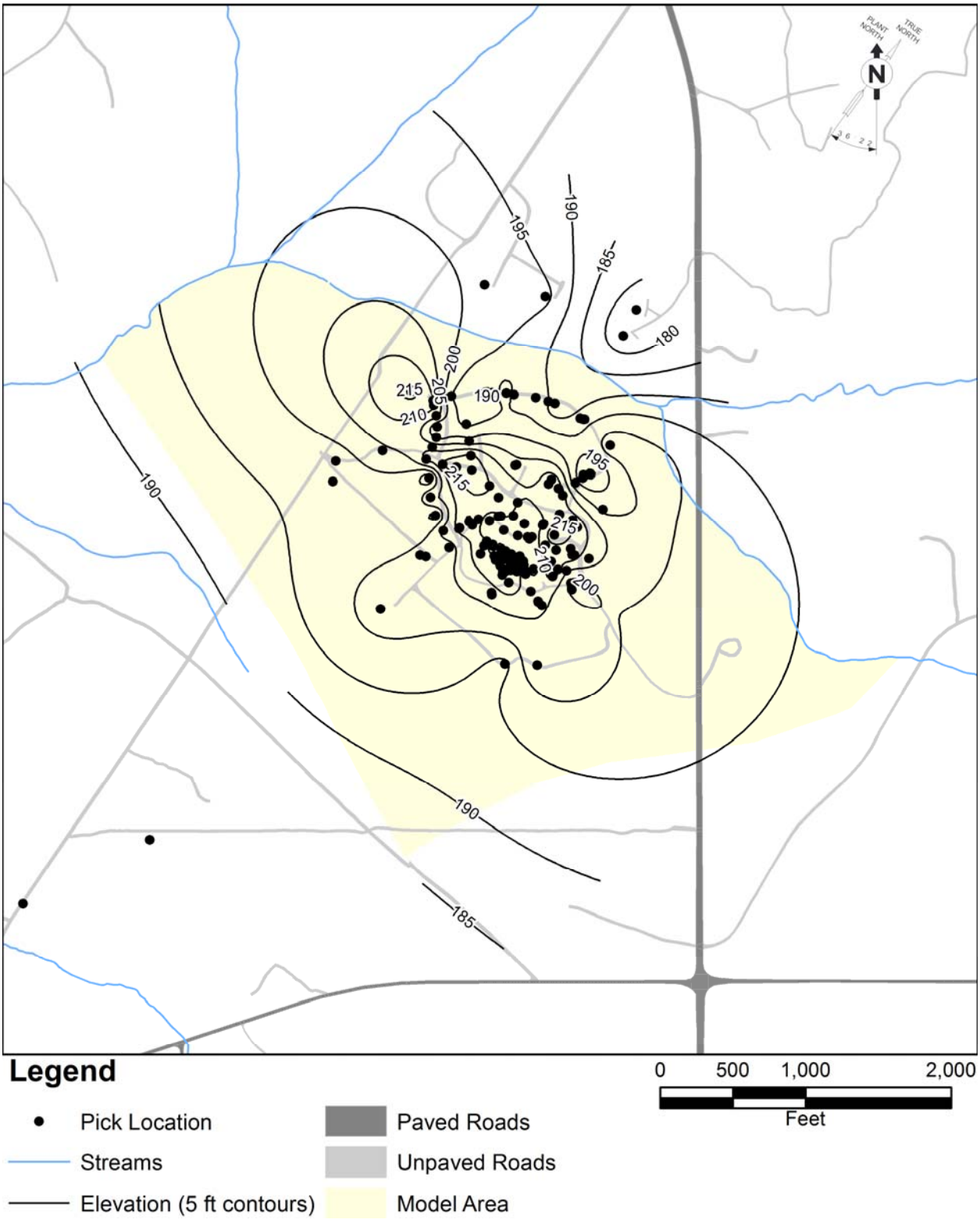

Figure 2.5 Elevation of the Top of the MAZ

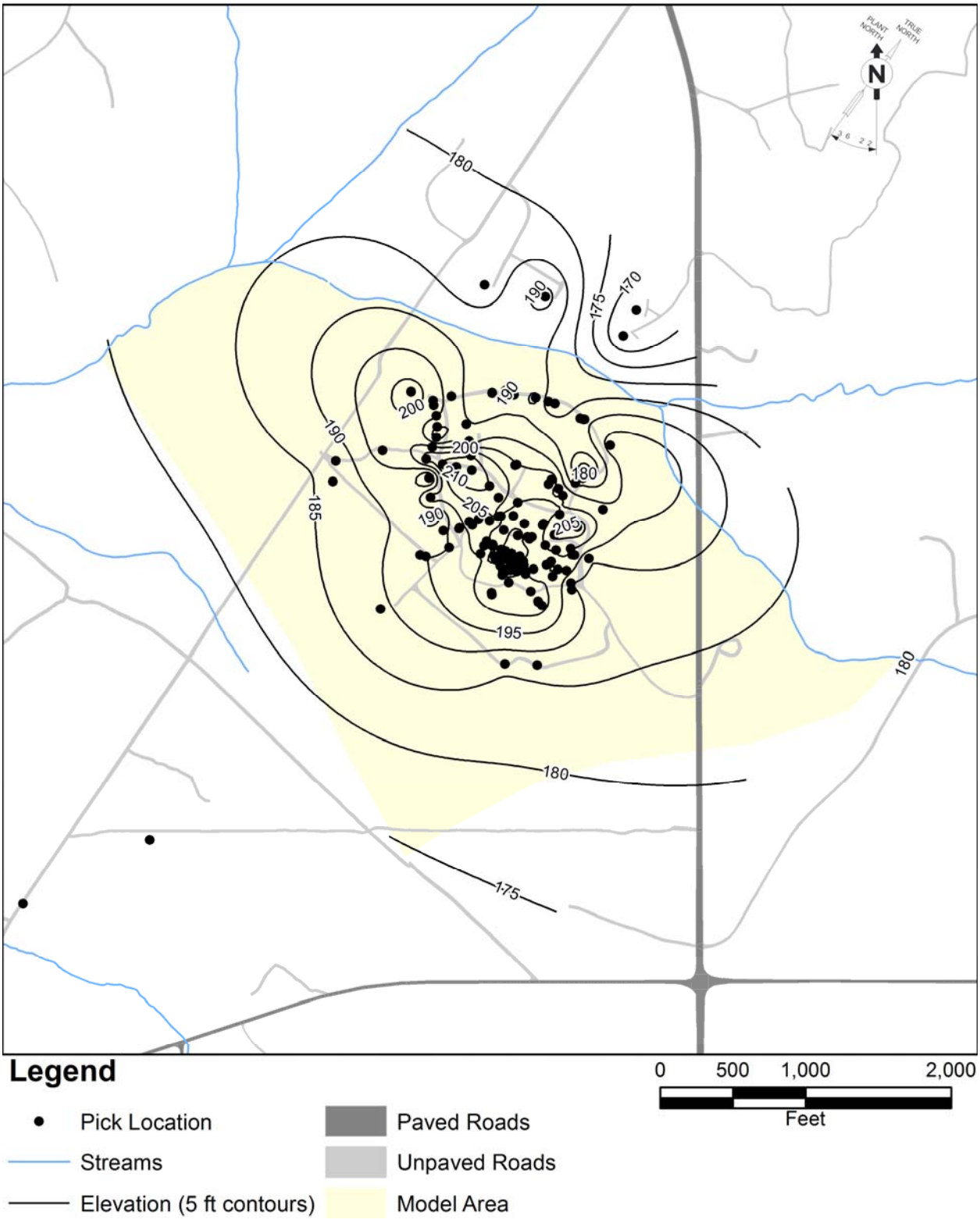

Figure 2.6 Elevation of the Top of the TCLC

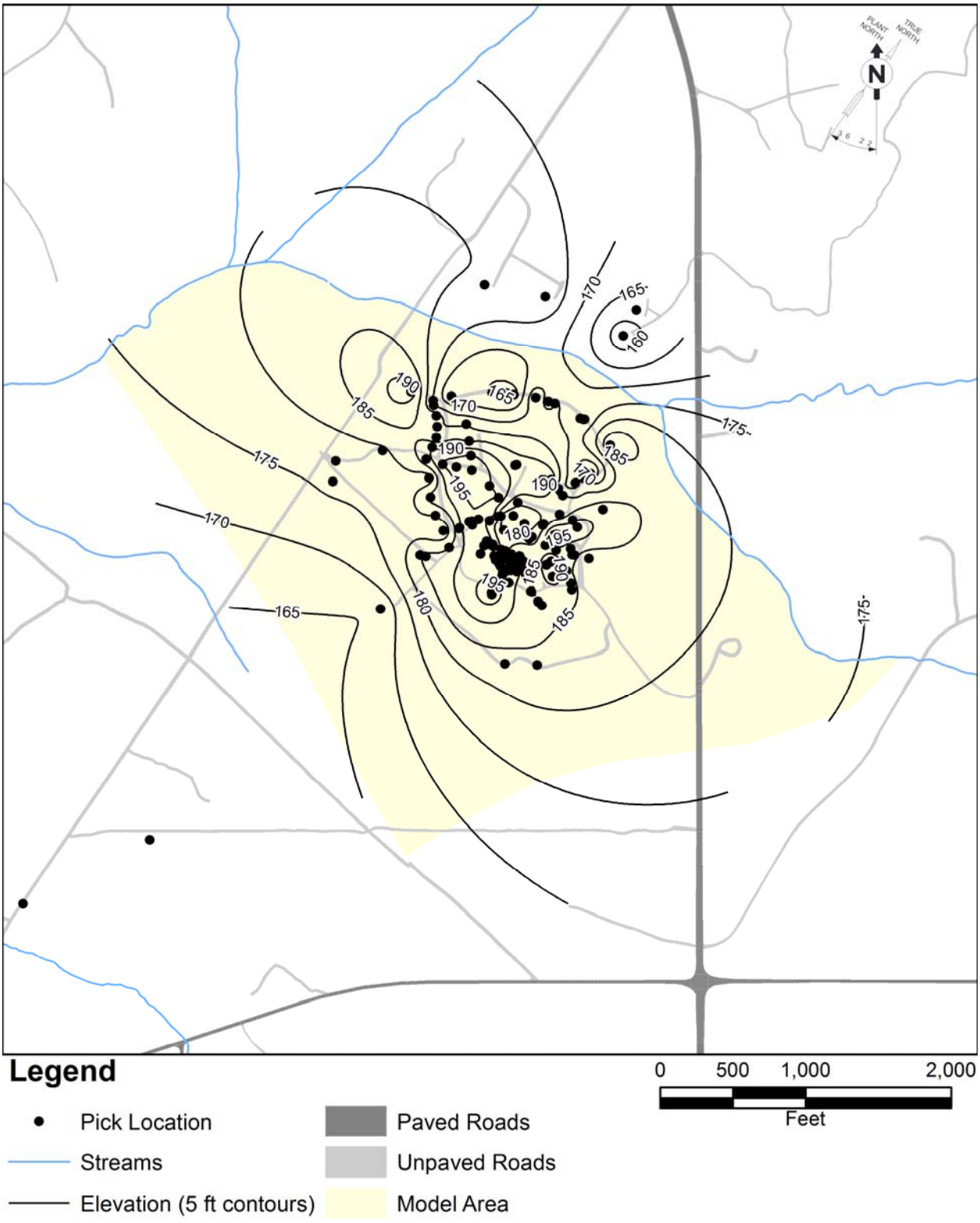

Figure 2.7 Elevation of the Top of the LAZ

Timeline	Activity	Water flux	Mass to water table	2002 Flow Model Calibration period	2017 F+T Calibration Period	Source Document
1970						
1971	CMP Pits received waste; CMP Pits backfilled in 1979	12 in/yr	In transit within vadose zone			Groundwater Modeling for CMP Pits 2002
1972						
1973						
1974						
1975						
1976						
1977						
1978			Enters water table			
1979						
1980						
1981						
1982						
1983						
1984	September excavated drums, NAPL, soils near surface; October removed VOC soil to 25 ft below 183G and pesticide soil to 10 ft below 171G; added liner, backfilled	1.2 in/yr	Source mass significantly reduced; slower transit time in vadose zone			2003 RFI/RI Addendum
1985	Pesticides/PCBs at/near ground surface west of pits (Ballast Area)--attributed to 1984 excavation stockpiling					2003 RFI/RI Addendum
1986						
1987						
1988						
1989						
1990						
1991						
1992						
1993						
1994						
1995						
1996	6 inches of soil spread over entire Ballast Area; then riprap, reseeding, and erosion protection fabric applied to ground surface					2003 RFI/RI Addendum
1997						
1998						
1999						
2000	216 yd^3 pesticide/PCB-contaminated soil excavated from Ballast Area					2003 RFI/RI Addendum
2001	600 yd^3 soil excavated from Ballast Area and bioremediation; April SVE in Field B			Steady State		2003 RFI/RI Addendum; 2017 SRS email from Shull
2002	January, SVE began operation in vadose zone of Field A. By May, Field B SVE removed 220 lb VOCs; Field B active system converted to passive (Baroballs) in July. By August 2002, both systems removed 6300 lb VOCS from CMP Pits area.					2003 RFI/RI Addendum; 2017 SRS email from Shull
2003			Reduction in vadose contribution		2003-2016 (from SOW intro)	2009 EMR CMP; 2014 EMR CMP
2004						
2005	Vadose/Ballast Area excavated: staged in windrows with enhanced bioremediation (nutrient amendments), post-remediation: soil placed back on Ballast and reseeded; Ballast Area successfully remediated in 2005					2009 EMR CMP; 2014 EMR CMP
2006						
2007	Heated SVE wells installed in CMP Pits Area					
2008	ERH/SVE conducted March 2008 to April 2009; ERH completed November 2008					2016 EMR CMP; 2009 EMR CMP; 2010 EMR CMP
2009	SVE shut down in April		Low vadose contribution			2009 EMR CMP
2010	Field B passive system abandoned					
2011						
2012						
2013						
2014						
2015						
2016						

Figure 2.8 Timeline for HCM at CMP Pits

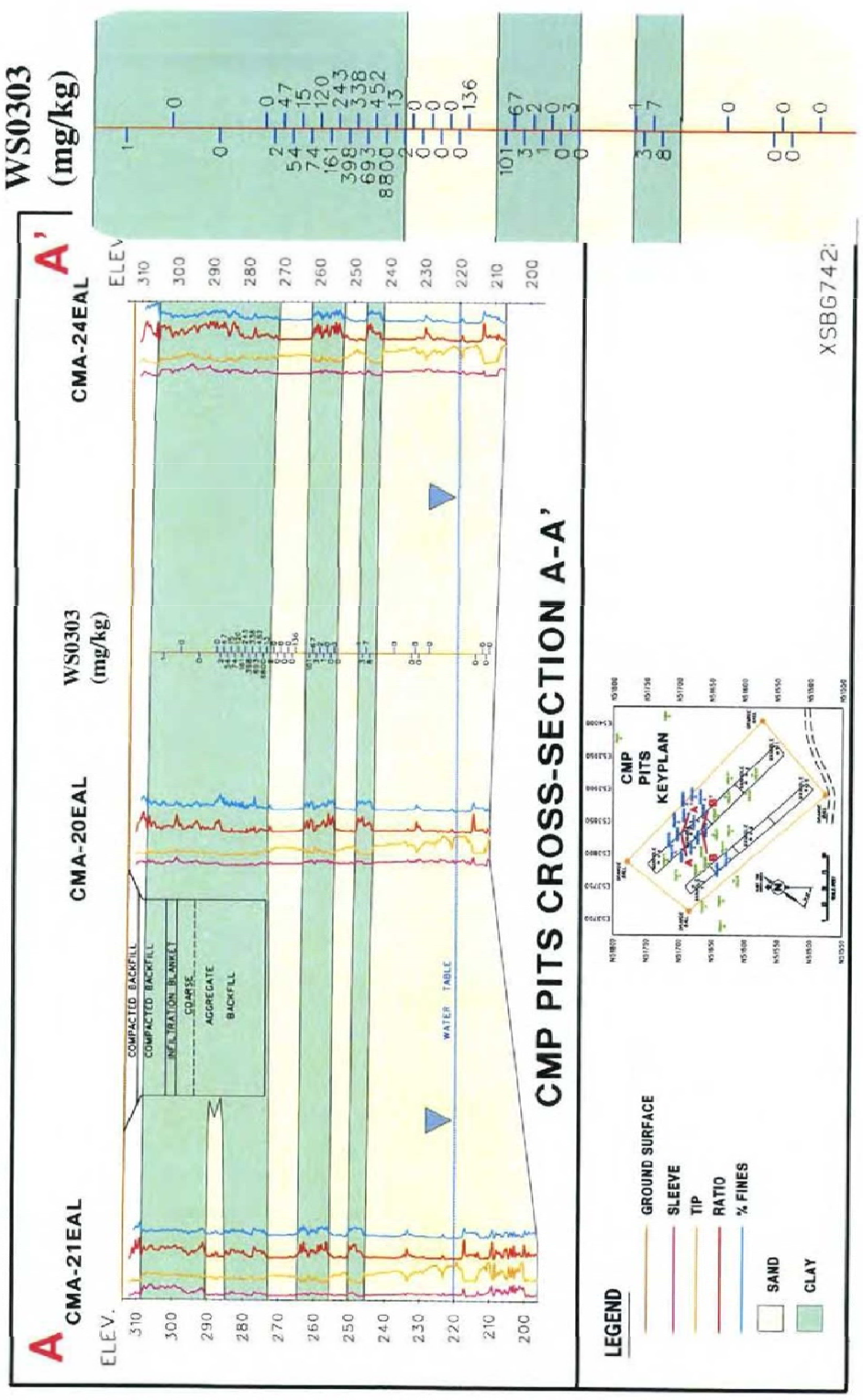

Figure 2.9 Initial PCE Concentration Profile Prior to ERH from Sample WS0303 (SRNS, 2010)

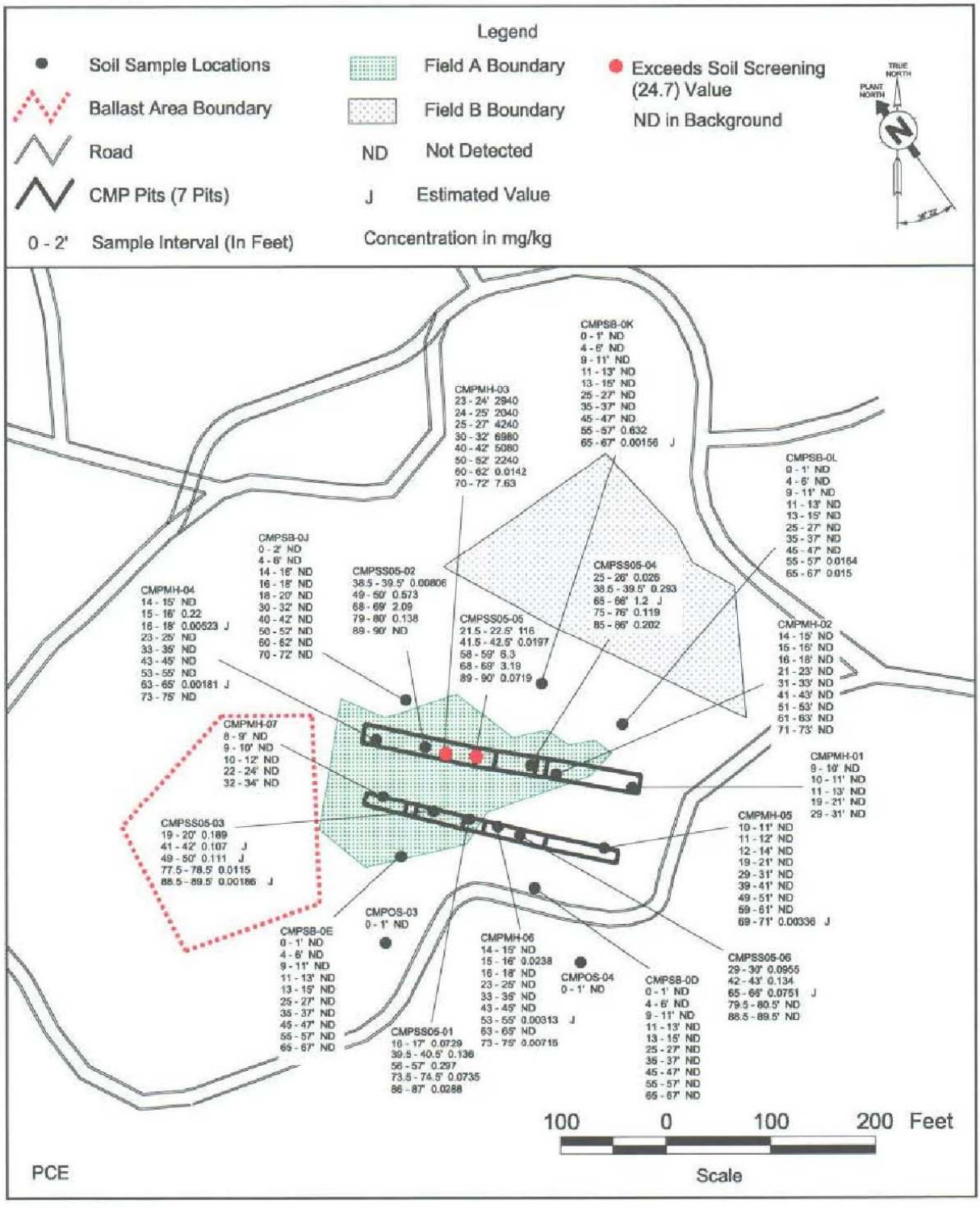

Figure 2.10 PCE Concentration in CMP Pits Area Soil (WSRC 2003)

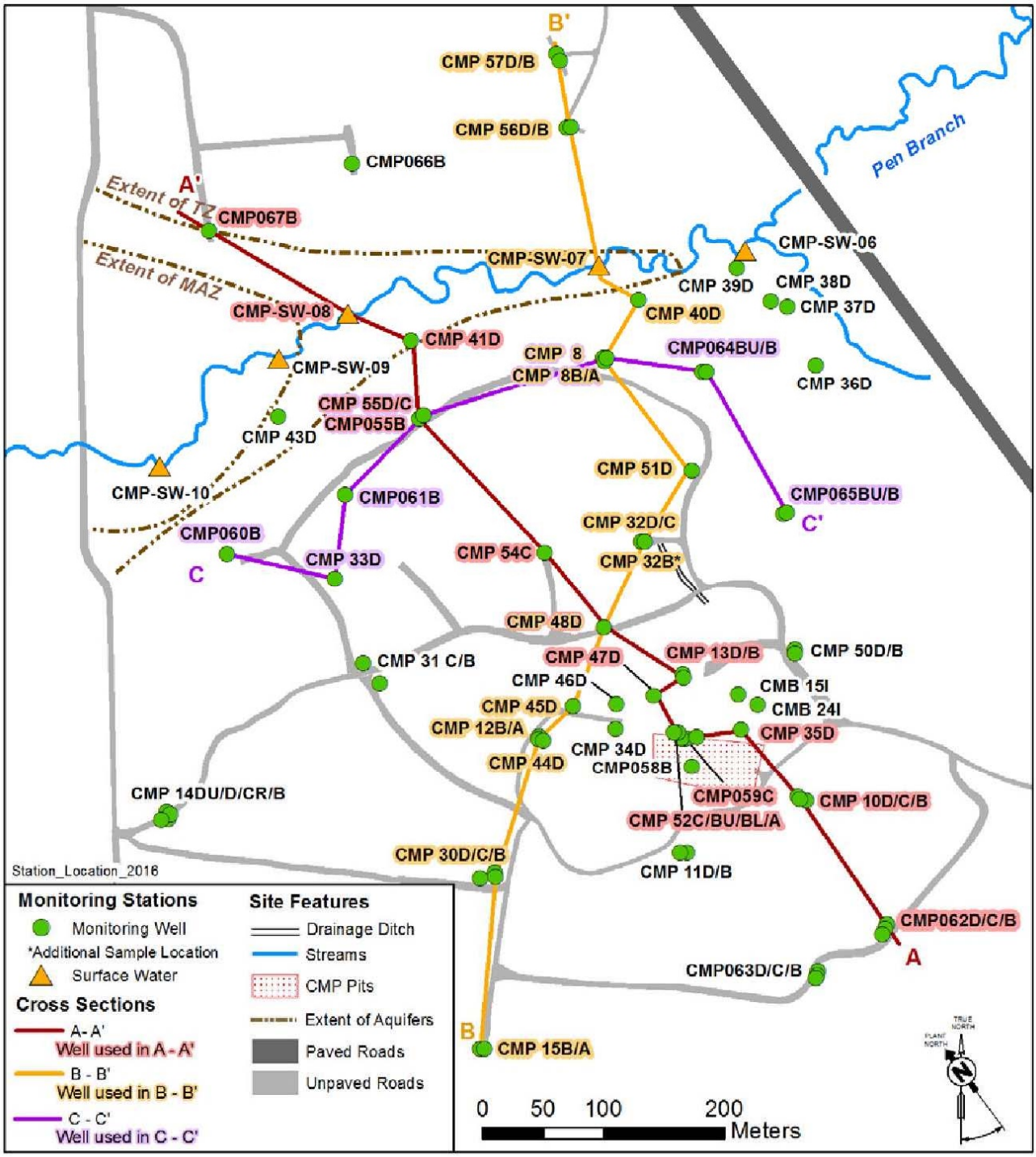

Figure 2.11 Monitoring Well Locations (SRNS 2017)

TZ Source, Distal

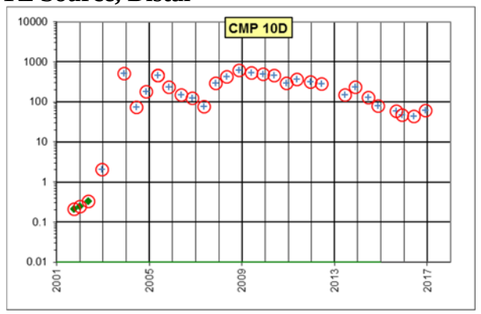

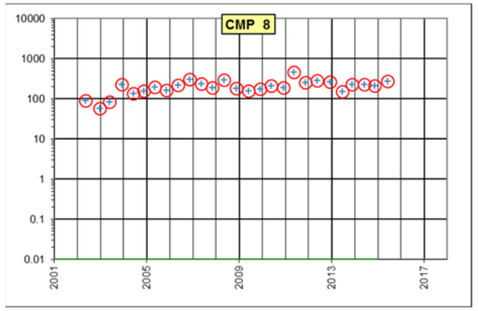

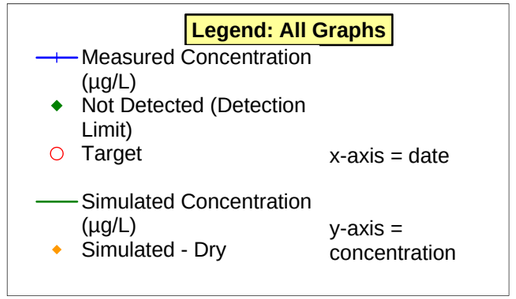

MAZ Source, Mid-Plume and Distal

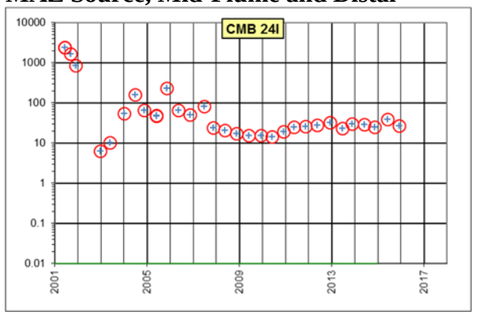

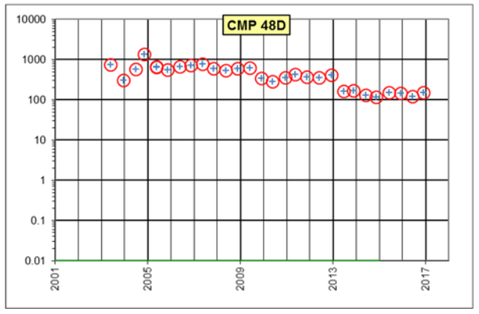

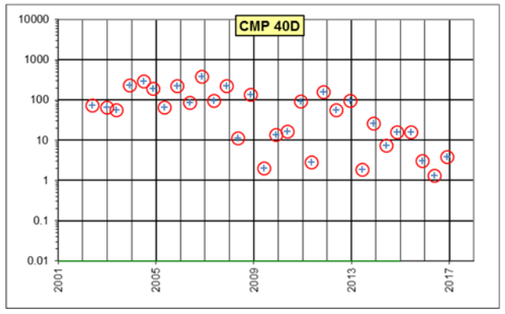

LAZ Source, Mid-Plume and Distal

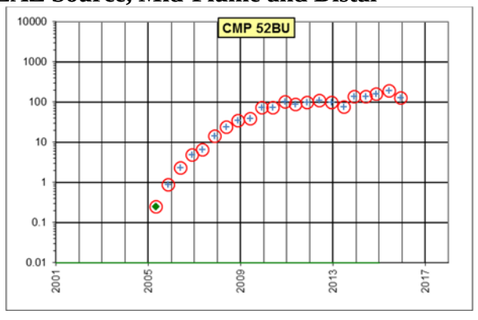

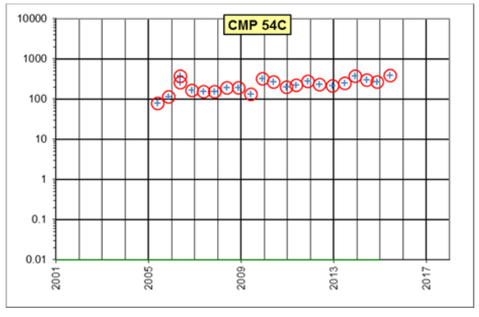

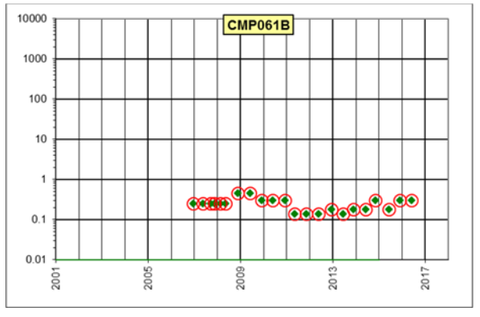

Figure 2.12 PCE Concentration vs. Time for Selected Wells

TZ Source, Distal

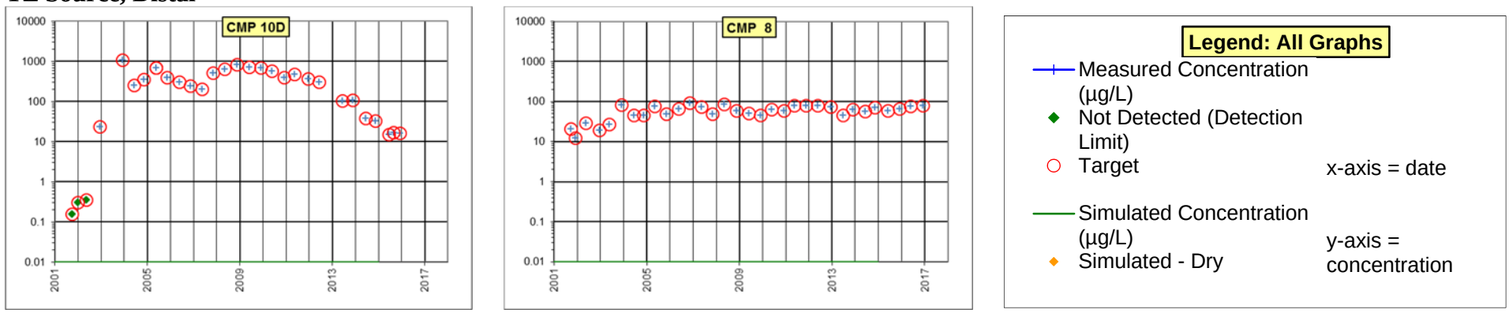

MAZ Source, Mid-Plume and Distal

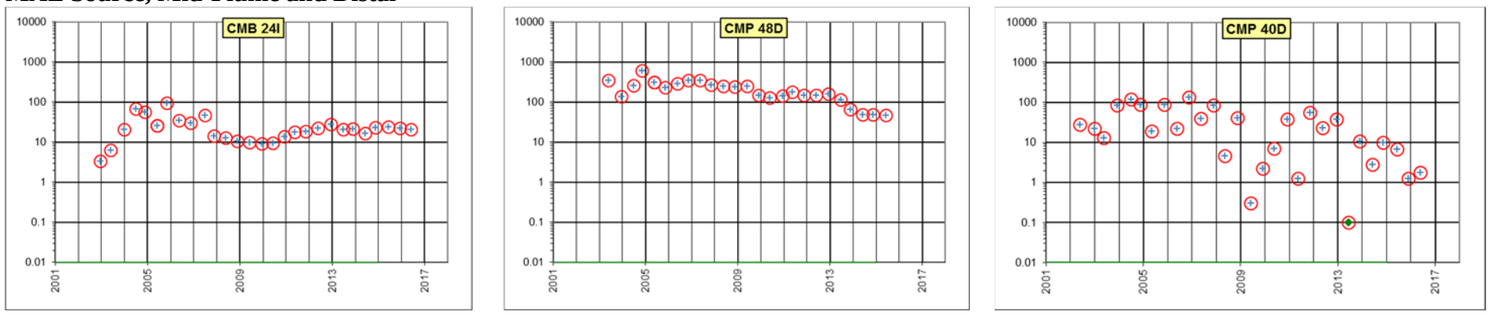

LAZ Source, Mid-Plume and Distal

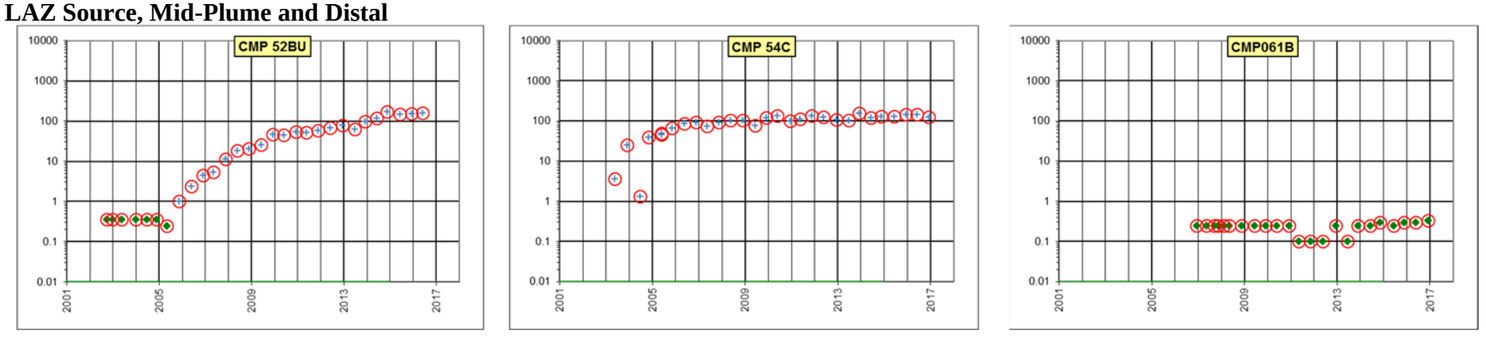

Figure 2.13 TCE Concentration vs. Time for Selected Wells

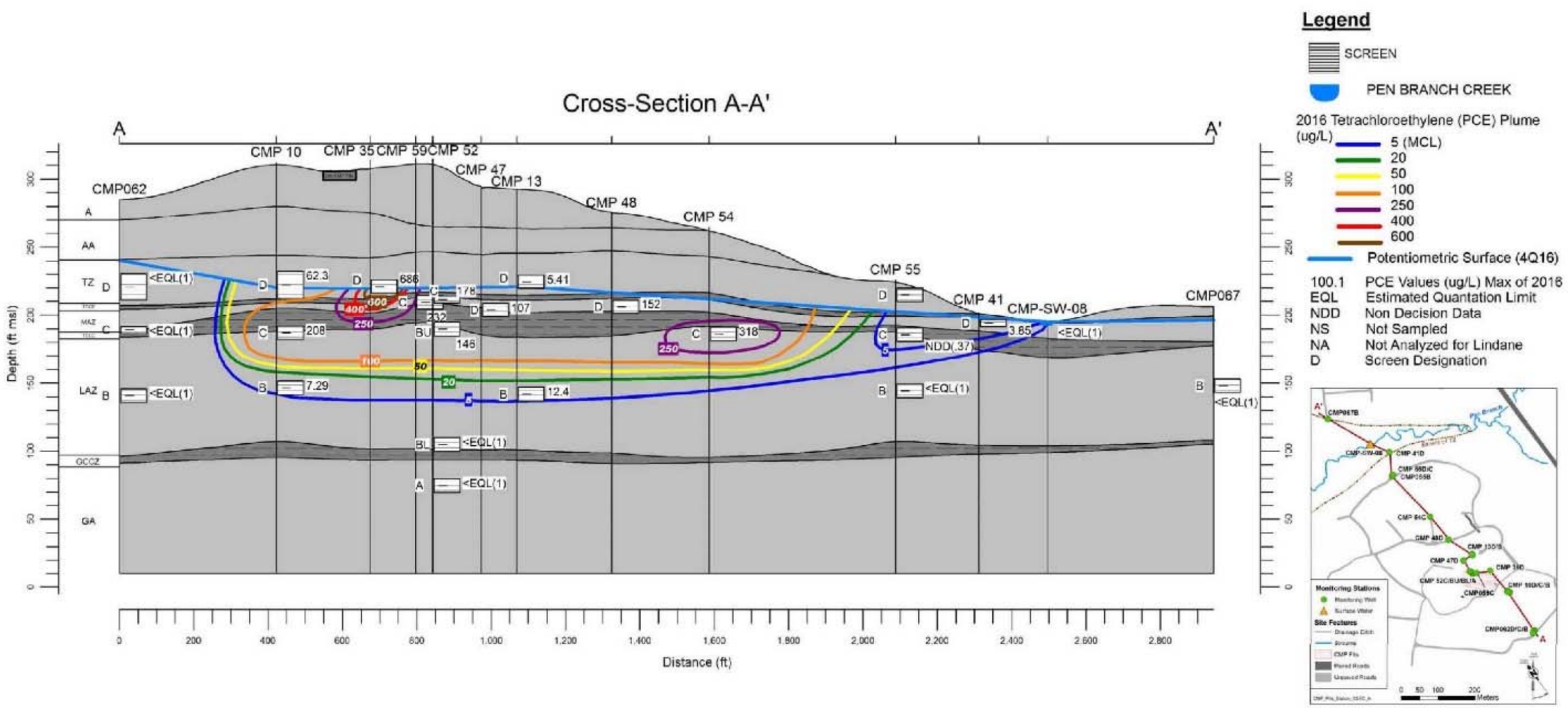

Figure 2.14 Cross-Section A-A' at CMP Pits OU with 2015 PCE Plume (SRNS 2017)

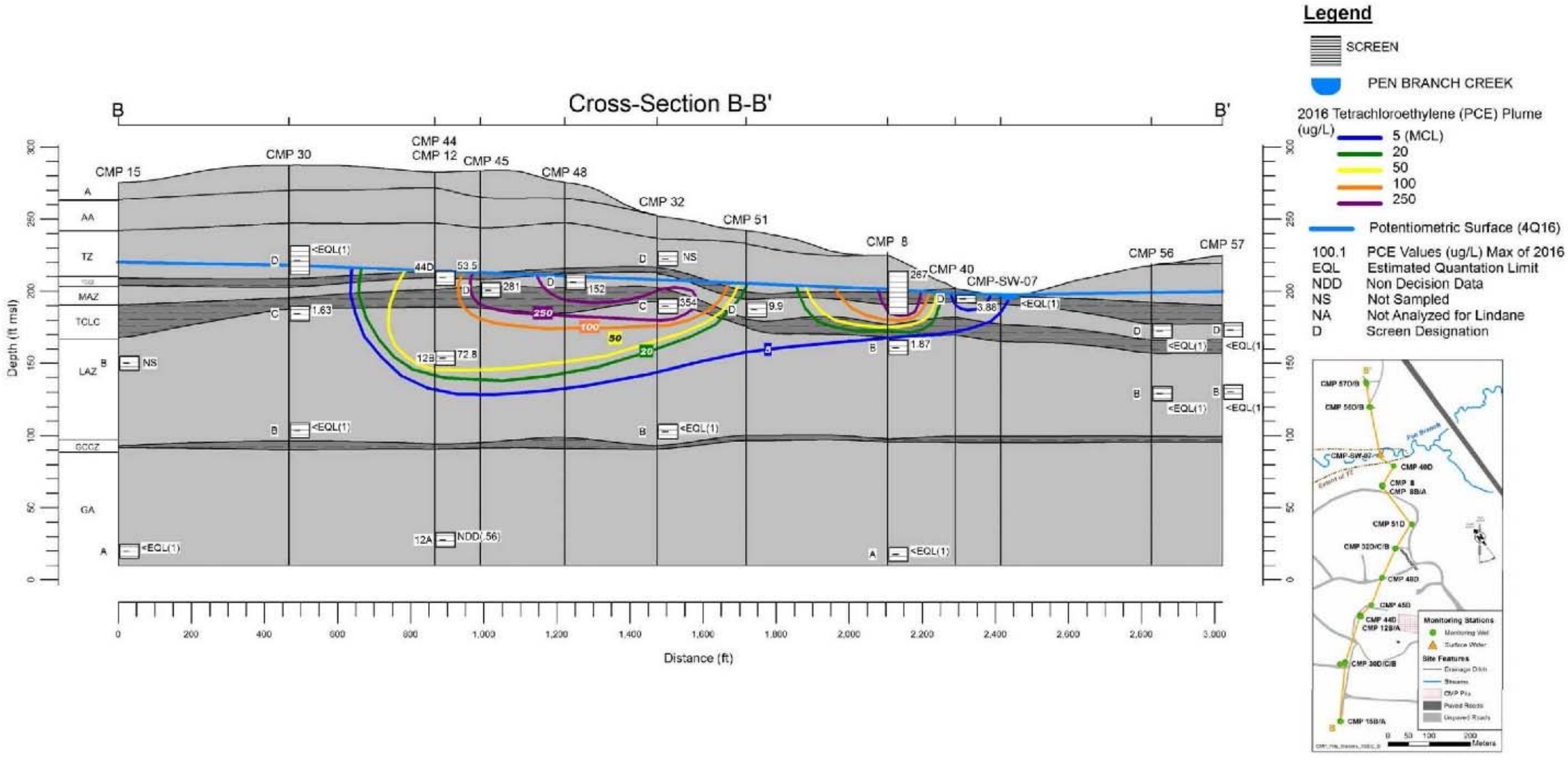

Figure 2.15 Cross-Section B-B' at CMP Pits OU with 2015 PCE Plume (SRNS 2017)

3.0 GROUNDWATER FLOW MODEL CONSTRUCTION AND CALIBRATION

In this section, development of a numerical groundwater flow model for the CMP Pits OU is documented. The development of the solute transport model for the CMP Pits OU is discussed separately in Section 4. The model is based on the HCM of Section 2, a prior groundwater flow and solute transport model (GeoTrans 2002a), and on site-specific data provided by SRNS.

3.1 Numerical Methods

In the saturated groundwater, a combination of continuity (mass conservation) and Darcy's Law leads to the following mathematical description of steady-state groundwater flow:

$$\frac{\partial}{\partial x}\left(K_x \frac{\partial h}{\partial x}\right)+\frac{\partial}{\partial y}\left(K_y \frac{\partial h}{\partial y}\right)+\frac{\partial}{\partial z}\left(K_z \frac{\partial h}{\partial z}\right)=0 \qquad (1)$$

In this equation, the dependent variable is the hydraulic head, h, which is defined in the traditional (x, y, z) Cartesian coordinate system. The horizontal and vertical hydraulic conductivities (K_x, K_y, and K_z) are known functions. Boundary conditions must also be specified to solve equation 1. The boundary conditions may be specified head (Dirichlet), specified flux (Neumann) or head-dependent flux (Cauchy). It is assumed that groundwater flow is unchanging in time (steady state).

The United States Geological Survey (USGS) groundwater flow modeling software MODFLOW (Harbaugh, et al, 2000) provides a means to solve equation 1 for h in a chosen domain, with specified values for hydraulic conductivity and specified boundary conditions. MODFLOW uses the finite difference method to approximate the groundwater flow equation as a set of algebraic equations in a discretized three-dimensional grid of rectangular cells.

MODFLOW is included in the Groundwater Modeling System (GMS) (Brigham Young University 2000) software package (version 9.0.5; Apr 19, 2013 build date). GMS is a standard suite of tools for modeling analyses at SRS and other United States Department of Energy and Department of Defense sites. In this model, the "conceptual model approach" is used in GMS to specify material properties, layer elevations, and boundary conditions independent of the finite-

difference model grid. This approach allows for great flexibility during the construction and calibration processes.

3.2 Model Construction

3.2.1 Model Domain and Grid

The horizontal domain of the CMP Pits numerical model (Figure 3.1) encompasses the contaminant plumes and extends, where practicable, to natural groundwater boundaries. Pen Branch and its tributary are natural groundwater boundaries to the north and east. Natural boundaries do not appear within a reasonable distance in other directions from the CMP Pits contaminant plumes. Therefore, regionally interpreted potentiometric surfaces (Hiergesell 1998) were initially used to set specified-head boundary conditions on the southern model edge, and the western model edge was chosen to approximate a groundwater flow line. These model edges are relatively distant (several hundred feet) from, and upgradient of, the CMP Pits contaminant plumes, which reduces the possibility of model accuracy errors due to inexact specification of boundary conditions.

The CMP Pits model has a uniform horizontal grid spacing of 25 ft by 25 ft (Figure 3.1). The model has 202 rows and 146 columns. Grid cells to the north of Pen Branch and its tributary are inactive (outside the modeled domain), as are grid cells outside the other chosen model boundaries. The lower left (southernmost) corner of the model has coordinates of 53,575 E and 48,887 N in the SRS plant coordinate system. The model extends 3,650 ft and 5,050 ft in the x and y directions, respectively. The grid is rotated 35° west of SRS north. The relatively fine 25 foot grid spacing is used throughout the model so that the resolution of transport results is increased and so that the error in the calculation of the concentration gradient ($\partial c/\partial x_i$) is decreased. This spacing (Δl) results in a Peclet number (P_e) of 2 or less for a characteristic dispersivity (α) of 12.5 ft or greater:

$P_e = \Delta l / \alpha$

$P_e = 25 \text{ ft} / 12.5 \text{ ft}$

$P_e = 2$

Maintaining a Peclet number of 2 or less helps to ensure stability of the numerical solution and to minimize numerical dispersion (Huyakorn and Pinder, 1983).

Nine model layers are used – two for the TZ, one for the TCCZ, one for the MAZ, one for the TCLC, and four for the LAZ (Figure 3.2). The first four layers are convertible and the remaining layers are confined (MODFLOW type 0). Vertically, the model layering is based on the reinterpreted hydrostratigraphic surface elevations described in Section 2.2. The ground surface, or top of the model, is based on a 2-ft contour topographic map as used in the 2002 model. In portions of the stream valleys, the TZ, TCCZ, and MAZ are absent (see HCM, Figure 2.1). There, the model layers representing these zones are set inactive (Figure 3.3). Note that portions of the TZ are absent in the plume area near Pen Branch.

The TZ is divided into two layers. This split includes a very thin (one half foot thick) layer and a second layer representing the remainder of the TZ. This representation was found in the 2002 study to be necessary to maintain a pathway to Pen Branch within saturated groundwater. The LAZ was divided into four layers that represent 12.5, 12.5, 25, and 50 percent of the LAZ thickness.

3.2.2 Hydrogeologic Properties

For steady-state groundwater flow, hydraulic conductivity values (K_x, K_y, K_z) are specified in each model cell. The value of hydraulic conductivity is much higher in aquifer/sand zones than in confining/clay zones, and may vary considerably within an aquifer or confining zone. Typically, hydraulic conductivity values are initialized for each hydrostratigraphic layer based on prior studies and the values are adjusted during flow model calibration to achieve a good match between modeled and observed head and/or flux conditions. In the current study, the calibrated parameters for the GeoTrans (2002a) model were used as initial values. The 2002 model had constant conductivity values across each aquifer with the confining units having zones along Pen Branch (Figure 3.4 and3.5). Section 3.3 provides details on the calibration process used in this study.

3.2.3 Groundwater Flow Boundary Conditions

Flow boundary conditions provide the sources and sinks of groundwater in the model. Three types of boundaries are used in the CMP Pits model – specified head, head-dependent flux, and specified flux boundaries.

Specified head boundaries are used on the southeast section of the model perimeter (Figure 3.4 through 3.7) in the aquifer units (layers 1-2, 4, and 6-9). The head values are based on a regional interpretation of potentiometric surfaces (Hiergesell 1998 and SRNS 2017). Adjustment of the specified head values for calibration is discussed in Section 3.3.

Pen Branch and its tributaries are modeled as head-dependent flux boundaries using MODFLOW's Drain Package (Figure 3.4 through 3.7). The boundary head is set to the stream elevation, and the conductance is treated as a calibration parameter (see Section 3.3). Because the modeled streams intersect different aquifer zones in different portions of the model, the boundary conditions are placed in different model layers along the stream. Where the boundary condition is applied to a confining unit, it is also applied to the underlying aquifer zone. The layers below the head-dependent flux boundaries are defined as no-flow (specified flux of zero). The wetlands in discharge areas near Pen Branch are modeled as seepage face drains, where the elevations are set to the top elevation of the cells. The wetland cells were placed in the top active layer and are applied to layers 1 through 6. Seepage faces were applied along the exposed faces of the TZ and MAZ in the downstream reaches where Pen Branch is defined in the lower aquifer, MAZ or LAZ respectively.

A specified flux is applied at the model top (uppermost active layer) in upland areas to represent precipitation recharge (Figure 3.8). The recharge rate is treated as a calibration parameter (see Section 3.3). A low-recharge condition is applied in capped or paved areas. In these areas, it is assumed that the recharge rate is reduced by 90%. The capped recharge rate was not adjusted during calibration. The 2002 model zonation included a zone of intermediate recharge along the steep slopes surrounding the CMP Pits was retained in the current study. Recharge was set to zero, a no-flow condition, in discharge areas along the creeks to the north and west matching the shape of the defined wetland seepage faces. Recharge was also set to zero on saturated confining beds

(TCLC) that are the highest active layer in the model. This representation prevents the unrealistic condition of a relatively large specified flux being injected into the confining bed.

A no-flow condition (specified flux of zero) is used on the western edge of the model to represent an inferred groundwater flow line in all aquifers. The confining units (layers 3 and 5) have no-flow boundary conditions for all edges of the active area, except in locations where the creek intersects and a head-dependent flux is defined.

3.2.4 Initial Conditions

Hydraulic heads in the active part of the model area were initialized to a uniform 250 ft. The value of initialized heads is of little consequence in a steady-state model. Specification of initial heads at a higher elevation than observed allows cells to desaturate cells when modeled water levels fall below the base of a layer, without the need to specify a-priori.

3.3 Groundwater Flow Model Calibration

The process of model calibration involves adjusting model specifications in order to achieve an optimal match to observed conditions. After calibration, the model can be more reliably used to predict future conditions. For this model of the CMP Pits, the groundwater flow model is calibrated by adjusting hydraulic conductivity values and boundary conditions until the model closely matches observed heads and flows.

3.3.1 Parameterization and Initial Values

Model hydraulic conductivity specifications and flow-model boundary conditions are treated as calibration parameters in the model. Initially, conductivities are estimated for each hydrostratigraphic unit based on field tests and prior studies (GeoTrans 2001). These were further refined during the calibration of the 2002 model (GeoTrans 2002a) and these values are used as the initial parameters in the current study. Table 3.1 lists the initial parameter values used in the groundwater flow model. For aquifers (TZ, MAZ, LAZ), flow is predominantly horizontal, and the important parameter is the horizontal hydraulic conductivity ($K_x = K_y$). In confining units

(TCCZ, TCLC), flow is predominantly vertical, and the parameter of interest is the vertical hydraulic conductivity (K_z). A hundred to one anisotropy ratio is assumed for hydraulic conductivity. Hydraulic conductivity zonation for the TCCZ and TCLC are found in Figures 3.4 and 3.5.

Table 3.1 Model Parameters and Initial Value

Parameter	Initial Value		
Hydraulic Conductivity (ft/d)	Unit	$K_x = K_y$	K_z
	TZ	60	0.6
	TCCZ Base	0.16	0.0016
	TCCZ High	10	0.1
	MAZ	50	0.5
	TCLC Base	0.08	0.0008
	TCLC High	8	0.08
	LAZ	20	0.2
Upland Recharge Rate (in/yr) Slope Recharge Rate (in/yr) Wetland Recharge Rate (in/yr)	12 10 0		
Drain Conductance (ft^2/d/ft)	0.5-10		
Specified Heads on Model Perimeter (ft)	Unit	Value	
	TZ	222	
	MAZ	213	
	LAZ	197-198	

The upland recharge rate is initially set to 12 in/yr, except in discharge areas and in capped areas (including the CMP Pits), as shown in Figure 3.10. Specified head values for the southeastern boundary are initially specified as uniform values in each aquifer zone based on earlier potentiometric surface interpretations (Hiergesell 1998). Stream conductances (per length of stream) are initialized at the 2002 model calibration values.

3.3.2 Calibration Process and Objectives

The flow model for the CMP Pits is the culmination of a calibration process that was used to increase model reliability. The process involved first setting calibration goals for flow simulations, and then using a trial-and-error approach to achieve the calibration goals through multiple

parameter value adjustments and simulations, along with the use of simple zone based parameter estimation (PEST (Doherty 2016)) to automate portions of the calibration.

The main goal of the flow model calibration is to optimally match observed aquifer heads using reasonable hydraulic properties and boundary conditions. Target heads were selected based on data quality and location. Water levels for 2016 were used in order to represent current conditions for simulation of contaminant transport into the future. The chosen set of 57 targets range in head from 193 ft to 221 ft. Polygonal areas presumed to be dry based on stratigraphic elevation relative to water surface were used as soft calibration targets to verify that the pattern of dry cells computed by the model matched those inferred from stratigraphic and observed water elevation surfaces.

For each flow model simulation, a head residual (or error) is computed for each head target by subtracting the observed head from the simulated head. The goodness-of-fit statistics for these residuals are then compared to commonly accepted criteria for groundwater flow model calibration. Specifically, a calibration is sought that has a mean error within 0.5 ft of zero, and has a root-mean-square error (RMSE) less than one-tenth of the observed head range across the area of interest. For this model, the RMSE should be less than 2.8 ft (in the plume area, the maximum observed head is 221 ft in the TZ, and the minimum is 193 ft in the LAZ). The RMSE is calculated by squaring each residual, taking the mean of the squares, and then taking the square root of that mean (when the mean error is zero, the RMSE is the same as the standard deviation). Another measure of calibration quality is the mean-absolute error (MAE), which is calculated as the mean of the absolute value of each residual. The MAE is less affected than the RMSE by outliers. When the MAE is much lower than the RMSE, a few poorly matched head targets are likely having a large effect on the statistics.

Head calibration alone is usually not sufficient to ensure that a groundwater flow model is a reasonable representation of reality. Another goal of groundwater flow calibration should be to match observed groundwater discharge conditions. Baseflow measurements at several locations along Pen Branch (Flach et. al 1999) were used to estimate a target for the volume of baseflow contributed from the model area. The estimated baseflow target for flow from the model to Pen

Branch and its tributary is 0.35 cfs, not including the discharge to the wetland, a large portion of which is assumed to evaporate or taken up and transpired by plants.

3.3.3 Model Adjustments Made for Calibration

The main parameters that were adjusted in the flow calibration were the horizontal and vertical hydraulic conductivities of the aquifers and confining units, recharge rate, drain conductance, seepage face elevation offset and specified head values. The constant head boundary in the TZ was modified to reflect the water table as shown in SRNS 2017 and the constant head boundary in the MAZ was adjusted to reflect current heads. As part of the transport calibration the flow model was further adjusted to ensure mass movement as observed in the LAZ (Figure 2.12 and 2.13). One of these adjustments was that constant heads in the LAZ were adjusted to steer the plume towards the upper reaches of Pen Branch (Figure 3.9). The final calibrated parameter values are listed in Table 3.2.

3.3.4 Calibrated Groundwater Flow Field

Goodness-of-fit calibration statistics of 2.15 ft for RMSE, -0.51 ft for mean error, and 1.62 ft for MAE were achieved for the calibration (Tables 3.3 and 3.4). This value for RMSE is within the calibration goal of 2.78 ft. Figures 3.11 through 3.13 show the modeled head field in the aquifers, and indicate the location and magnitude of computed head residuals. In general, the computed flow fields closely resemble the interpreted potentiometric maps of Figures 6 and 7 of SRNS (2017). In addition, the head residuals are randomly distributed, indicating minimal spatial bias. Also shown in Figures 3.11 and 3.12 is a good match between the dry areas computed by the model and those areas presumed to be dry prior to calibration. Plots of modeled vs. observed head and modeled residual vs. observed head are included in Figure 3.14. Figure 3.15 shows a histogram of the flow model residuals. The overall water budget for this model is shown in Figure 3.16. In this simulation, Pen Branch and all wetlands and seepage faces receive about 0.43 cfs, with 0.21cfs directly discharging into Pen Branch, which is consistent with the baseflow target of 0.35 cfs. Figure 3.16 shows that the model domain is dominated by downward hydraulic gradients; however slight upward flow is predicted in the TCCZ, MAZ, TCLC, and LAZ at locations near surface water. This is consistent with observations, and with groundwater flow theory.

Table 3.2 Model Parameters and Final Values

Parameter	Final Calibrated Value			
Hydraulic Conductivity (ft/d)	Unit	$K_x = K_y$	K_z	
	TZ TCCZ Base TCCZ High MAZ TCLC Base TCLC Low LAZ	8 0.21 0.58 50 0.22 0.0003 30	0.08 0.0021 0.0058 0.5 0.0022 0.000003 0.30	
Upland Recharge Rate (in/yr) Slope Recharge Rate (in/yr) Capped Recharge Rate (in/yr) Wetland Recharge Rate (in/yr)	16.0 13.34 1.2 0			
Drain Conductance ($ft^3/d/ft$)	Unit	Pen Branch	Seepage Face	Wetlands
	TZ MAZ LAZ	0.16 0.5-50 0.75	10 1.0 N/A	0.01 1.5 1.5
Specified Heads on Model Perimeter (ft)	Unit		Value	
	TZ MAZ LAZ		230-240 213-215 194-200	

Table 3.3 Head Calibration Statistics

Aquifer	Mean Error (ft)	Mean Absolute Error (ft)	Root Mean Square Error (ft)
TZ	-0.27	0.96	1.13
MAZ	-0.29	1.96	2.41
LAZ	-0.72	1.62	2.28
All Targets	**-0.51**	**1.62**	**2.15**

In general, modeled hydraulic heads are slightly lower than observed in all three aquifers. The hydraulic heads are, on average, lower in the TZ due to large residuals in a few wells. These wells could be measuring perched water in the TZ and not the actual water table. The distribution of residuals shows no inherent areal bias in Figures 3.11 through 3.13. There are residuals in five wells over 5 ft (CMP15B, CMP050D, CMP063C, CMP064B and CMP31C). CMP31C is located in the dry zone in the MAZ and is screened in the MAZ and the TCLC. The target was placed in the TCLC to be consistent with the observed presence of water in the well.

Table 3.4 Head Residuals in the Calibration Simulation

Name	Unit	Observed (ft)	Computed (ft)	Residual (ft)
CMP063D	TZ	220.28	221.91	1.63
CMP10D	TZ	220.67	220.15	-0.52
CMP11D	TZ	220.40	219.66	-0.74
CMP14D	TZ	214.28	215.01	0.73
CMP14DU	TZ	214.44	214.85	0.41
CMP30D	TZ	219.20	218.64	-0.56
CMP34D	TZ	220.72	218.94	-1.78
CMP35D	TZ	220.84	218.91	-1.93
CMP8	TZ	202.10	202.46	0.36
CMB24I	MAZ	211.03	209.87	-1.16
CMP059C	MAZ	210.62	209.73	-0.89
CMP063C	MAZ	205.76	213.16	7.40
CMP065BU	MAZ	206.23	207.35	1.12
CMP14CR	MAZ	207.91	204.31	-3.60
CMP30C	MAZ	207.70	209.44	1.74
CMP31C	TCLC	206.63	197.85	-8.78
CMP36D	MAZ	204.46	203.79	-0.68
CMP37D	MAZ	201.57	200.49	-1.08
CMP38D	MAZ	200.69	199.94	-0.75
CMP39D	MAZ	198.76	198.33	-0.43
CMP40D	MAZ	198.39	197.64	-0.75
CMP41D	MAZ	196.43	196.34	-0.09
CMP44D	MAZ	211.31	208.88	-2.43
CMP45D	MAZ	206.44	208.78	2.34
CMP46D	MAZ	209.04	208.84	-0.20
CMP47D	MAZ	209.08	208.92	-0.16
CMP48D	MAZ	208.23	207.60	-0.63
CMP50D	MAZ	204.84	209.84	5.00
CMP51D	MAZ	204.75	203.68	-1.07
CMP52C	MAZ	210.45	209.53	-0.92
CMP43D	TCLC	193.07	190.49	-2.58
CMP55C	TCLC	196.55	195.88	-0.67
CMP8B	TCLC	197.50	197.15	-0.35
CMP055B	LAZ	196.31	194.02	-2.29
CMP058B	LAZ	195.76	195.83	0.07
CMP060B	LAZ	193.78	192.72	-1.06
CMP061B	LAZ	194.01	193.53	-0.48

Name	Unit	Observed (ft)	Computed (ft)	Residual (ft)
CMP062B	LAZ	199.14	196.24	-2.90
CMP063B	LAZ	195.63	195.98	0.34
CMP064B	LAZ	200.27	195.04	-5.23
CMP064BU	LAZ	198.68	195.10	-3.58
CMP065B	LAZ	194.00	195.33	1.33
CMP10B	LAZ	194.20	195.92	1.72
CMP10C	LAZ	199.10	196.19	-2.91
CMP11B	LAZ	194.30	195.72	1.41
CMP12B	LAZ	193.86	194.90	1.04
CMP13B	LAZ	193.97	195.39	1.42
CMP14B	LAZ	193.67	192.72	-0.95
CMP15B	LAZ	201.82	195.20	-6.62
CMP30B	LAZ	194.20	194.72	0.52
CMP31B	LAZ	193.74	193.87	0.13
CMP32C	LAZ	194.60	195.17	0.57
CMP33D	LAZ	195.30	193.61	-1.69
CMP50B	LAZ	194.04	195.81	1.77
CMP52BL	LAZ	195.45	195.30	-0.15
CMP52BU	LAZ	195.20	195.69	0.49
CMP54C	LAZ	194.91	194.77	-0.14

3.4 Particle Tracking Results

Particle tracking was used to verify that flow paths from the CMP Pits source area coincide with the observed plume locations (Figure 3.17). The particle tracking analysis indicates that the majority of lateral particle movement occurs in the MAZ. Particles that start on the southern end of the pits move through the MAZ until they reach the vicinity of CMP 54C and 32C where they enter the LAZ and head to the lower reaches of Pen Branch. A slight upward hydraulic gradient in the LAZ near Pen Branch, which is observed in the CMP064B/BU cluster, is confirmed by particle tracks in the LAZ, shown in Figure 3.17. It takes approximately five years for particles to move from the water table at the CMP Pits to discharge locations along Pen Branch in the MAZ and 25 years when in the LAZ. The residence time in the confining beds (TCCZ and TCLC) is much greater than in the aquifers. The 5 to 25-year travel time is relatively short when compared to the estimated travel time in the vadose zone. However, it should be noted that the particle tracking

does not consider retardation due to sorption/desorption; this is addressed in the solute transport model.

3.5 Sensitivity Analysis

Sensitivity analysis is performed on groundwater models to assess the effects of parameter, boundary condition, or conceptualization uncertainty on the calibrated results. The procedure generally involves changing a single aspect (parameter, boundary condition, etc.) of the model by a pre-determined amount (usually within a reasonable range of certainty) and comparing the result to the calibrated model. This procedure is repeated several times, where independent changes are made to assess low and high ranges of uncertainty for a suite of parameters, boundary conditions, or conceptualizations.

The process of calibrating a model involves making independent changes and noting the result; consequently, the analyst has an indication of model sensitivity prior to performing the formal sensitivity analysis that is documented. During the model calibration, hydraulic conductivity, and boundary conditions were identified as key elements of the flow model.

Another method of performing sensitivity analysis is to extract data regarding response to parameter perturbations from a parameter estimation simulation (PEST software). Parameter estimation by its nature, involves perturbation of calibration parameters by a specified amount (generally a few percent) and noting the response of water levels at calibration targets. These responses are called sensitivity coefficients and may be summarized to present a comprehensive view of model sensitivity. The sensitivity of key flow model parameters is summarized in Table 3.5. The vertical hydraulic conductivity of the TCCZ and recharge are the most sensitive. These are followed by the horizontal hydraulic conductivity of the upper parts of the aquifer, the TZ and MAZ.

Table 3.5 Summary of Sensitivity of Key Flow Model Parameters

Parameter	Current value	Relative Sensitivity	Rank
Wetland Cond (Lower Reaches) $(ft^2/d)/ft^2$	1.00E-02	5.41	1
Recharge (ft^3/d)	3.65E-03	1.30	2
K_v Base TCCZ (ft/d)	0.21	0.90	3
K_v Base TCLC (ft/d)	0.22	0.77	4
Wetland Cond (Center Reaches) $(ft^2/d)/ft^2$	1.00E-02	0.53	5
K_h TZ (ft/d)	8	0.45	6
K_h LAZ (ft/d)	30	0.33	7
K_h MAZ (ft/d)	50	0.22	8
K_v High TCCZ (ft/d)	0.58	0.074	9
K_v Low TCLC (ft/d)	3.00E-04	0.0071	10
Wetland Cond (Upper Reaches) $(ft^2/d)/ft^2$	1.5	0.0020	11

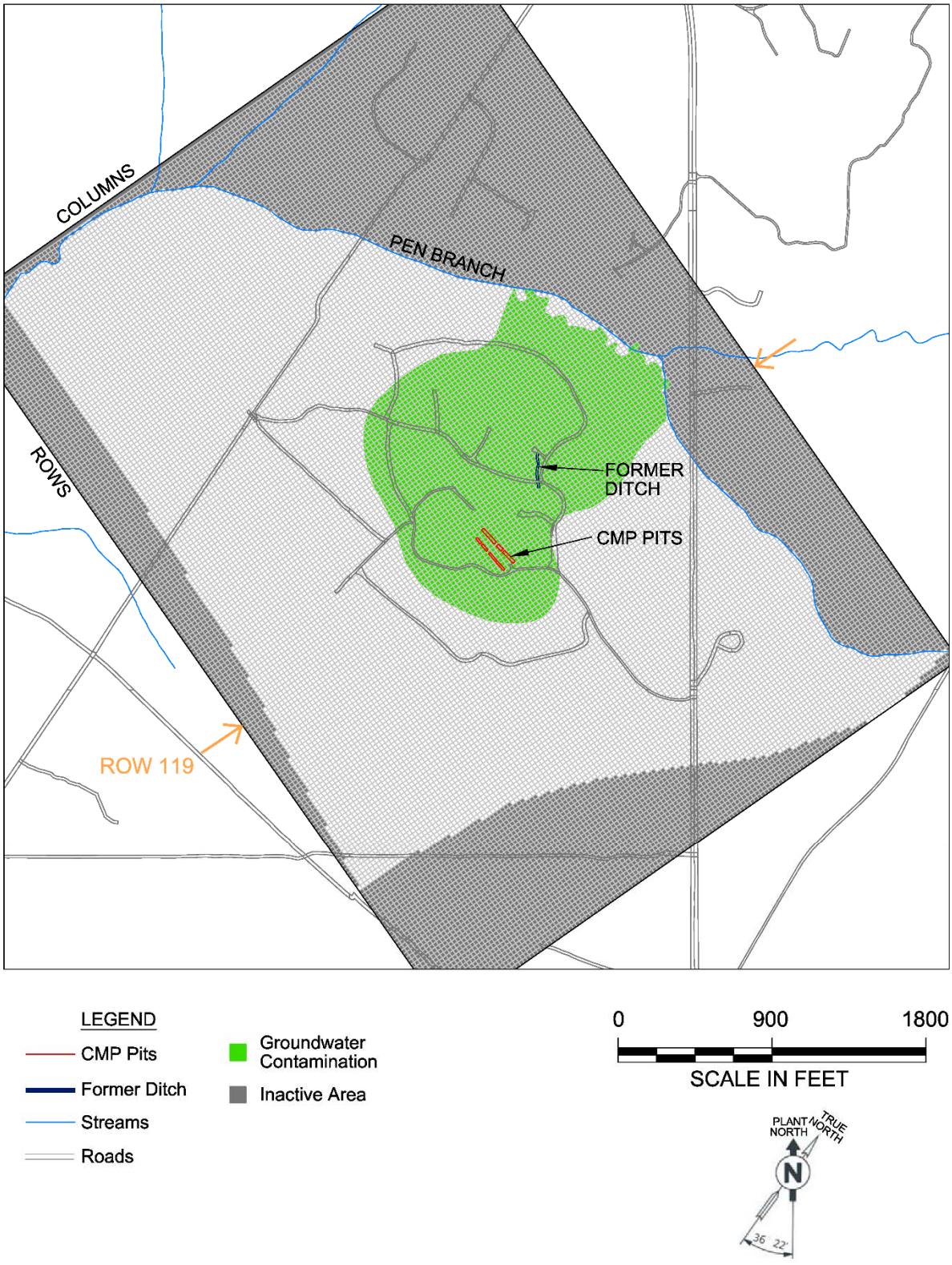

Figure 3.1 Model Domain and Grid

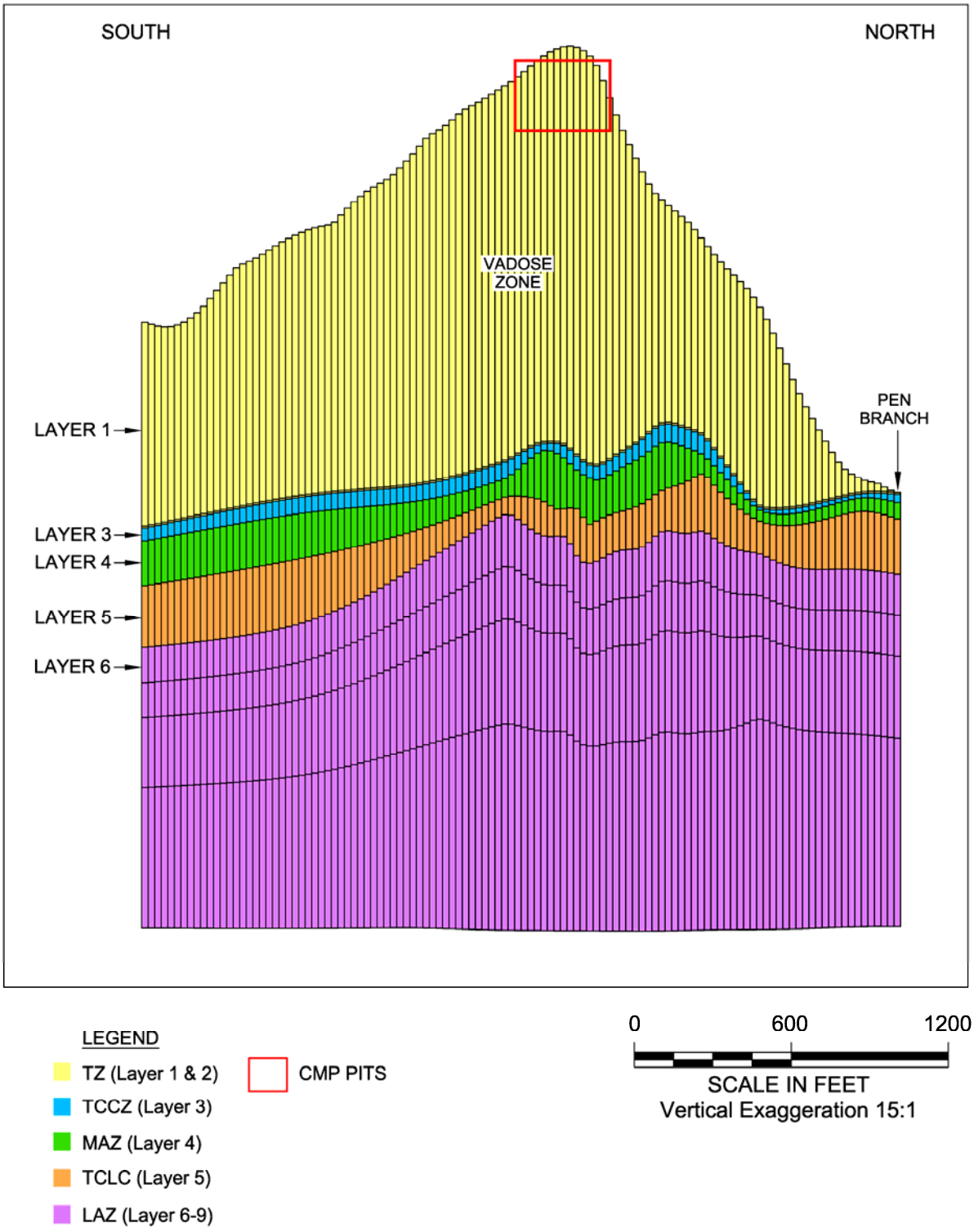

Figure 3.2 Cross Section Along Row 119 Showing Model Layering

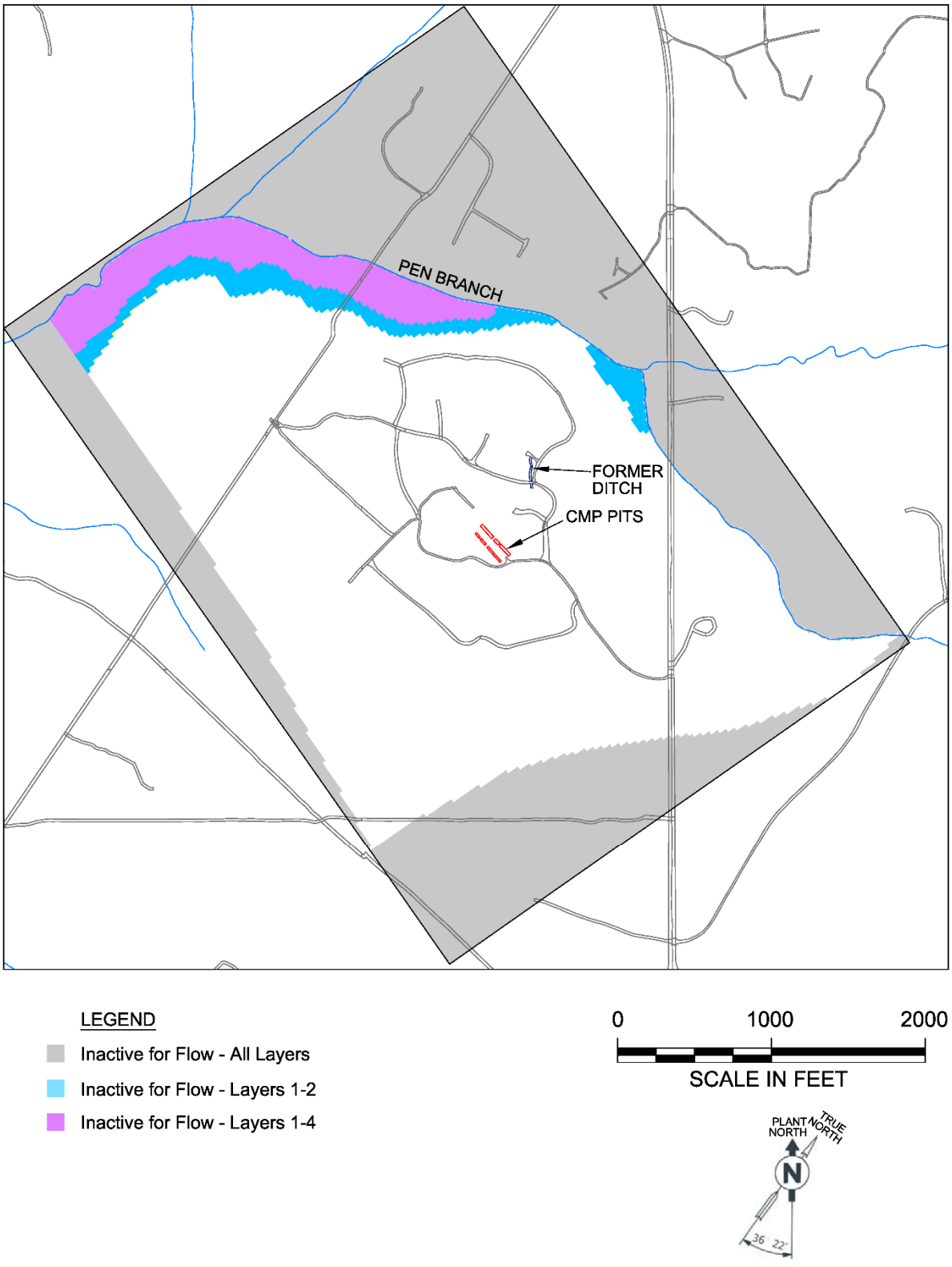

Figure 3.3 Inactive Area in the Model

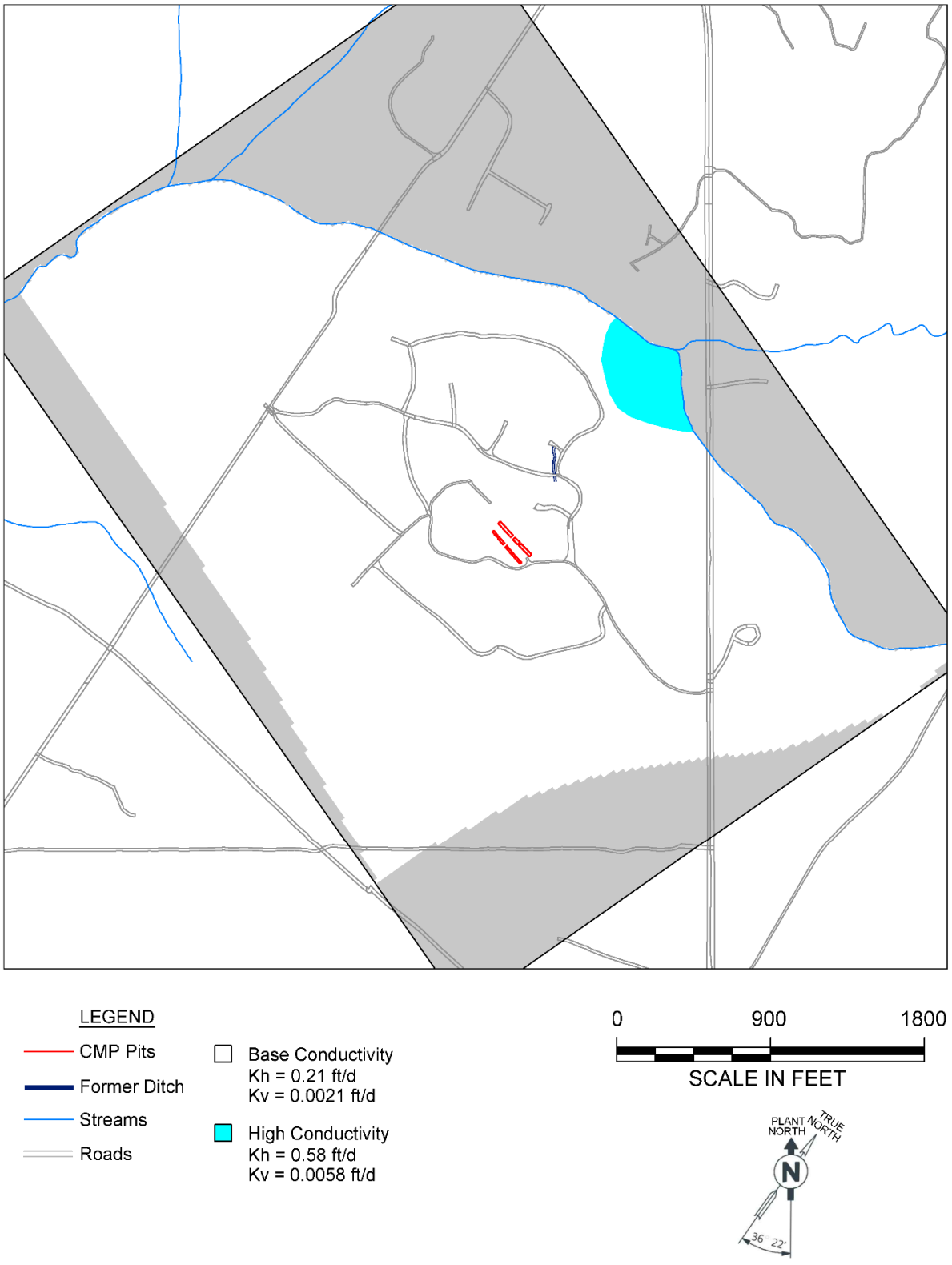

Figure 3.4 Hydraulic Conductivity Zonation of TCCZ

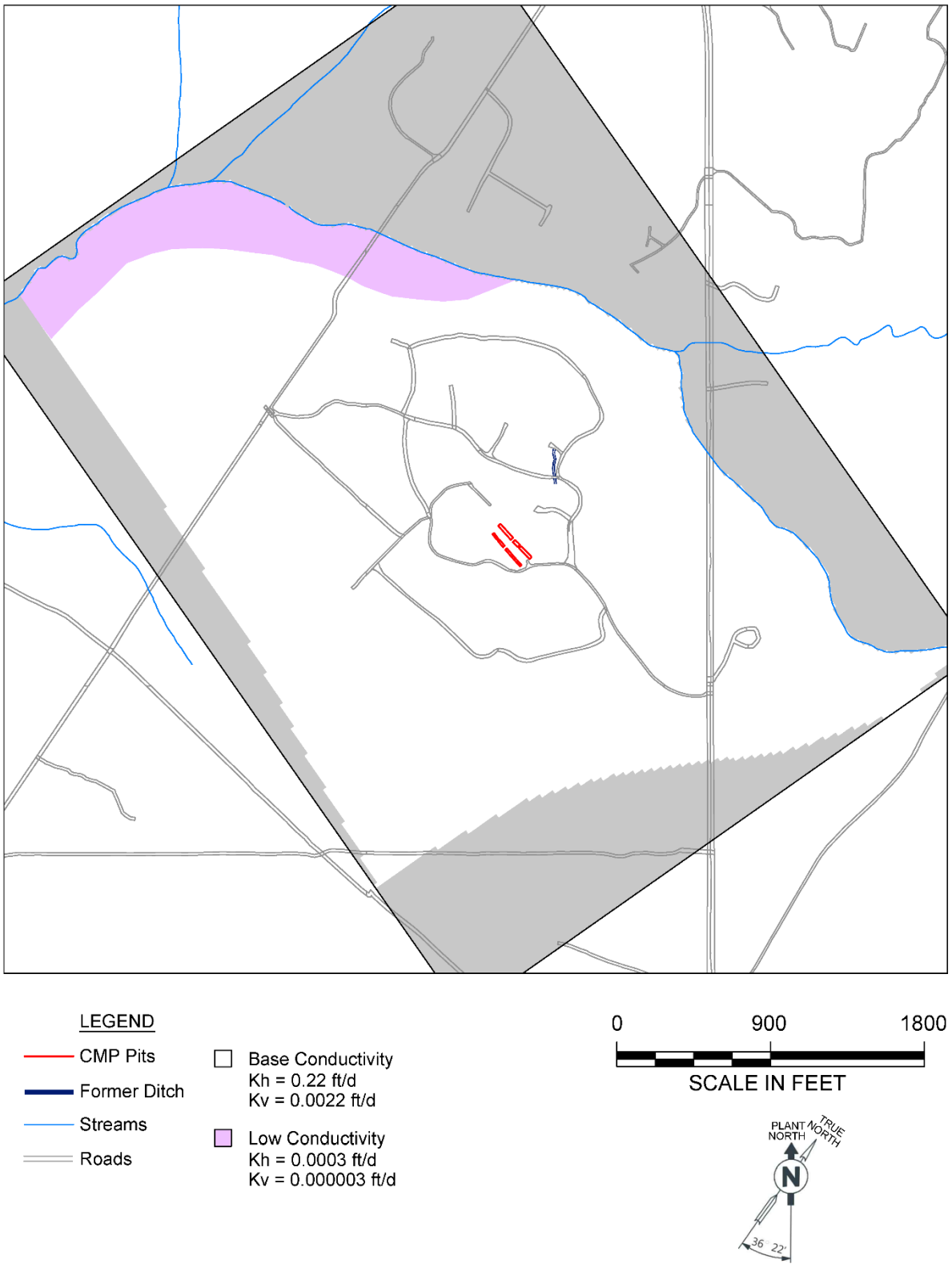

Figure 3.5 Hydraulic Conductivity Zonation of the TCLC

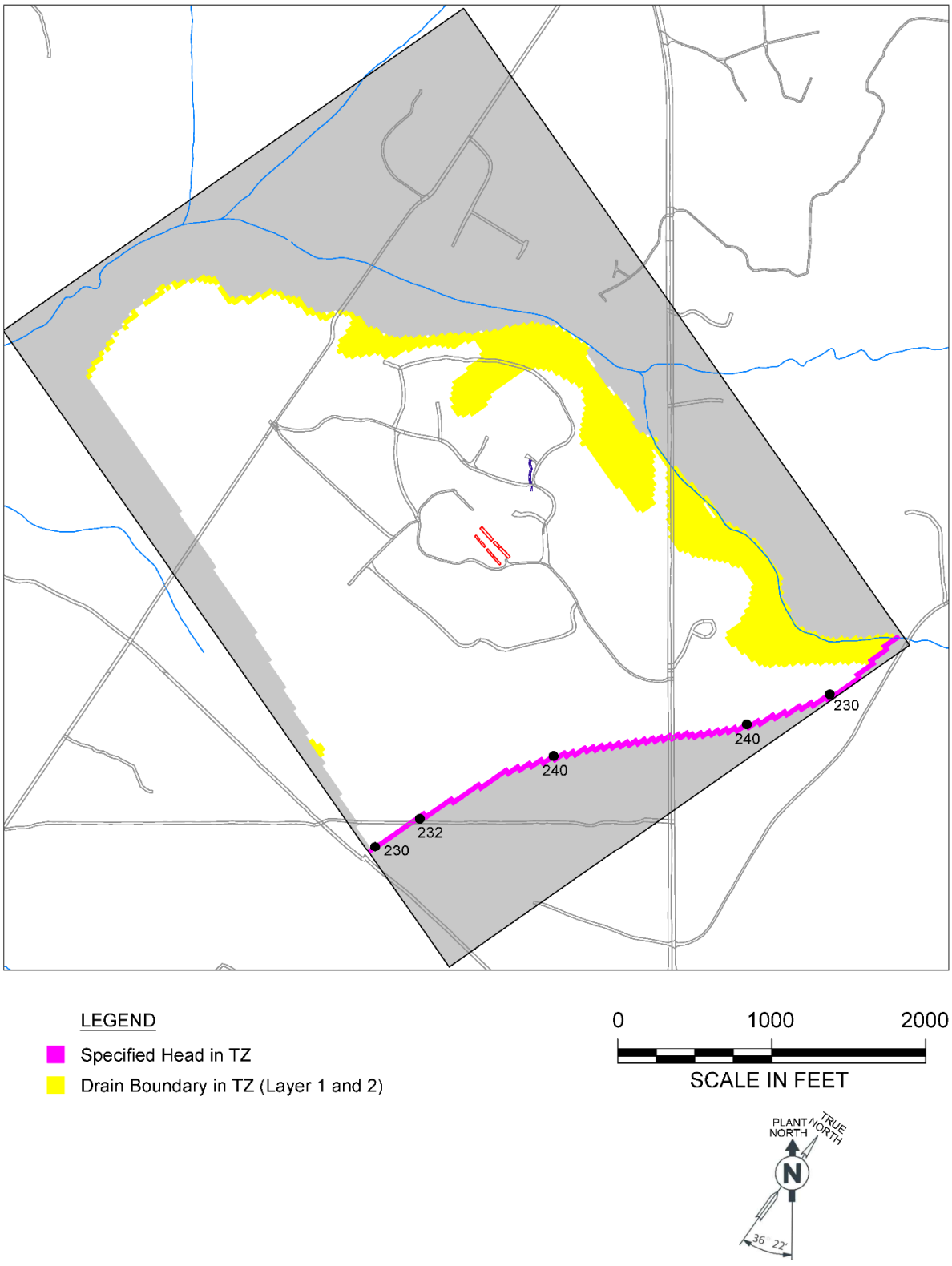

Figure 3.6 Model Boundary Conditions in TZ

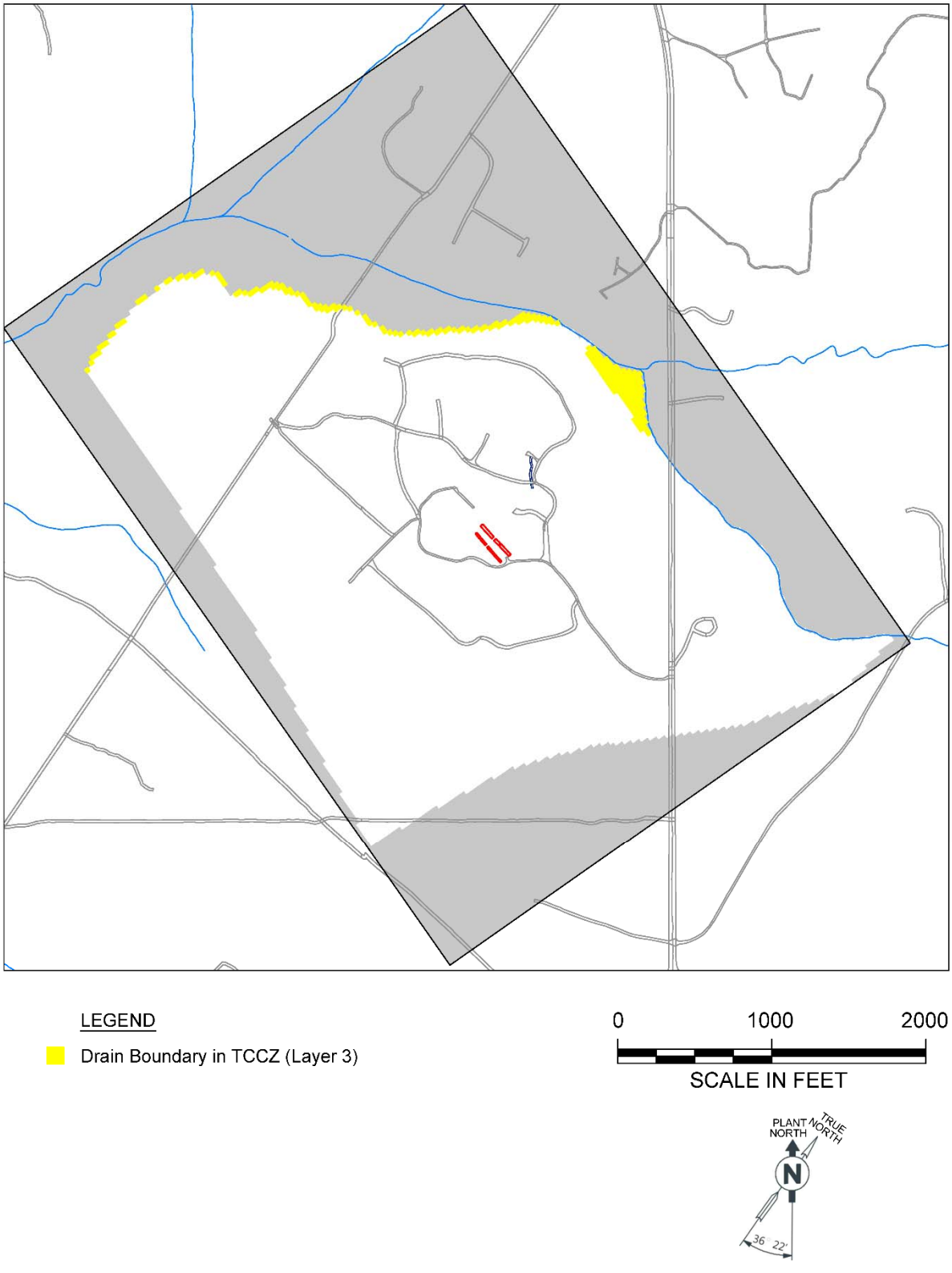

Figure 3.7 Model Boundary Conditions in TCCZ

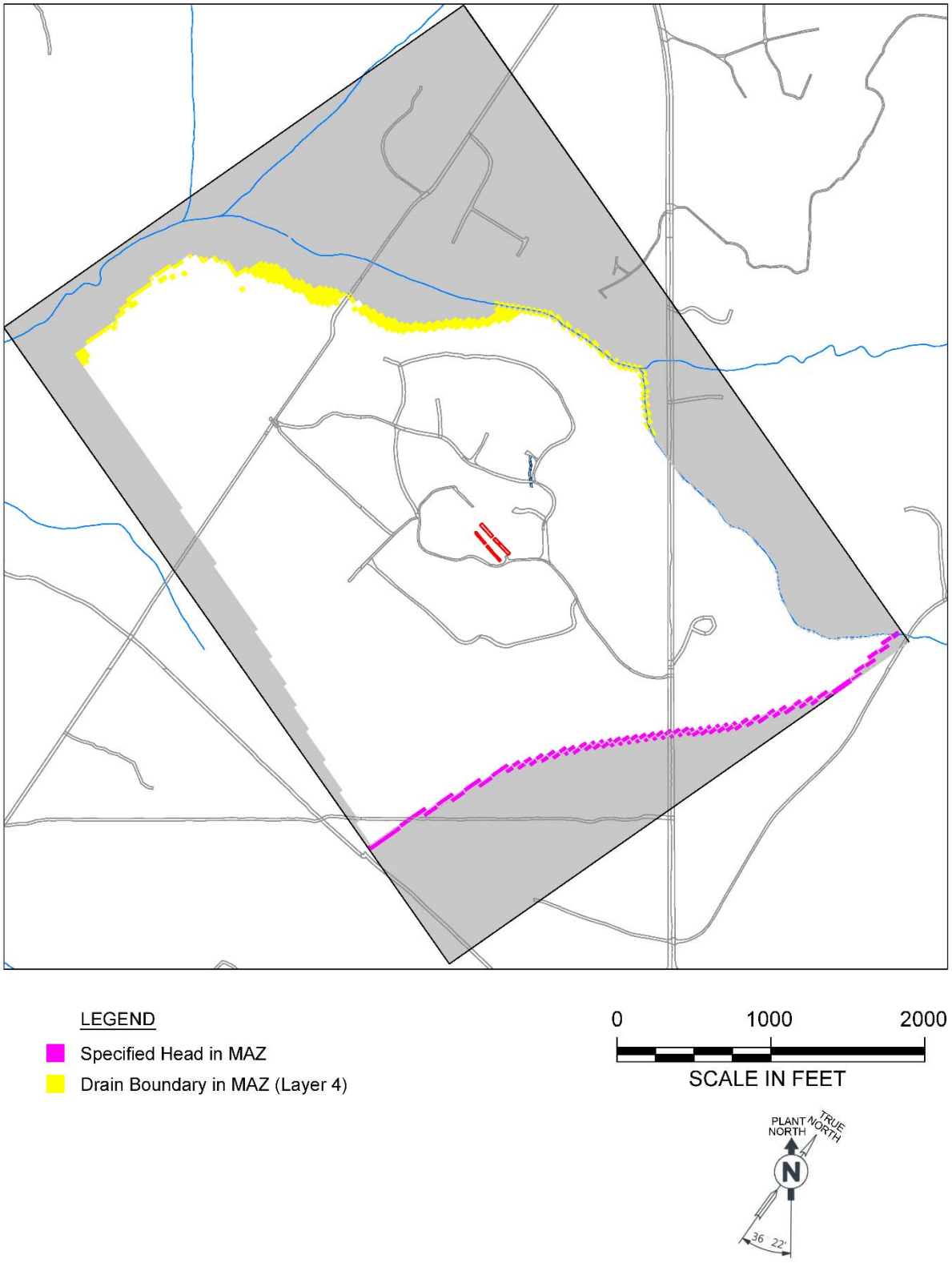

Figure 3.8 Model Boundary Conditions in MAZ

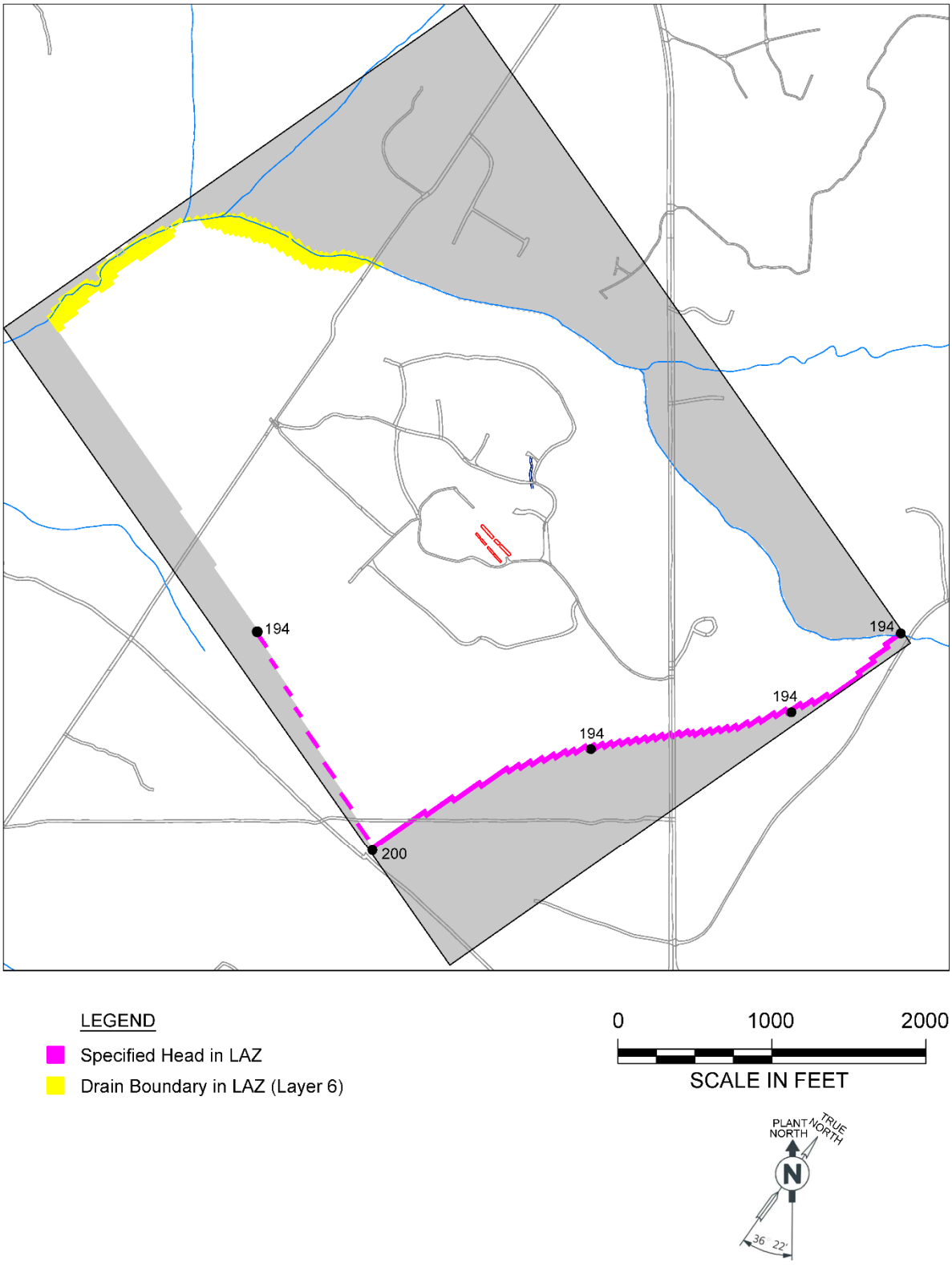

Figure 3.9 Model Boundary Conditions in LAZ

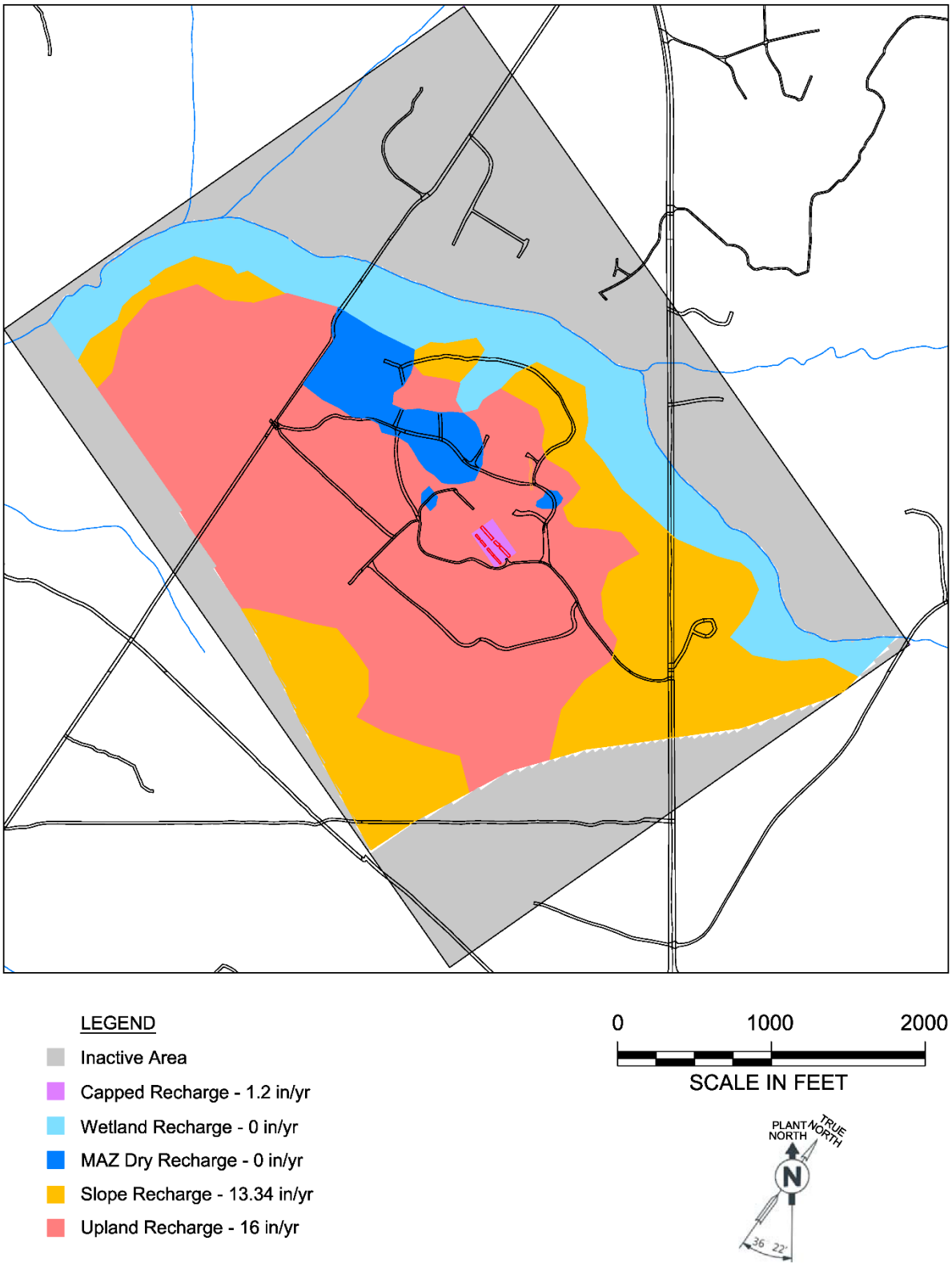

Figure 3.10 Areal Distribution of Recharge

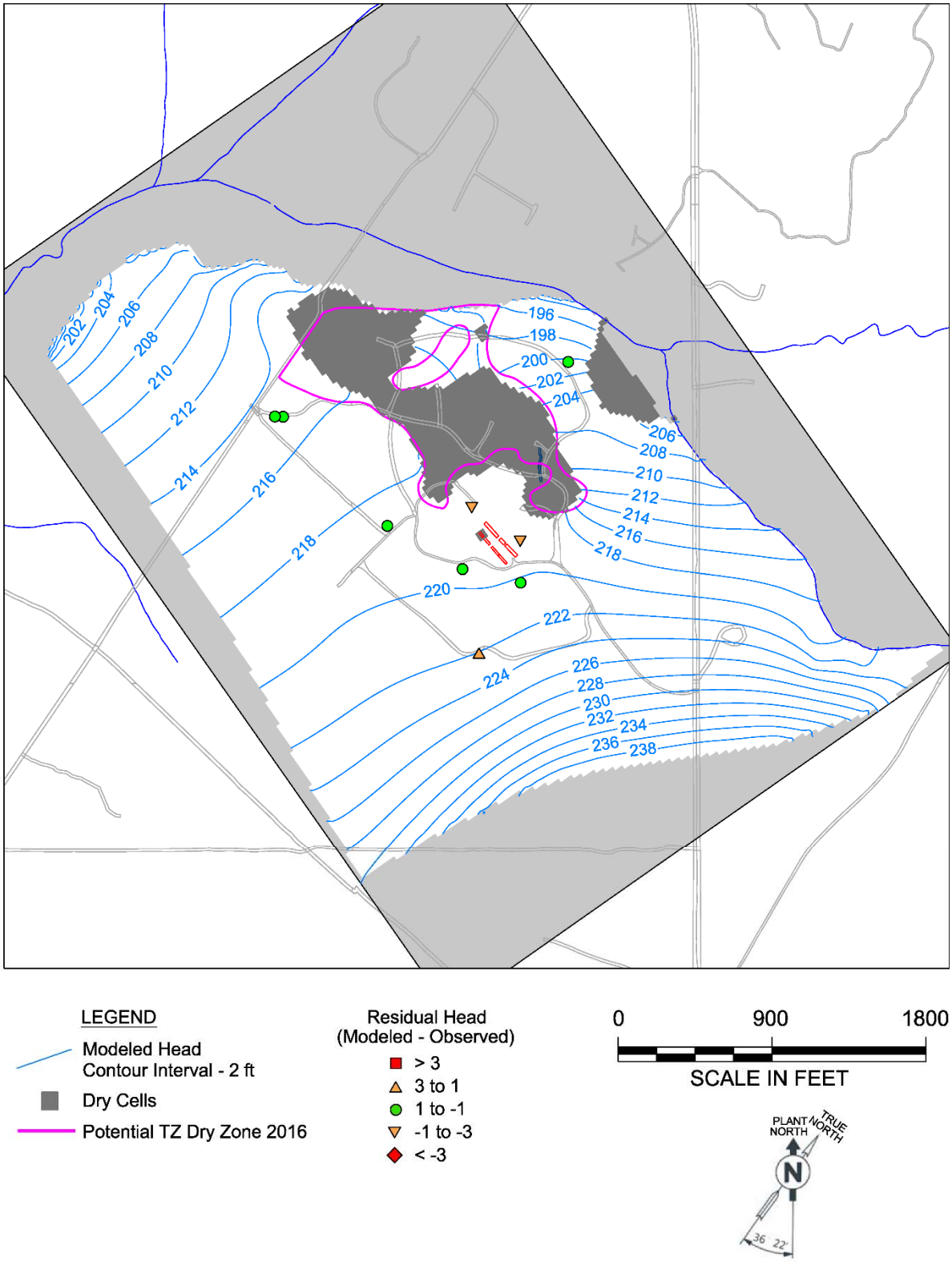

Figure 3.11 Model Head and the Head Residuals in the TZ

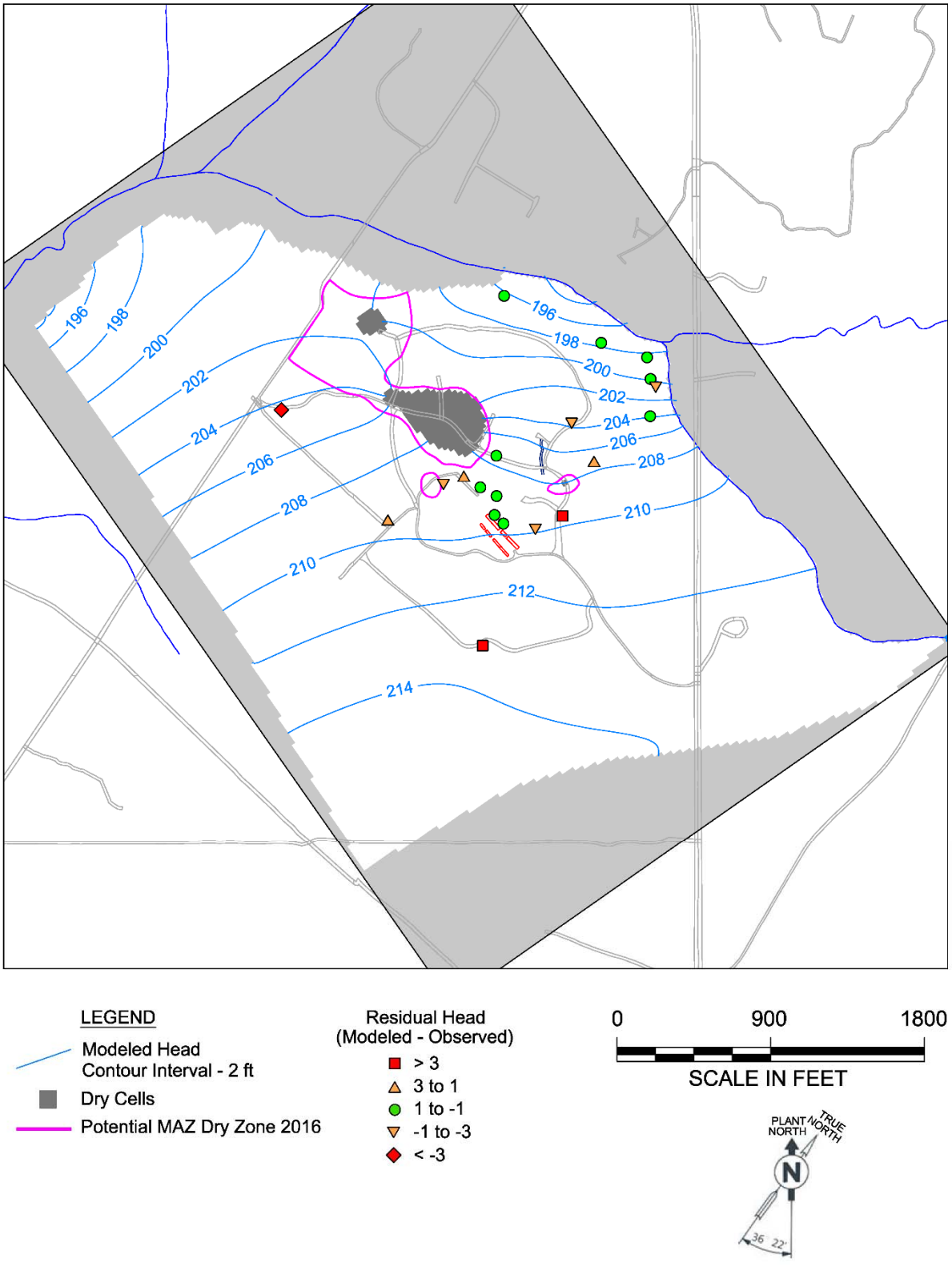

Figure 3.12 Model Head and the Head Residuals in the MAZ

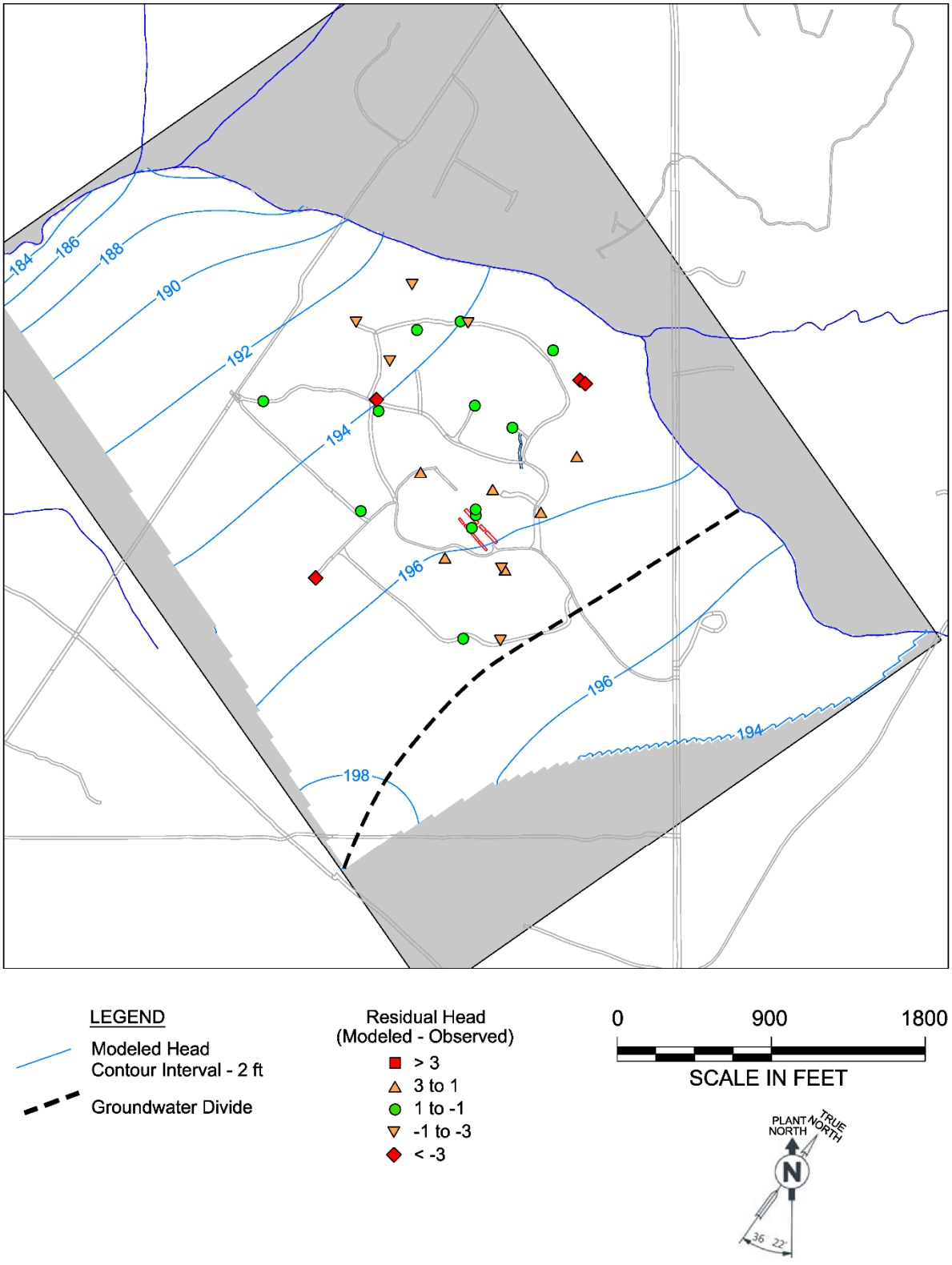

Figure 3.13 Model Head and the Head Residuals in the LAZ

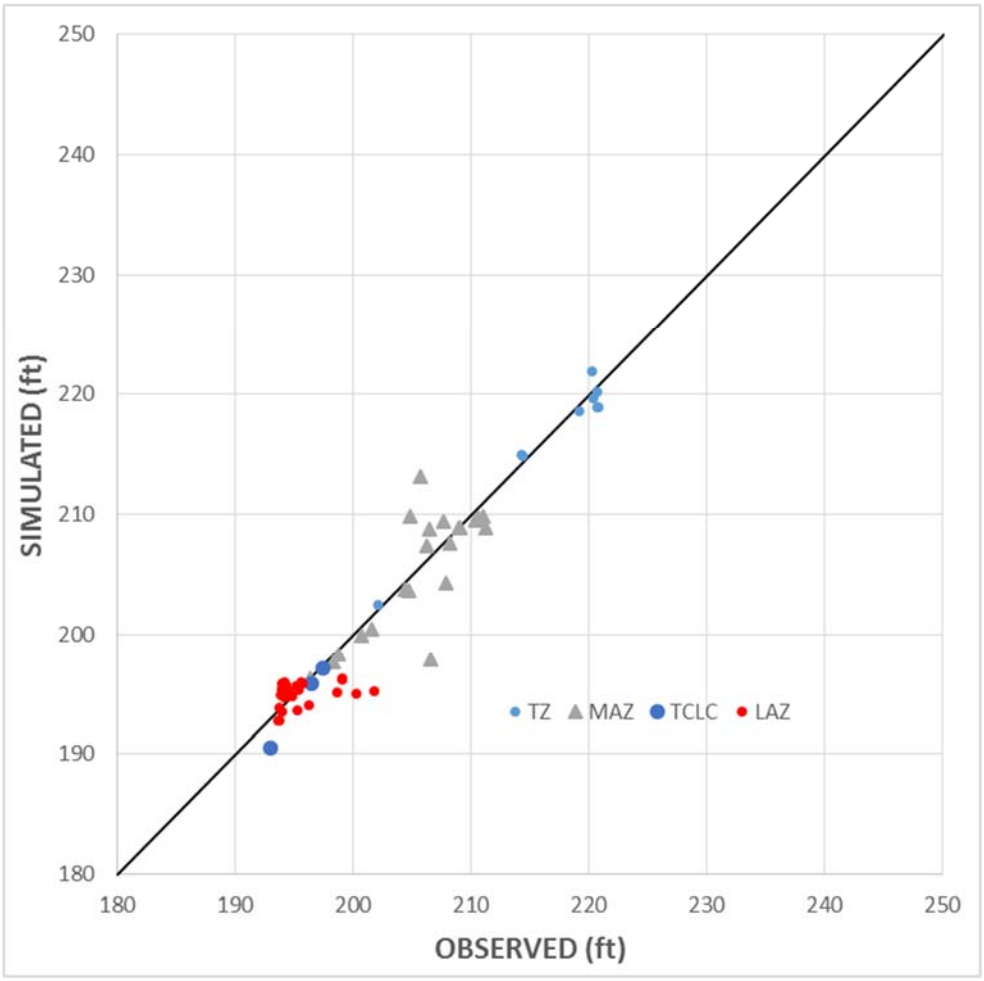

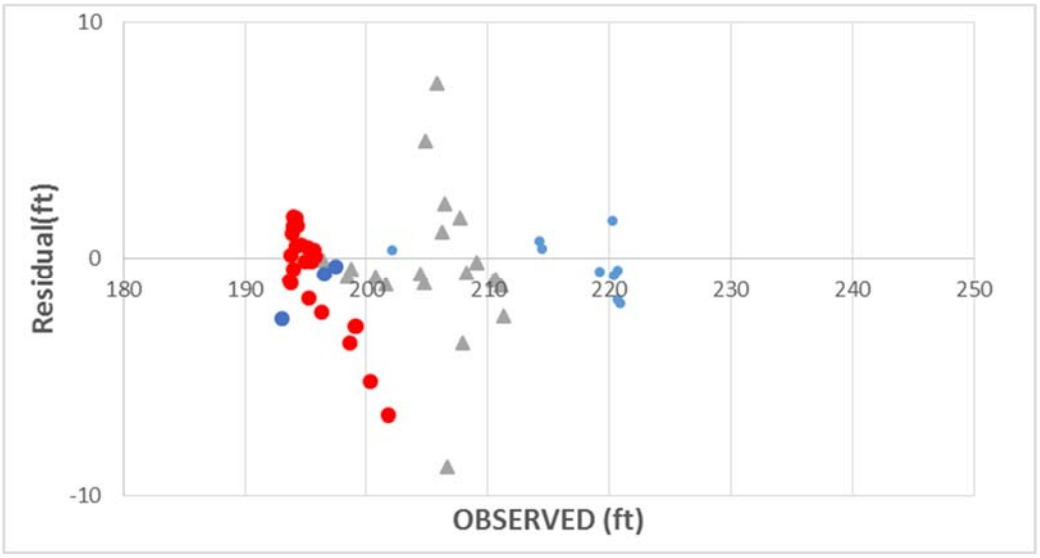

Figure 3.14 Comparison of Modeled Head and Head Residuals to Observed Head

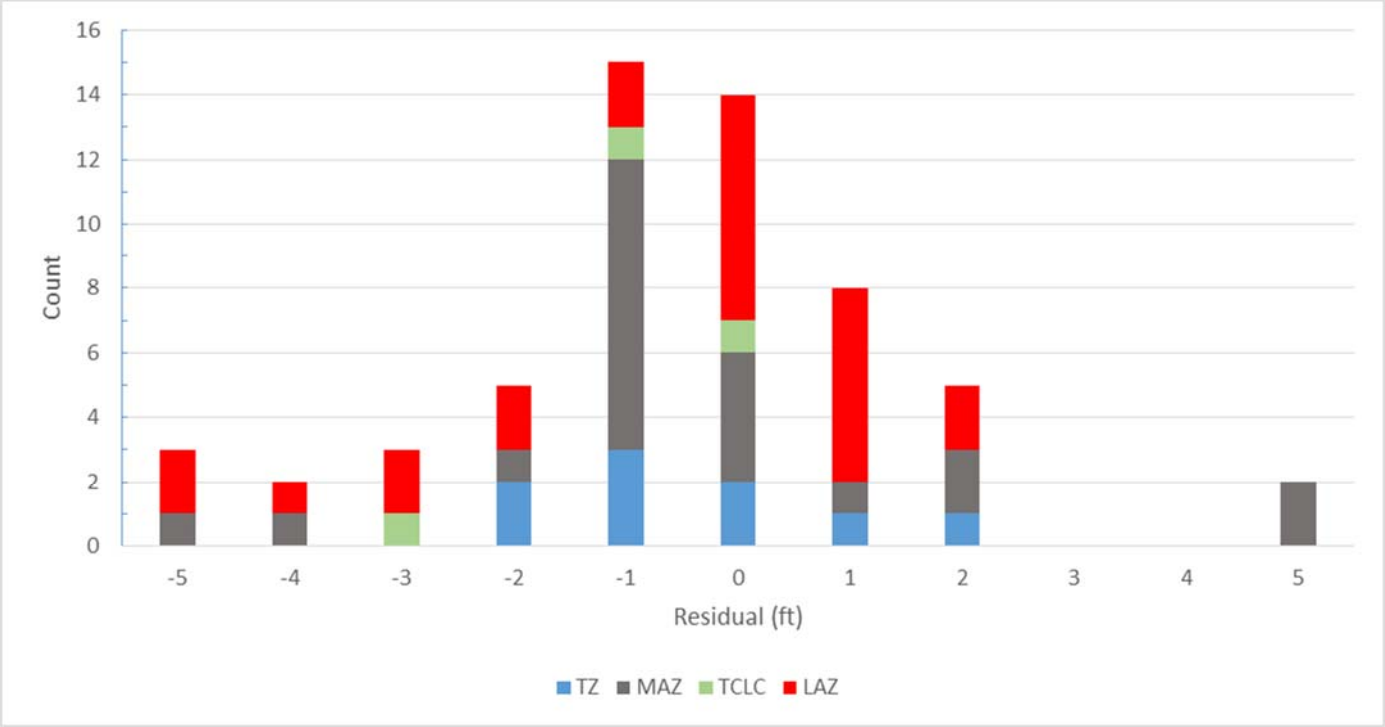

Figure 3.15 Histogram of Flow Model Residuals

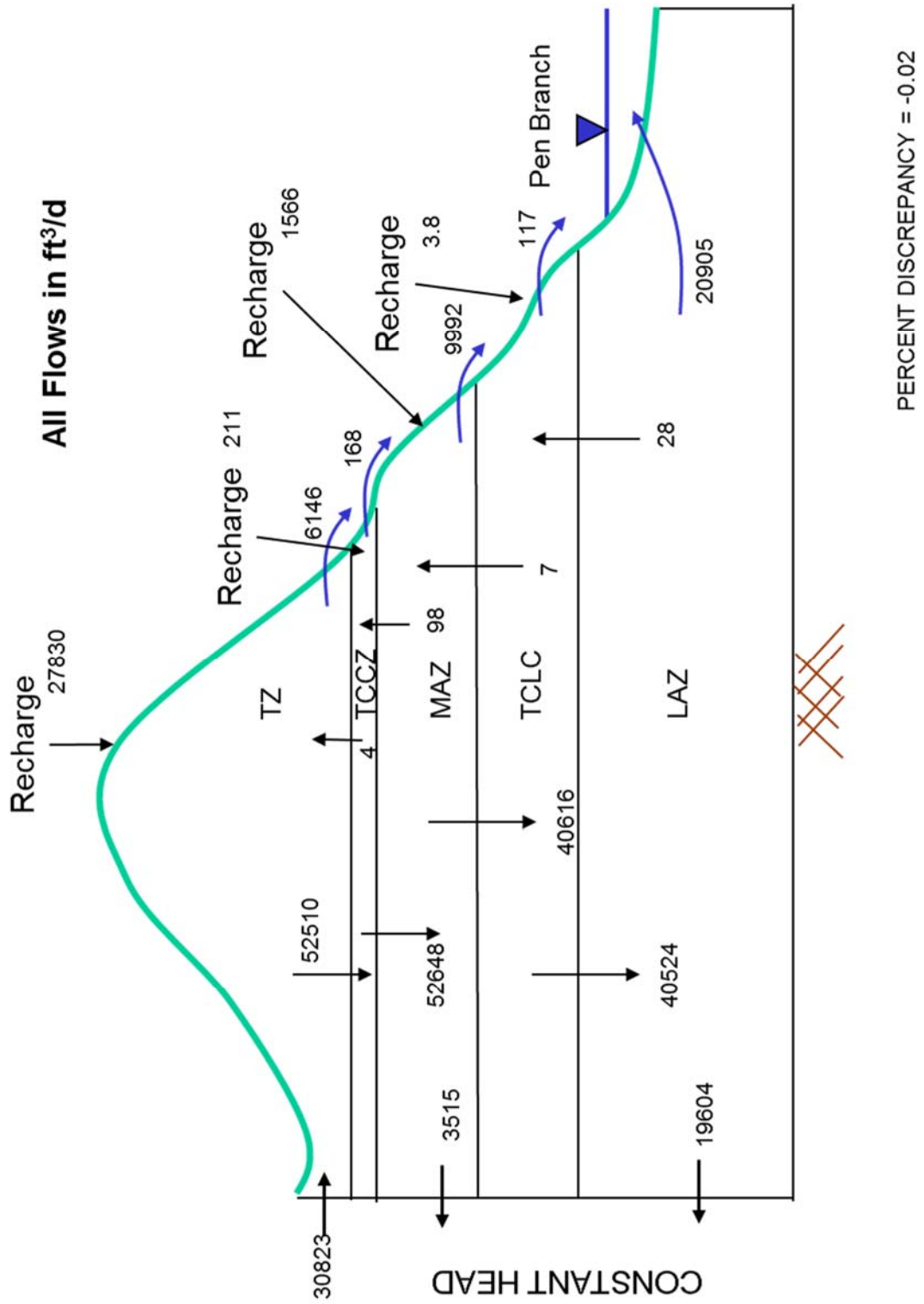

Figure 3.16 Calibrated Model Flow Budget

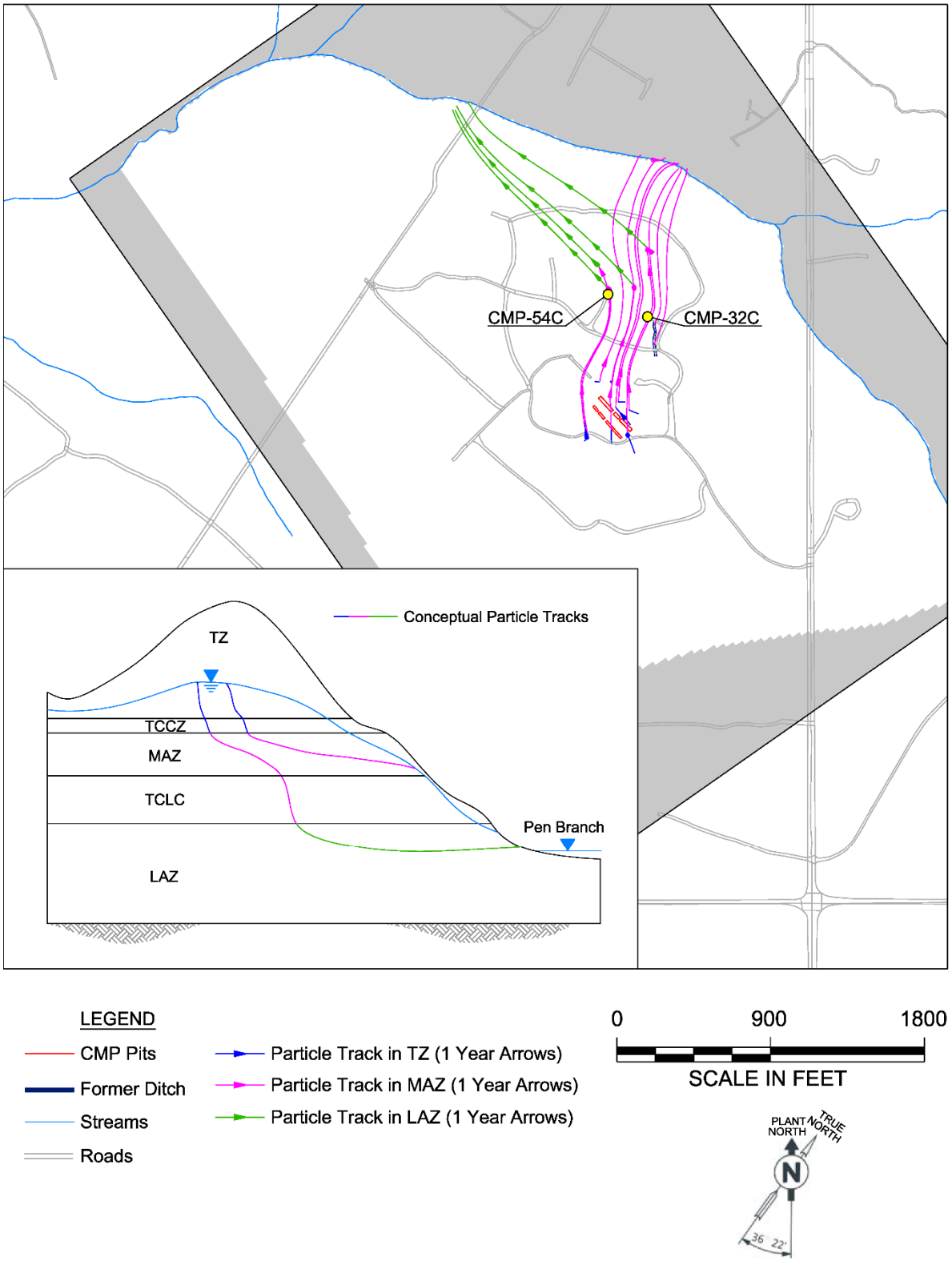

Figure 3.17 Particle Tracking from the CMP Pits

4.0 SOLUTE TRANSPORT MODEL CONSTRUCTION AND CALIBRATION

In this section, development of a numerical model for solute transport within the CMP Pits OU is documented. The numerical model is based on the HCM of Section 2 and on site-specific data provided by SRNS.

4.1 Numerical Methods

The transport of contaminants in groundwater is governed by the advection-dispersion-reaction equation, which can be written as follows:

$$\left(\theta + \rho_b K_d\right)\frac{\partial c}{\partial t} + \frac{\partial}{\partial x_i}\left(\theta v_i c\right) = \frac{\partial}{\partial x_i}\left(\theta D_{ij}\frac{\partial c}{\partial x_j}\right) - \lambda\left(\theta + \rho_b K_d\right)c + q_s c_s \qquad (2)$$

In this equation, the Cartesian coordinates are represented by x_i (i = 1, 2, 3), and the dependent variable is the contaminant concentration in groundwater, c. The velocity field (vi) is determined from the flow solution and Darcy's Law. The effective porosity is θ, and the porous medium bulk density is ρ_b. First order (exponential) decay is assumed at a rate of λ. Equilibrium, linear sorption is also assumed, with a sorption coefficient of K_d. Contaminant sources and sinks are represented by the source/sink groundwater flow rate per unit volume of the aquifer (q_s) and the source/sink concentration (c_s). The dispersion coefficient tensor, D_{ij}, is dependent on the groundwater velocity and specified length scales for dispersion, called dispersivities. Dispersivities are usually specified as longitudinal (along the direction of flow, α_L), horizontal-transverse (α_H), and vertical-transverse (α_V). The initial value of c must also be specified in order to solve equation 2.

MT3DMS (Zheng and Wang 1998) is a software program for solving equation 2 that uses the same finite-difference framework as MODFLOW, the groundwater flow simulator used in Section 3. Once the steady-state values of h are determined from MODFLOW, and the independent variables of equation 2 are specified, MT3DMS can be used to solve for contaminant concentration (c) as a function of space and time in the modeled domain. For the simulations presented in this report, the standard finite-difference (upstream weighting) solution method is used to simulate solute advection. While this method can lead to numerical error (sometimes called numerical or artificial

dispersion), it is inherently mass-conservative and typically free of spurious oscillations in the solution. Small grid-cell sizes (25 feet) are used in the model to minimize numerical error in the finite-difference solution. Also, the MT3DMS simulator automatically chooses model time steps that are small enough to limit numerical error.

4.2 Model Domain

Contaminant plumes generally travel northward from the source area toward and entering Pen Branch. Stage in Pen Branch is lower than groundwater levels on either side of the stream indicating that the stream (and surrounding wetlands) is the discharge point for groundwater. Further, the relative elevations of groundwater to surface water indicate that there is no underflow beneath Pen Branch. The model domain for solute transport is identical to the domain for groundwater flow.

4.3 Solute Transport Properties

Transport modeling also requires specification of values for effective porosity (θ), sorption coefficient (K_d) and dispersivity (α_L, α_H, and α_V) for every active cell in the model. The effective porosity (volume-fraction of connected pores in a soil medium) is a factor in determining groundwater velocity (v_i). The effective porosity is set to a typical value of 30% for this model. Dispersivity is a parameter that describes the degree of plume spreading, and is often determined by calibration to an existing plume. Dispersivity values depend on the scale of the plume and are typically higher in highly heterogeneous formations. As a practical rule of thumb, the longitudinal dispersivity (α_L) should be no greater than one-tenth of the problem length scale, the horizontal-transverse dispersivity (α_H) should be about one-tenth of α_L, and the vertical dispersivity (α_V) should be about one-hundredth of α_L. The CMP Pits TCE plume is approximately 700 ft long from the source to the estimated plume toe in the LAZ, meaning that acceptable values for longitudinal dispersivity are 70 ft or lower. However, prior studies at SRS (e.g., Fogle and Brewer 2001, GeoTrans 2001) suggest that the relatively homogeneous soils at SRS lead to plumes exhibiting much lower dispersivities. As in these prior studies, dispersivities are set to 5 ft (longitudinal), 0.5 ft (horizontal-transverse) and 0.05 ft (vertical-transverse). Dispersivity and porosity are treated as space-uniform constants for transport modeling.

The bulk density (ρ_b) and sorption coefficient (K_d) determine the degree to which the COIs (PCE, TCE, lindane and 1,4 dioxane) mass is adsorbed to solids in the porous medium (an equilibrium sorption is assumed). Greater adsorption effectively results in slower movement of the COIs. A bulk density of 1.48 kg/L (92.4 lb/ft^3 or 4.19e^7 mg/ft^3) was used throughout the model domain. Sorption is a function of the constituent organic-carbon partition coefficient (K_{oc}) and fractional organic content (F_{oc}) of the sediment.

$$K_d = F_{oc} K_{oc} \tag{2}$$

Organic-carbon partition coefficients (K_{oc}) for both TCE and PCE are 265 L/Kg (from Lester and Council 2008). As outlined in Shukla, et al. (2000) the K_{oc} of lindane is 1.10 m^3/Kg. According to EPA (2014), the K_{oc} of 1,4-dioxane is 16.98 L/Kg. The assumed organic carbon content in the solids (F_{oc}) by hydrostratigraphic unit is shown in Table 4.1, along with the calculated K_d values for TCE and PCE. K_d values for lindane are shown in Table 4.2, and 1,4-dioxane in Table 4.3.

The retardation factor (R) describes the adsorption process through the use of the contaminant specific sorption coefficient, the material specific bulk density and total porosity. R can also be defined as the ratio of the average groundwater velocity to the velocity of the contaminants. A retardation factor of 1.0 results in the contaminant moving along with the groundwater. A factor of 2.0 results in the contaminant moving at one-half the velocity of groundwater.

The equation for retardation factor is:

$$R = (1 + K_d (\rho_b / \theta)) \tag{3}$$

Where:

R = retardation factor

K_d = equilibrium sorption coefficient

ρ_b = bulk density

θ = total porosity (assumed to equal effective porosity)

Table 4.1 Fractional Organic Content by Hydrostratigraphic Unit for TCE and PCE

Layer	F_{oc} (%)	K_d (L/kg)	R	F_{oc} Source
Transmissive Zone	1.0	2.65	14.1	1
Tan Clay Confining Zone	1.2	3.18	16.7	2
Middle Aquifer Zone	0.3	0.80	4.9	3
Tan Clay Lower Clay	0.3	0.80	4.9	3
Lower Aquifer Zone	0.3	0.80	4.9	3

Source 1: Average total organic carbon content of the 27- to 30-ft-depth intervals of boreholes RAG001, RAG003, and RAG005 are from the *RCRA Facility Investigation/Remedial Investigation (RFI/RI) Report with Baseline Risk Assessment and Corrective Measures Study (CMS/FS) for the R-Area Operable Unit (U)* (SRNS 2009).

Source 2: Fraction of organic carbon (F_{oc}) value represents 2 times the average lignite percentage of the layer in six borings (P19TA, P20TA, P24TA, PPC1, GCB7LI, and LAW1TD) from P-, R-, and L-Areas. Total organic carbon is assumed to be 2 times the visible lignitic carbon.

Source 3: Default Savannah River Site value from *Sampling and Analysis of Fraction of Organic Carbon (foc) in Soil* (Ohio EPA 2003).

Table 4.2 Fractional Organic Content by Hydrostratigraphic Unit for Lindane

Layer	F_{oc} (%)	K_d (L/kg)	R	F_{oc} Source
Transmissive Zone	1.0	11	55.3	1
Tan Clay Confining Zone	1.2	13.2	66.1	2
Middle Aquifer Zone	0.3	3.3	17.3	3
Tan Clay Lower Clay	0.3	3.3	17.3	3
Lower Aquifer Zone	0.3	3.3	17.3	3

Table 4.3 Fractional Organic Content by Hydrostratigraphic Unit for 1,4-Dioxane

Layer	F_{oc} (%)	K_d (L/kg)	R	F_{oc} Source
Transmissive Zone	1.0	0.17	1.8	1
Tan Clay Confining Zone	1.2	0.2	2.0	2
Middle Aquifer Zone	0.3	0.05	1.3	3
Tan Clay Lower Clay	0.3	0.05	1.3	3
Lower Aquifer Zone	0.3	0.05	1.3	3

Biodegradation is modeled as a first order decay process that is characterized by a half-life. Half-lives for TCE and PCE are assumed to be 25 yrs (personal communication, Jeff Ross, SRNS, 2015), as was done in P-area (SRNS 2015); these are applied throughout the saturated zone in the CMP Pits model. Degradation in the vadose zone source is not modeled. Significant biodegradation is believed to be occurring in the Pen Branch wetland. The environment there is conducive to reductive dechlorination, and is similar to the Twin Lakes portion of C-Area, where degradation is known to be occurring. At Pen Branch, there are multiple lines of evidence that indicate that significant degradation is occurring. These include the very low concentrations of PCE and TCE in surface water, often below detection, along with the verified presence of cis-1,2-dichloroethylene, and collaborating contaminant data provided by SC State University (which is included in the CMP Pits Effectiveness Monitoring Reports). However, for this model, no credit is taken for degradation in the Pen Branch wetlands, beyond the 25-year half-life.

Shukla, et al. (2000) indicate that the half-life of lindane is on average 400 days and Adamson, et al. (2015) found the half-life of 1,4-dioxane to be 31 months. However, degradation depends on many site-specific factors; lindane and 1,4, dioxane are conservatively assumed to not degrade in the solute transport model.

4.4 Solute Sources and Other Transport Boundary Conditions

The nature of the CMP Pits source was described in Section 2.3. The source is simulated as a mass flux boundary condition (specified concentration of recharge) in the MT3DMS transport model. A summary of the sampling dates, depths and concentrations is shown in Table 4.4.

Table 4.4 Analytical Soil Results Summary

Analyte	Sampling Date Range	Sampling Depth Range (ft)	Results Range (µg/kg)
TCE	2001 - 2009	0 - 130	ND - 25,607
PCE	2001 - 2009	0 - 130	ND - 8,800,000
lindane	1999 – 2005	0 - 89	ND – 18,400
1,4-dioxane	2002	0 – 5	ND

ND – Not Detected

On average the water table at the CMP Pits Area occurs 90 feet below ground surface (bgs). After analyzing the soil data, it was determined that the soil concentrations closest to the water table were the most representative for input in a given stress period for the groundwater model; thus, the deepest result for each boring was selected for further processing. Thus, soil concentrations less than 60 feet deep were excluded since these COIs will not reach the water table before 2016.

For lindane, the range of concentrations at greater than 60 feet was ND to 115 µg/kg, with an average concentration of 0.94 µg/kg. Based on the very low average concentration, the vadose zone source contribution to groundwater for lindane was considered negligible and not included for input into the transport model. Because 1,4-dioxane had solely non-detect results from near ground surface, it also was not included as a source to the model. Thus, only TCE and PCE soil data were processed for input into the transport model.

The available soil data were solely for the CMP Pits Area. Thus, stress periods were determined based on remediation events at the CMP Pits as shown in Table 4.5.

Table 4.5 Duration of Transport Model Stress Periods

Stress Period	Time Range (yr)
1	1999 - 2002
2	2003 - 2008
3	2009 - 2016

The transport model requires water concentrations as input. By definition, the distribution coefficient K_d is:

$$K_d(L/kg) = \frac{\text{Soil Concentration } (\mu g/kg)}{\text{Water Concentration } (\mu g/L)} \quad (4)$$

Thus, to convert to a water concentration:

$$\text{Water Concentration } \left(\frac{\mu g}{L}\right) = \frac{\text{Soil Concentration } (\mu g/kg)}{K_d(L/kg)} \quad (5)$$

For both TCE and PCE, the deepest soil concentrations were converted to an equivalent water concentration. Values of K_d were determined from Riley et al. (2006). The K_d results listed in Table 3 of that report were averaged and used in Equation 5 to determine groundwater concentrations for TCE and PCE.

After the deepest soil concentrations were selected and converted to water concentrations, groundwater concentration contours were developed. The area between two contours was given the value of the lesser contour, e.g., the area between 1 µg/kg and 100 µg/kg was given a value of 1 µg/kg. These areas were used to assign concentration values in each model cell in the transport model.

The deepest soil concentration data, typically near 88 feet bgs, was rarely the maximum concentration. The maximum soil concentrations were typically around 68 feet bgs, at the approximate location of an observed low-permeability unit. Based on historical groundwater monitoring data showing stable concentrations of TCE and PCE, it was assumed that unless soil samples showed a decrease in concentration, the concentration from the previous stress period should be applied, as shown in Figures 4.1 and 4.2.

In addition, groundwater data indicated soil sources to the southeast of the CMP Pits, where no soil data was available. It was assumed the maximum groundwater concentration for each stress period was the best representation of soil contributions to groundwater concentrations. Thus,

groundwater data for the shallow wells CMP-10D and CMP11D was used to determine a contour around each well for input into the transport model.

Figure 4.3 shows the calculated mass input (kg/yr) to the water table for PCE and TCE, respectively. Groundwater flow sinks (discharge-area streams) are also contaminant sinks, since the water being removed through the groundwater flow sinks may contain a concentration of the contaminant mass (i.e. have non-zero concentration). Pen Branch, the unnamed tributary, and associated discharge wetlands are the main contaminant sinks in the model.

4.5 Initial Conditions

The initial 2002 plumes were created by mapping the highest sampled groundwater concentration between January 2000 and April 2002 and inferring the plume pattern using information on groundwater flow direction, and hydrostratigraphy. Concentration data taken from CPT samples between 1998 and April 2002 were also used to develop the initial plumes. The plumes were generated for each hydrostratigraphic layer (TZ, TCCZ, MAZ, TCLC, and LAZ) for each COI. The LAZ plume was placed only in the top two LAZ layers (layers 6 and 7 representing the upper one-fourth of the LAZ), where LAZ contamination has been observed. Figure 4.4 and 4.5 show the initial plumes for PCE and TCE. Note that specification of contamination in the confining beds (TCCZ, TCLC) results in creating areas where transport is much slower than in the aquifers. Contamination specified in the confining beds may appear as continuing sources in long-term simulations.

No attempt has been made to simulate the source(s) that led to the 2002 plume configuration. Such an exercise would be impractical due to large uncertainties in past conditions. Because the initial concentrations come from one source (inferred from concentration measurements) and the continuing source input comes from another source (the computation described above), there may be some inconsistency in predictions between early-time conditions (in the next several years) and later-time conditions. Early plume behavior will be governed in large part by the initial conditions. After the initial plume discharges to Pen Branch, the continuing vadose-zone source may influence plume behavior, depending on its strength relative to mass in place.

4.6 Solute Transport Model Calibration

The process of calibrating the groundwater flow model was described in Section 3.3. The solute transport model was also calibrated for the time period 2002 until 2016, using the hydraulic parameters obtained from the groundwater flow model calibration. Calibration of the solute transport model initially involved adjusting input/source boundary conditions to match transient plume behavior from 2002 to 2016. It became apparent early in the solute transport calibration that it would be necessary to alter the hydrologic conceptual model and to recalibrate hydraulic parameters from the groundwater flow model in order to match the 2016 plume configuration.

Challenging aspects of the solute transport calibration included the presence of contamination in wells CMP10, upgradient of the CMPP source, and CMP11, side-gradient to the CMPP source. It was postulated that contamination in these locations may be the result of non-vertical vadose transport of DNAPL or DNAPL-like constituents. This concept is illustrated in Figure 4.6. Contamination traverses vertically until it encounters low-permeability layers that cause water to be perched or DNAPL to pool, followed by lateral flow along the dip of the low permeability layer, lens, or bedding plane. Note that saturated stratigraphic layers in this area dip to the south, suggesting that localized low permeability layers may also dip to the south, resulting in DNAPL flow to the south. The relatively short distance of CMP10 (150 feet) and CMP11 (275 feet) from the pit area, relative to the 90 foot vadose zone transit, support the plausibility of this conceptual model.

A second challenging aspect of the solute transport calibration was the presence of contamination at the confluence of an unnamed tributary and Pen Branch, in the northeastern part of the model domain. Particularly confounding was the relatively high concentration (617 ug/L PCE or 286 ug/L TCE) that was measured in a new well, CMP064BU in the LAZ. Inspection of potentiometric maps showing desaturated or "dry" areas suggest that these areas can influence lateral flow directions, especially in the highly conductive TZ and MAZ. Figure 4.7 shows a conceptual model wherein flow directions in the TZ are diverted around the desaturated area, taking a more circuitous route to the east and ultimately discharging into Pen Branch further upgradient on the stream than if the TZ had been fully saturated. This conceptual model explains

the presence of contamination near the unnamed tributary and Pen Branch, particularly when it is considered that the areas of desaturation are not static, as indicated in Figure 4.7, but rather expand and contract over time with changes in climate and water level. Note that the flow field in the groundwater model is assumed to be steady state, that is, not changing with time. This assumption has bearing on the trajectory and spreading of contamination because the areas of desaturation also do not change with time. Thus, the situation shown in Figure 4.7 occurs occasionally, but may not be represented in the model's steady state condition.

A reasonable calibration to both water levels and contaminant concentrations was obtained once these challenging aspects were addressed. The groundwater flow model calibration was documented in Section 3.3; a description of the solute transport model results are presented below. Figures 4.8, 4.9, and 4.10 compare the modeled and interpreted PCE plumes in the TZ, MAZ, and LAZ for 2016 conditions. Figure 4.11 shows a PCE concentration profile along cross-section A-A' shown in Figure 2.11. Similar plots are shown for TCE (Figures 4.12, 4.13, 4.14, and 4.15).

Figure 4.16 shows modeled and observed PCE concentration versus time for the eight wells shown in Figure 2.12. Similar graphs are shown for TCE in Figure 4.17. Note that the model captures the general trends of solute transport over the past 14 years in the CMPP OU: predominantly decreasing concentrations in the MAZ and increasing in the LAZ; decreases in the source area due to the remediation.

Modeled vs observed concentrations at monitoring wells for 2016 are shown for PCE in Figure 4.18 and TCE in Figure 4.19. Note that the plotted time interval is the most challenging to match because by 2016 the simulation has progressed 14 years. The general trend of the plume configuration and movement is represented by the model, despite the scatter of points in these figures. Note that the model generally over-predicts concentrations on the lower end of the concentration scale <10 ug/L), particularly for PCE.

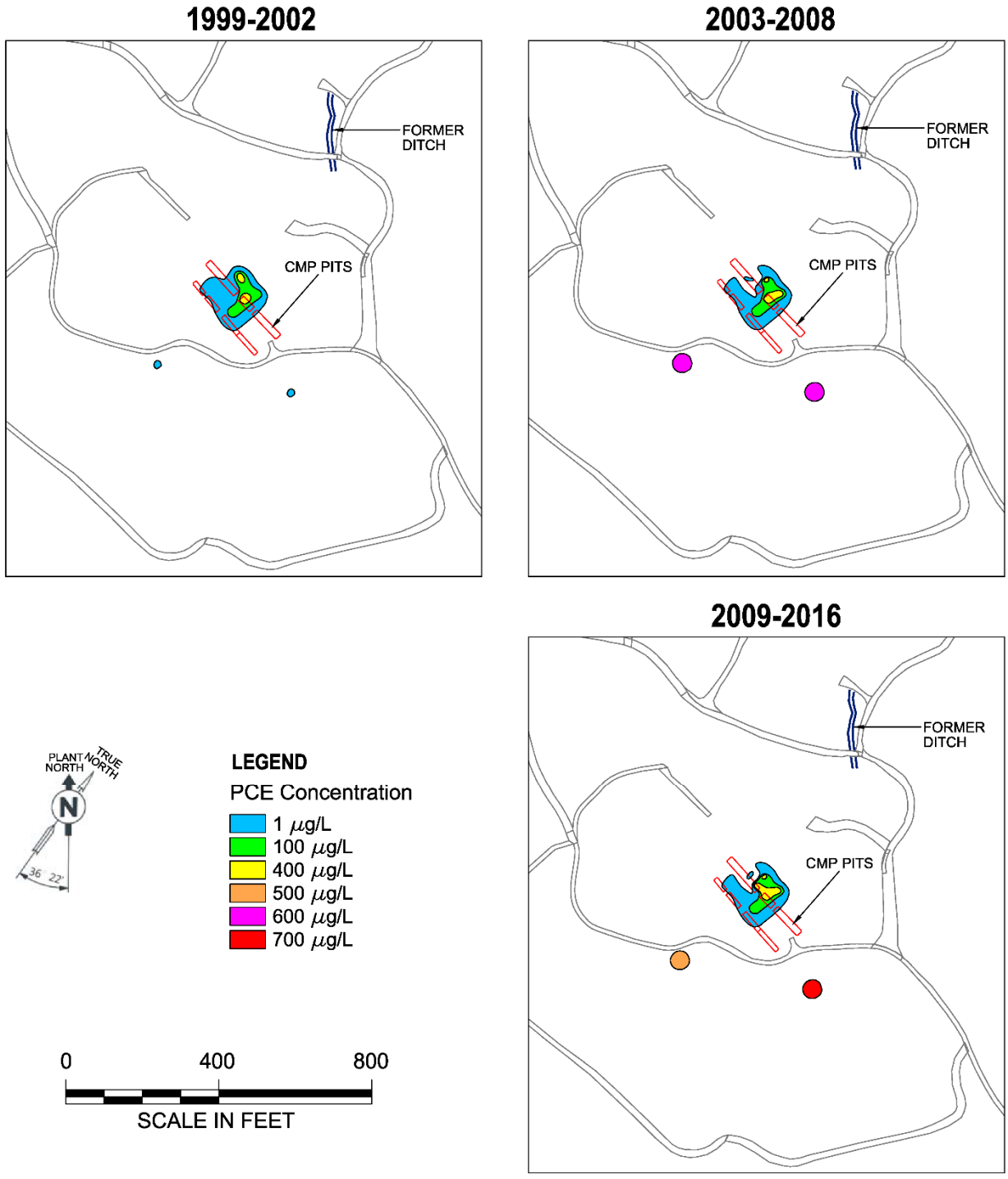

Figure 4.1 Source Concentrations for PCE for Stress Periods 1, 2, and 3 of the Calibration, Corresponding to Years 1999-2002, 2003-2008 and 2009-2016, Respectively

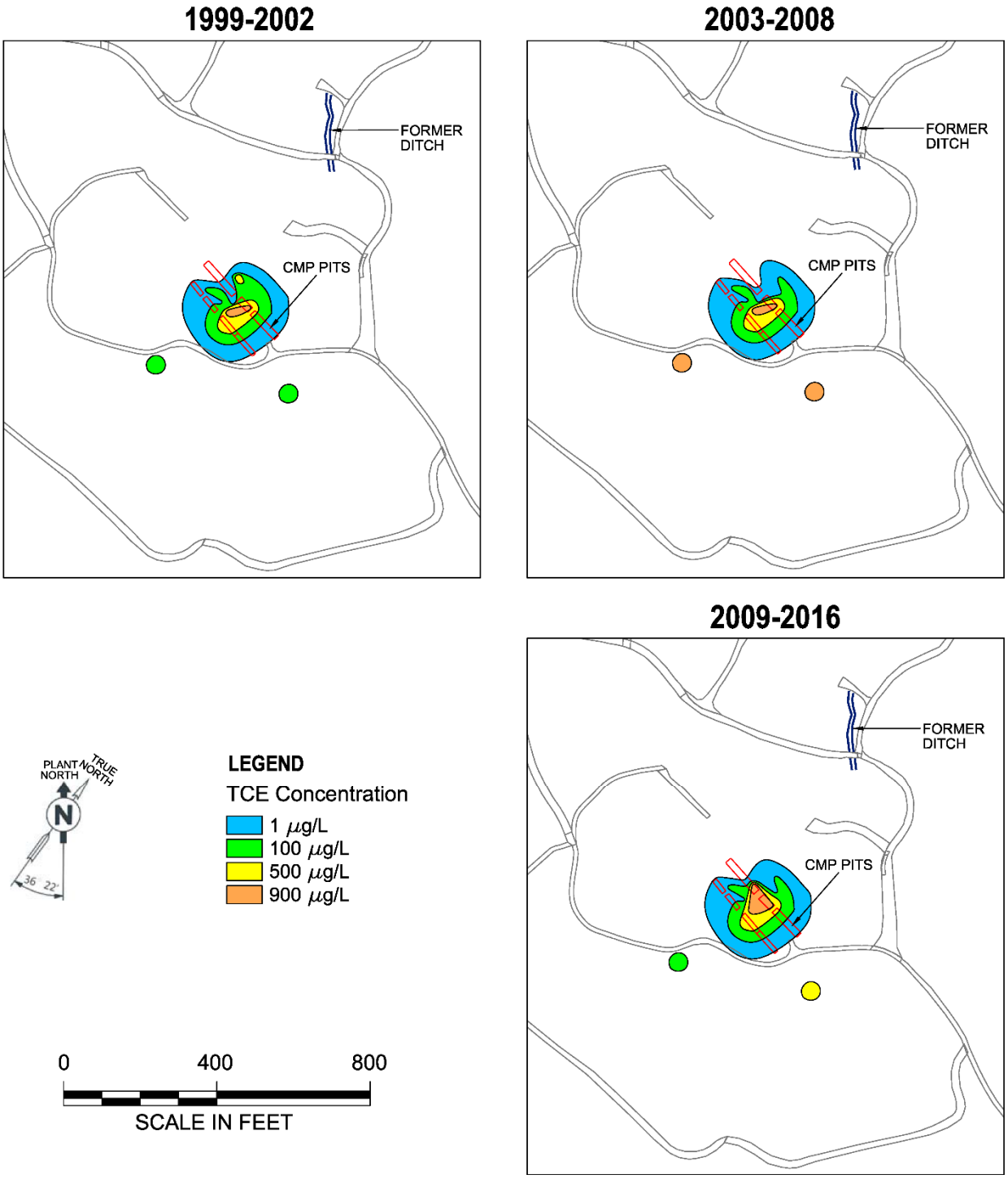

Figure 4.2 Source Concentrations for TCE for Stress Periods 1, 2, and 3 of the Calibration, Corresponding to Years 1999-2002, 2003-2008 and 2009-2016, Respectively

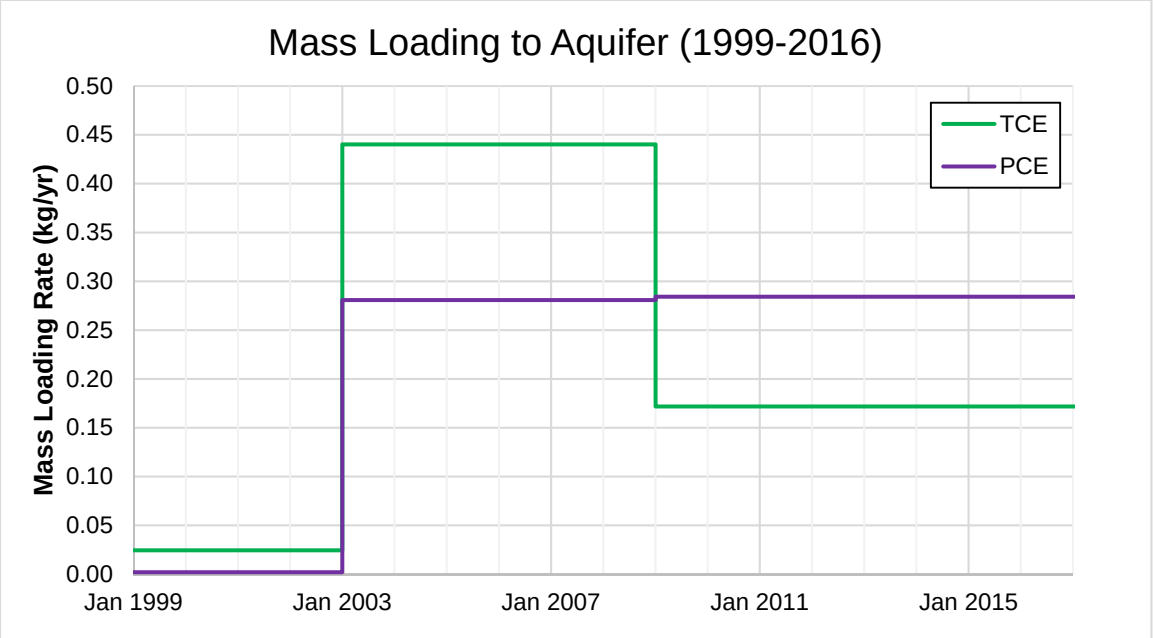

Figure 4.3 Calculated Mass Input (kg/yr) to the Water Table for PCE and TCE for the Calibration Period.

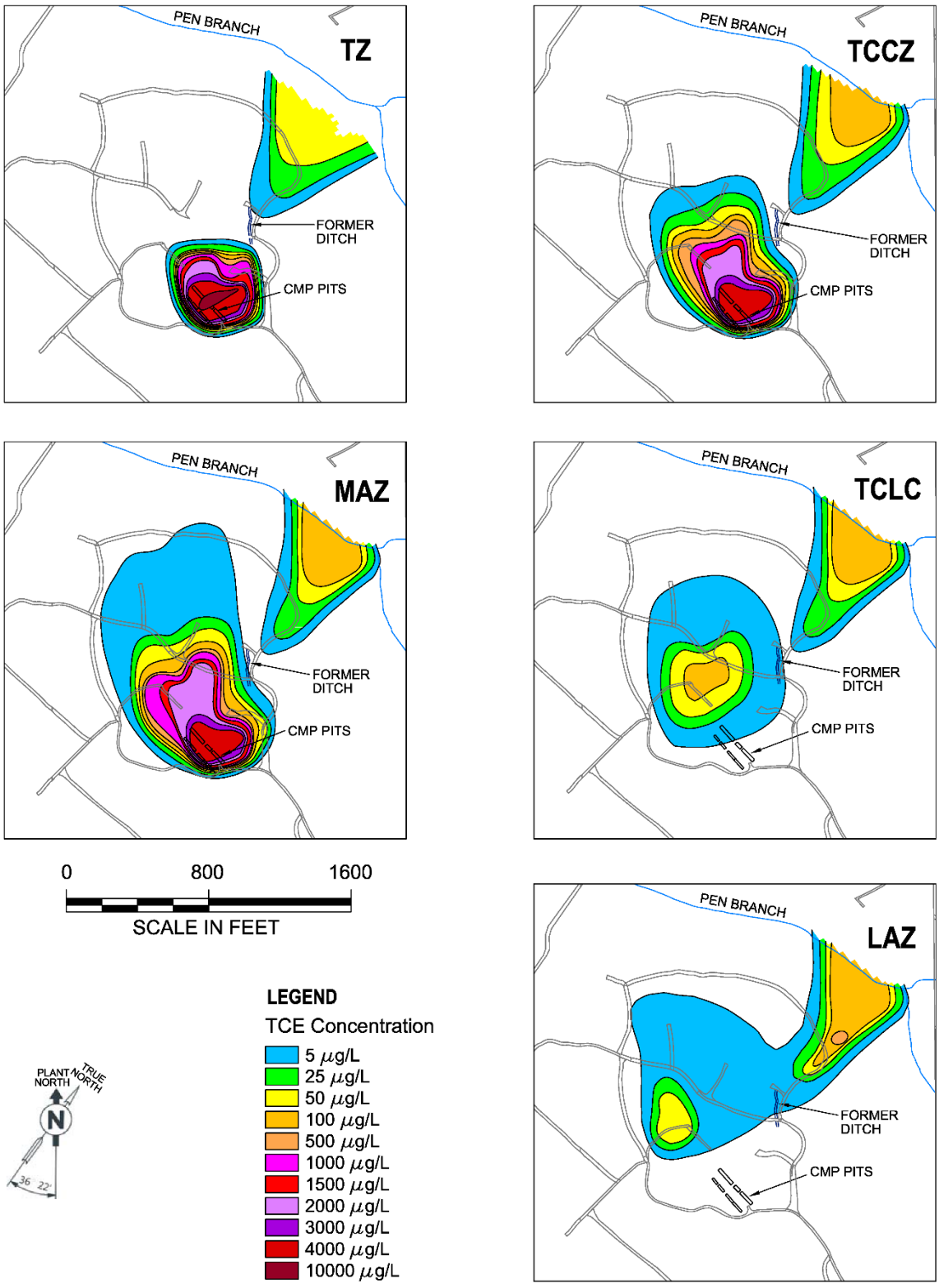

Figure 4.4 Initial Plumes (2002) for PCE for the a) TZ, b) TCCZ, c) MAZ, d) TCLC, and e) LAZ

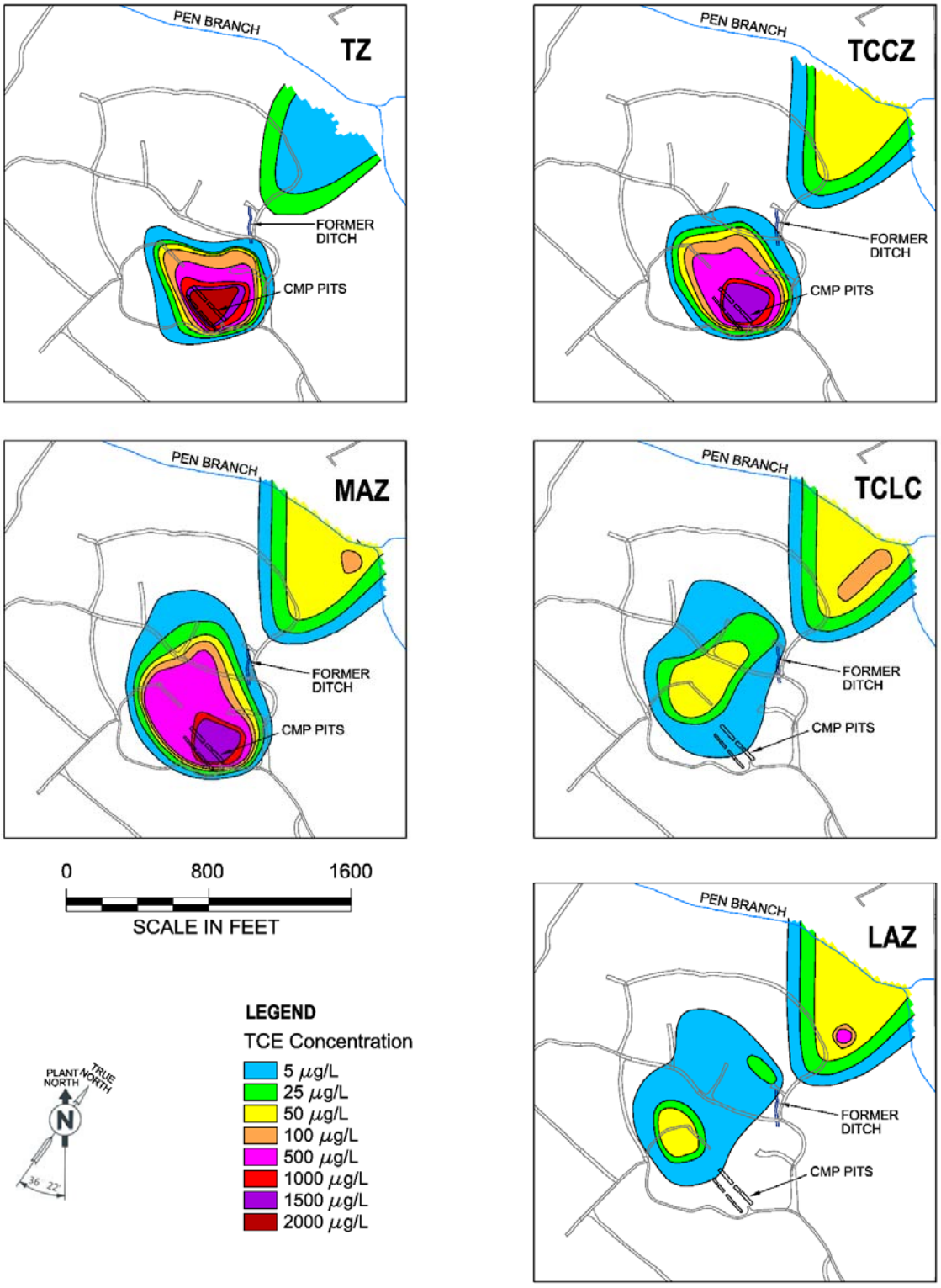

Figure 4.5 Initial Plumes (2002) for TCE for the a) TZ, b) TCCZ, c) MAZ, d) TCLC, and e) LAZ

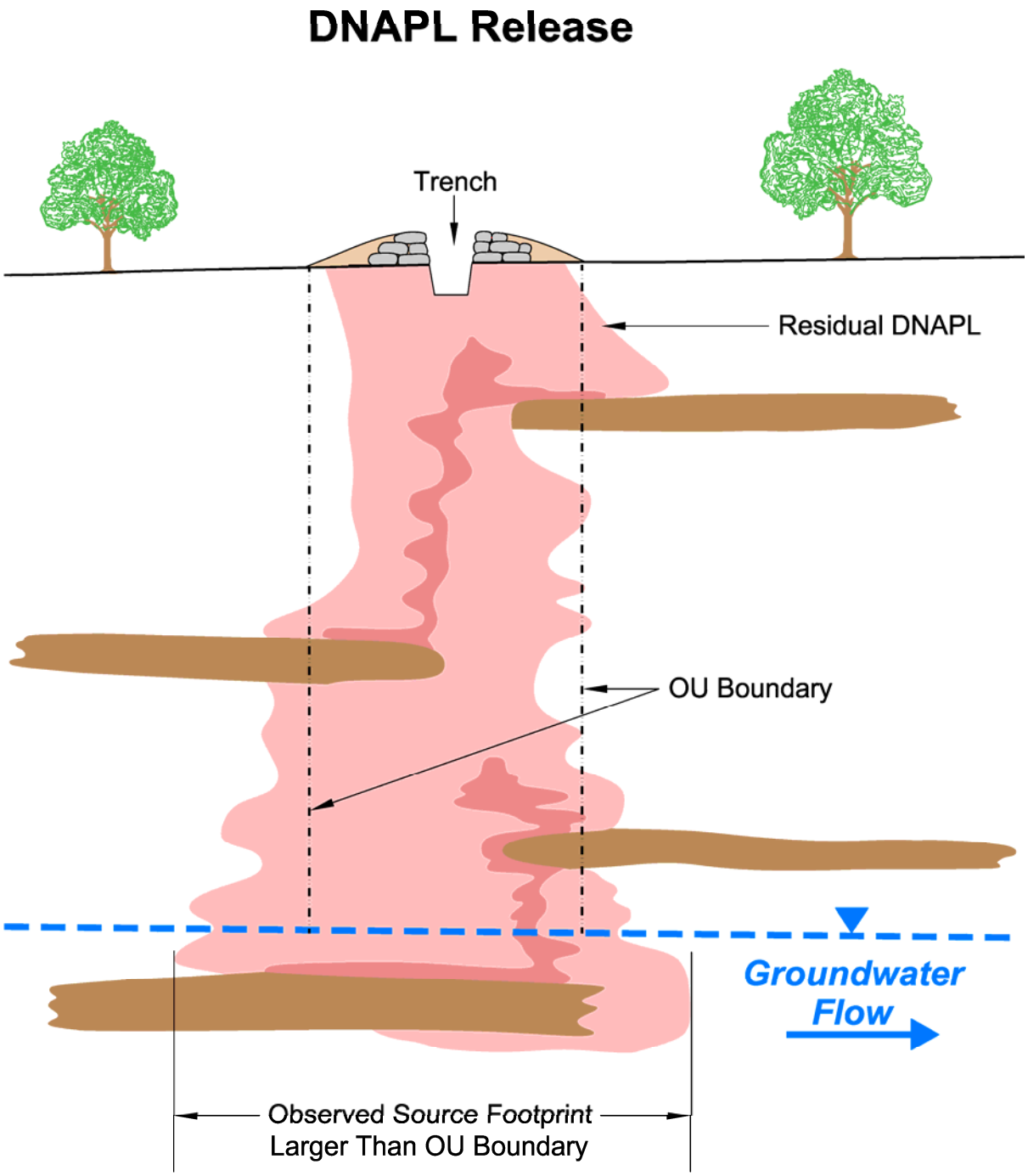

Figure 4.6 Conceptual Model for Presence of Contamination at Wells CMP10 and CMP11

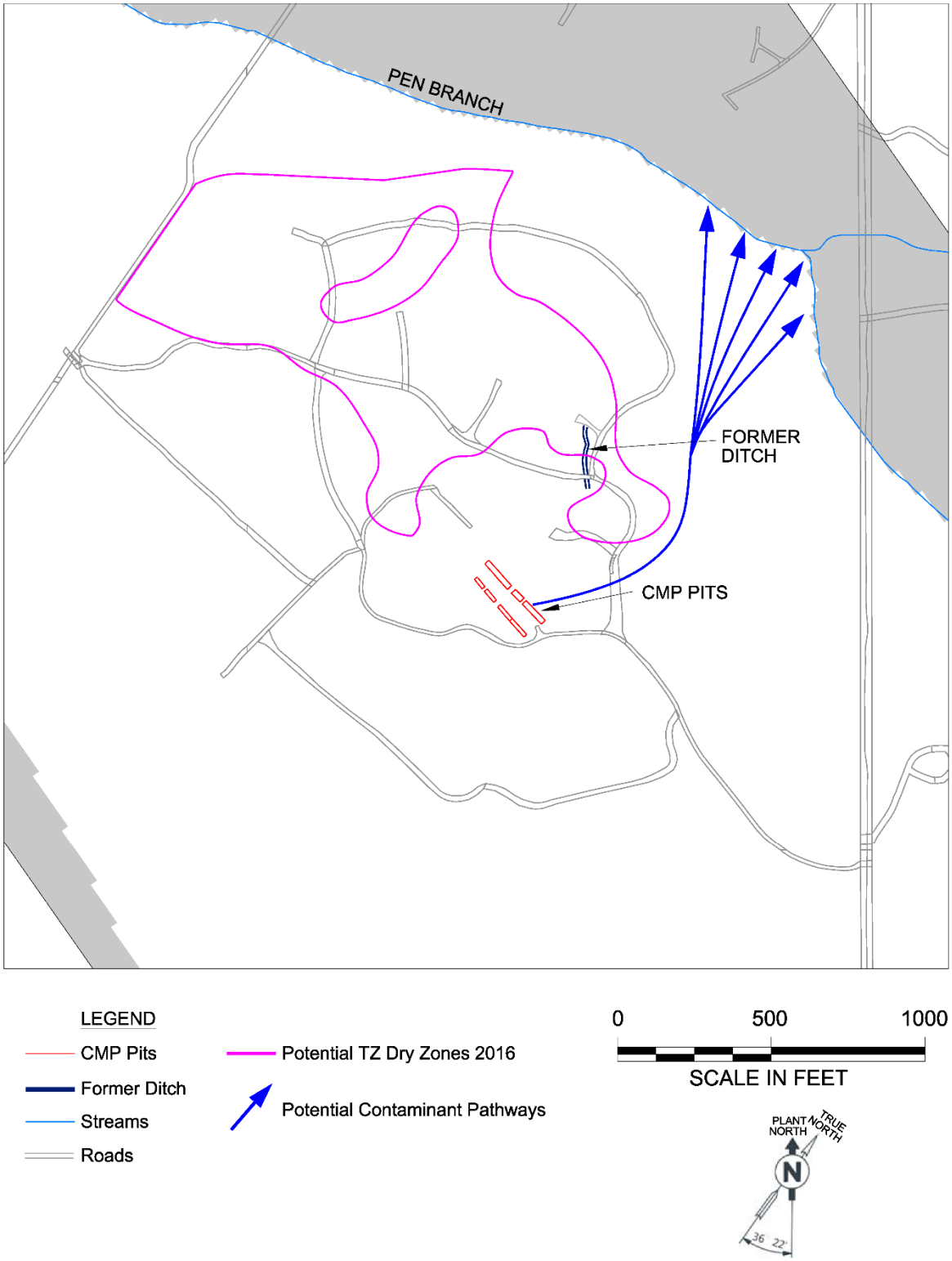

Figure 4.7 Conceptual Model for Presence of Contamination at Northern Corner of Model Domain Near Well CMP064BU

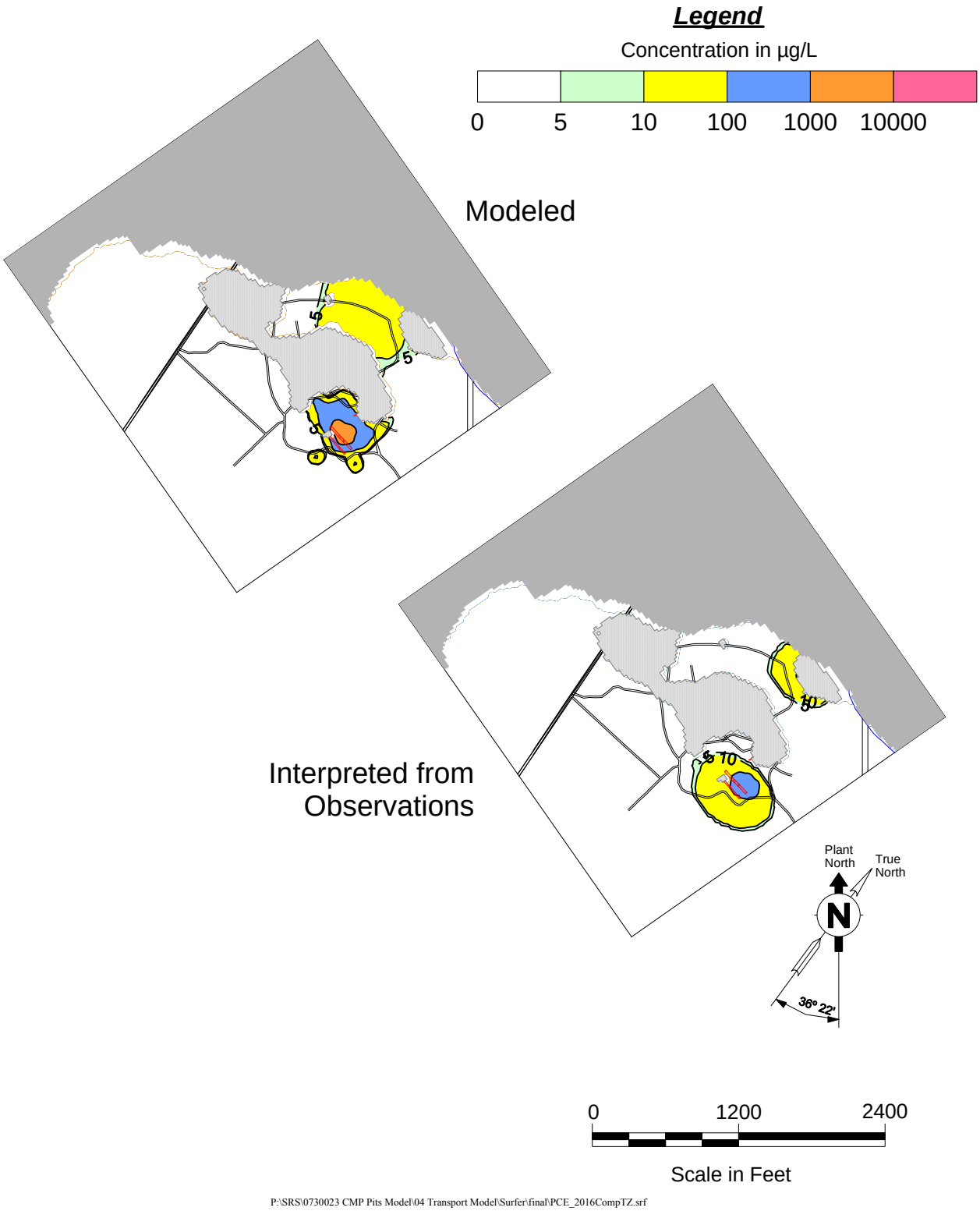

Figure 4.8 Modeled (a) and Interpreted (b) PCE Plume in the TZ in 2016.

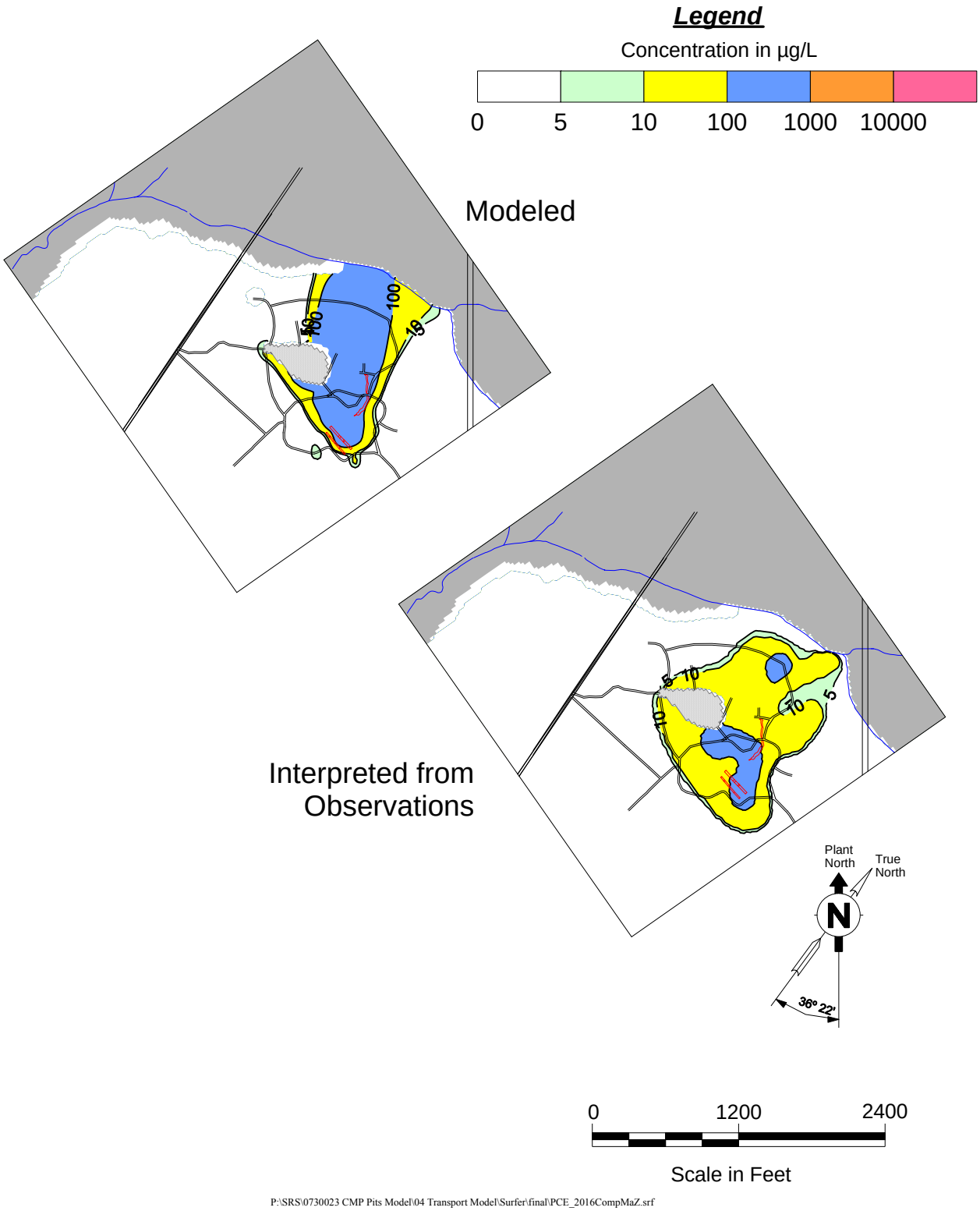

Figure 4.9 Modeled (a) and Interpreted (b) PCE Plume in the MAZ in 2016.

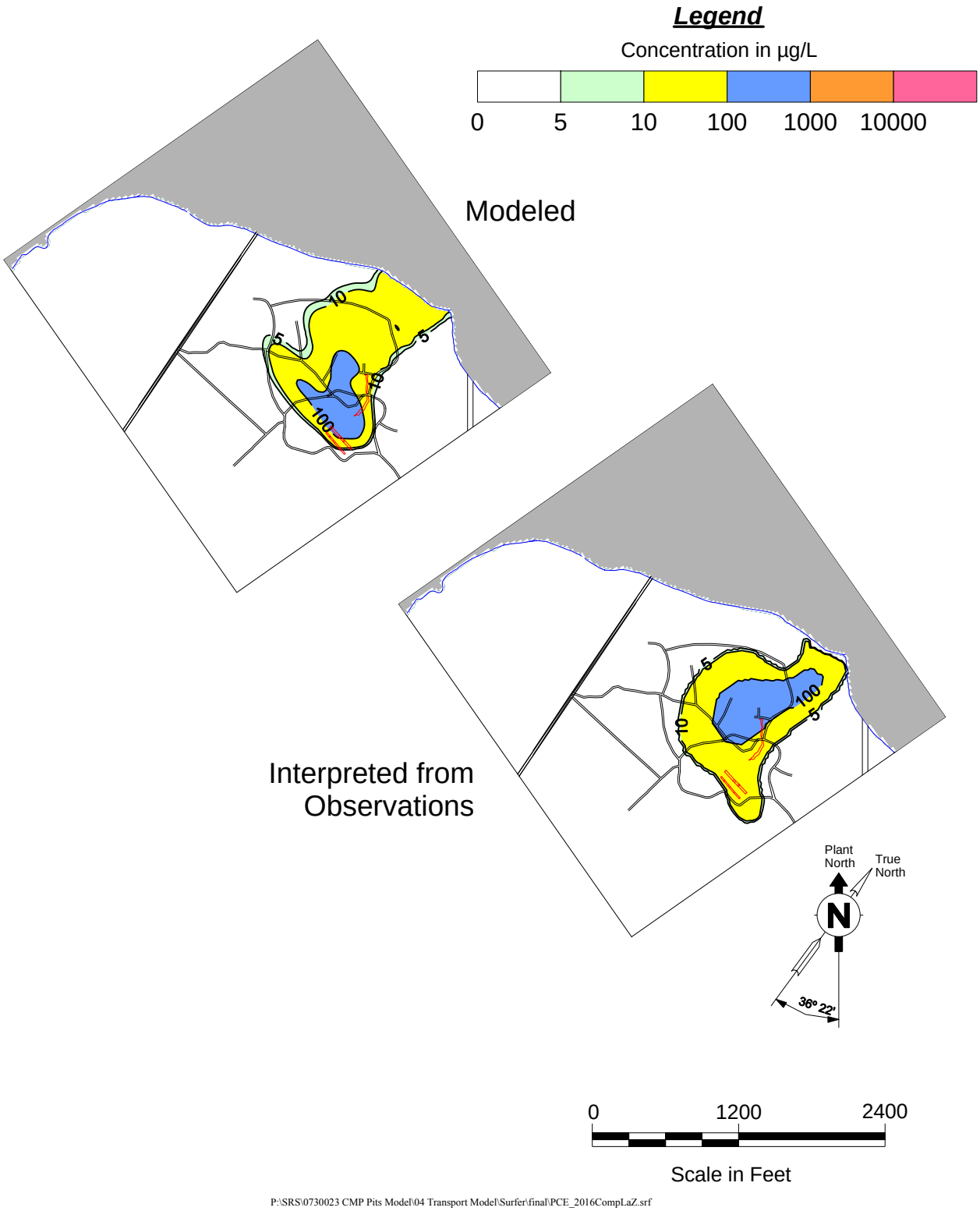

Figure 4.10 Modeled (a) and Interpreted (b) PCE Plume in the LAZ in 2016.

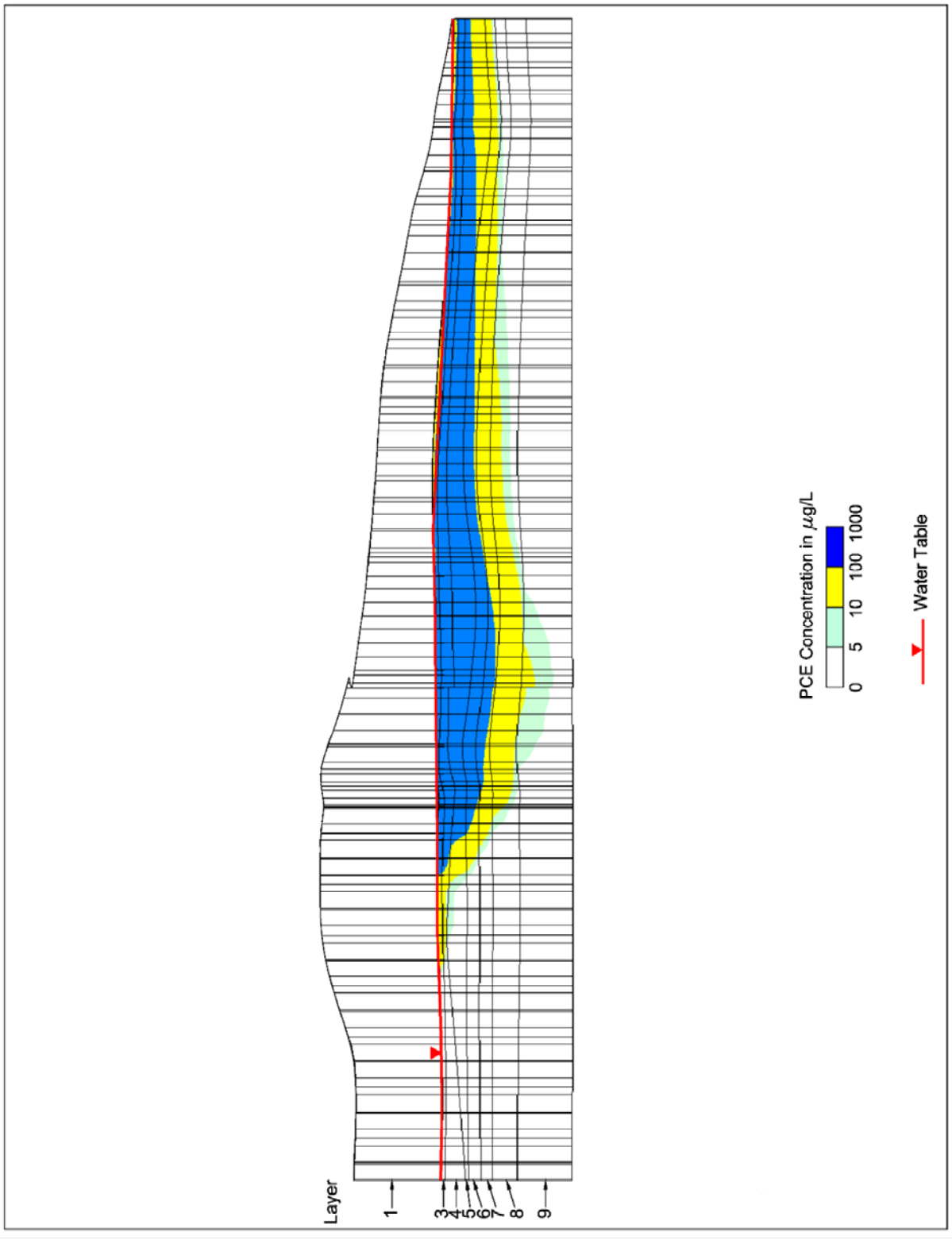

Figure 4.11PCE Concentration (µg/L) Along Cross-section A-A'

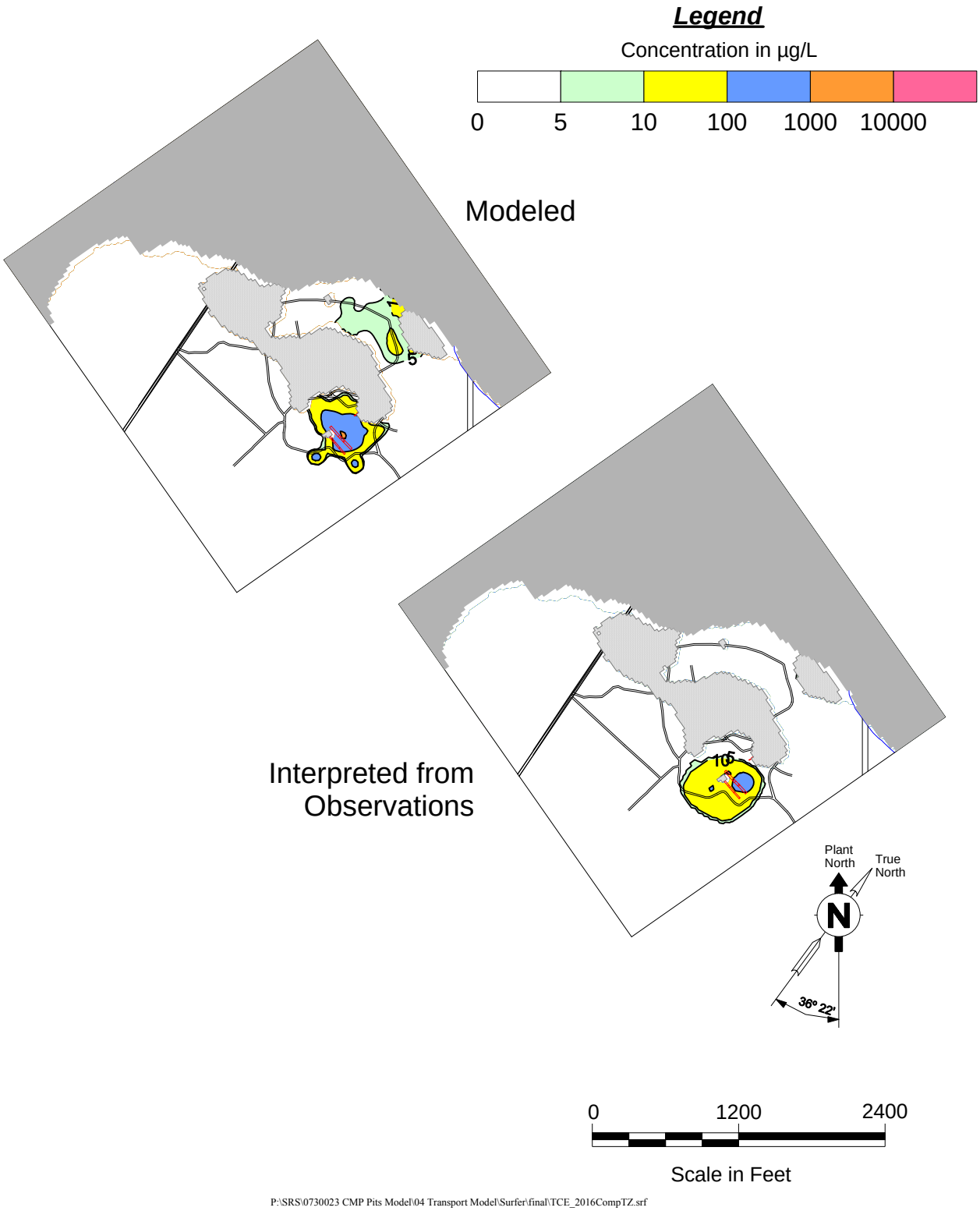

Figure 4.12 Modeled (a) and Interpreted (b) TCE Plume in the TZ in 2016.

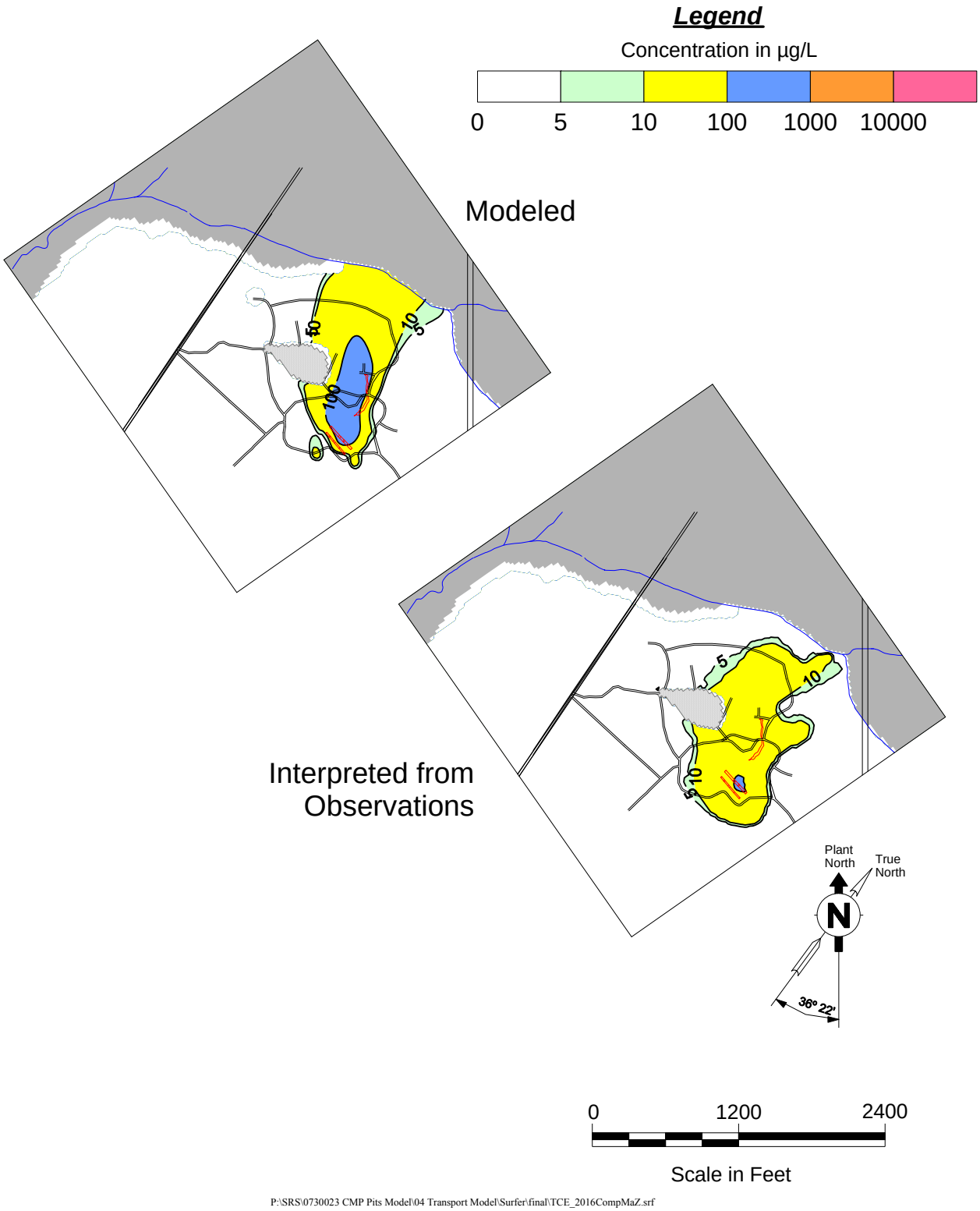

Figure 4.13 Modeled (a) and Interpreted (b) TCE Plume in the MAZ in 2016.

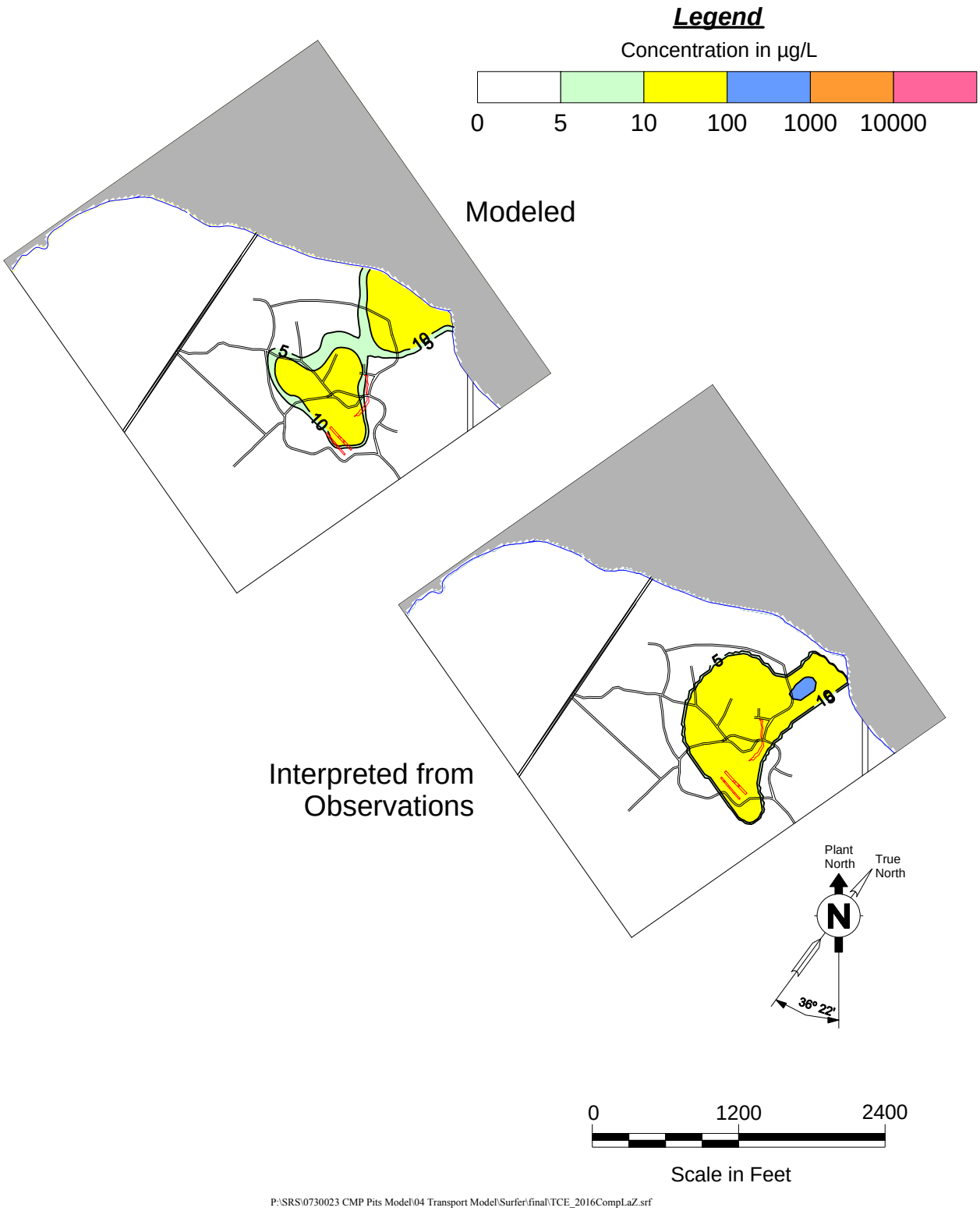

Figure 4.14 Modeled (a) and Interpreted (b) TCE Plume in the LAZ in 2016.

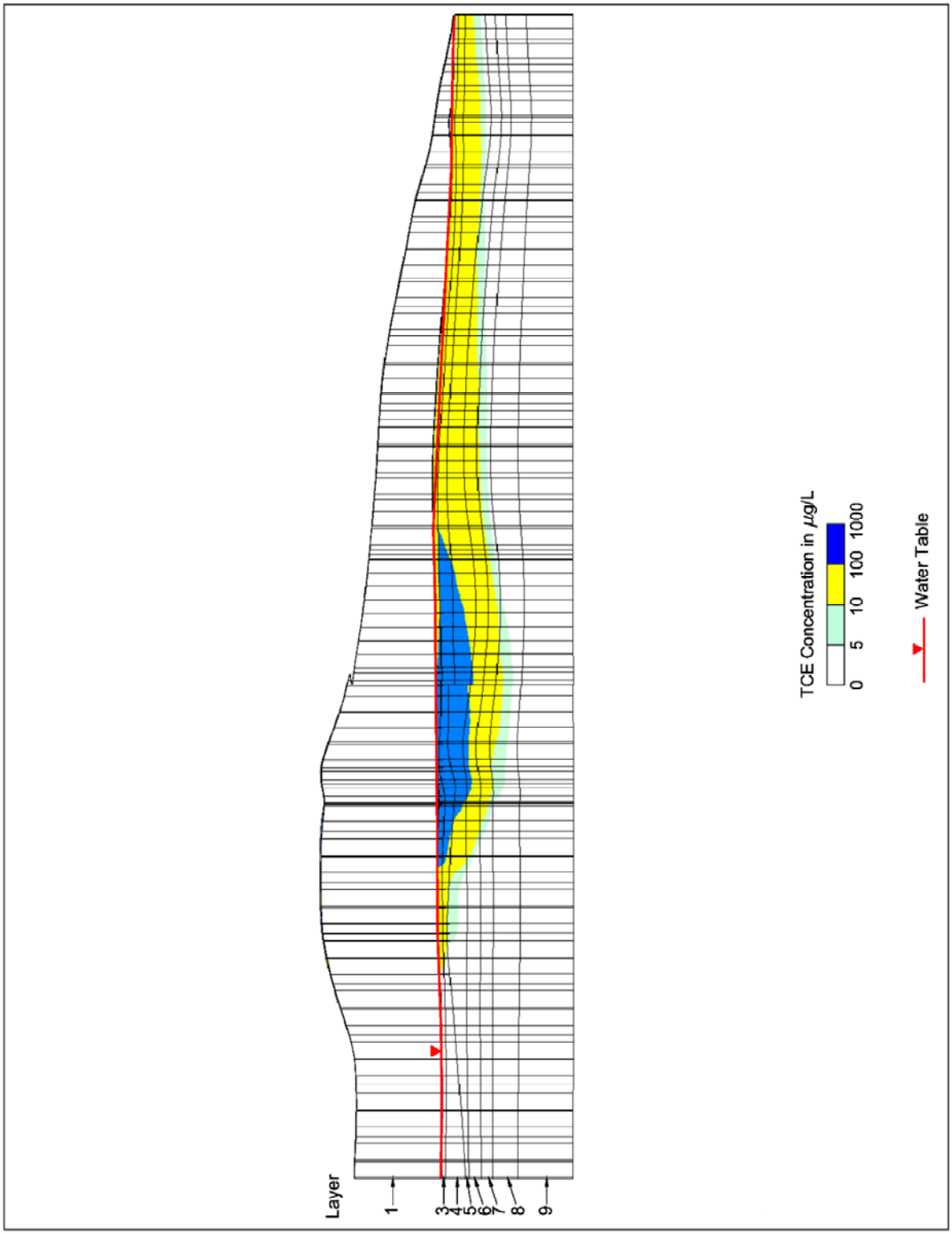

Figure 4.15 TCE Concentration (µg/L) Along Cross-section A-A'

Page intentionally left blank

TZ Source, Distal

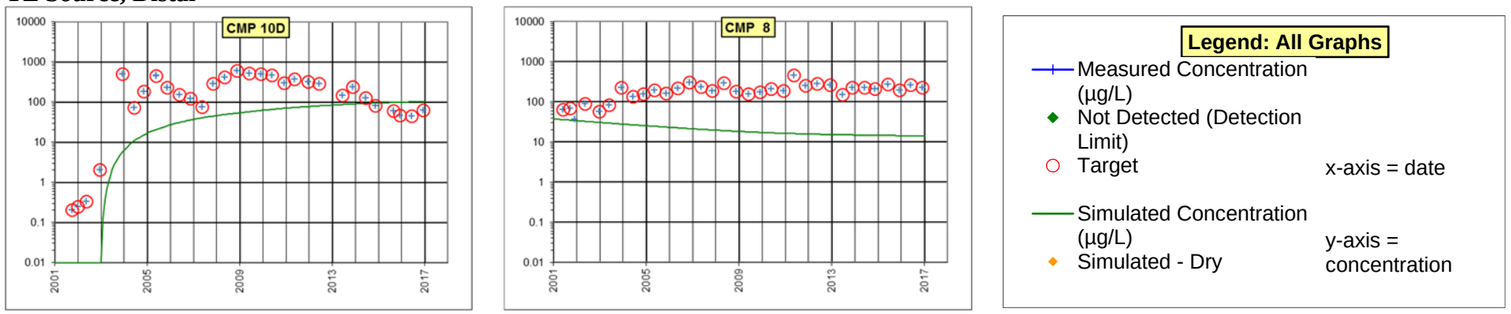

MAZ Source, Mid-Plume and Distal

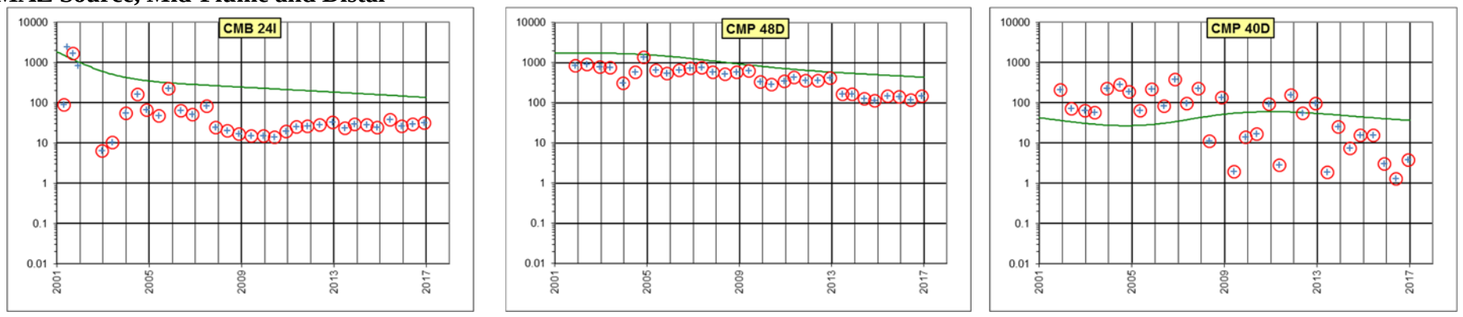

LAZ Source, Mid-Plume and Distal

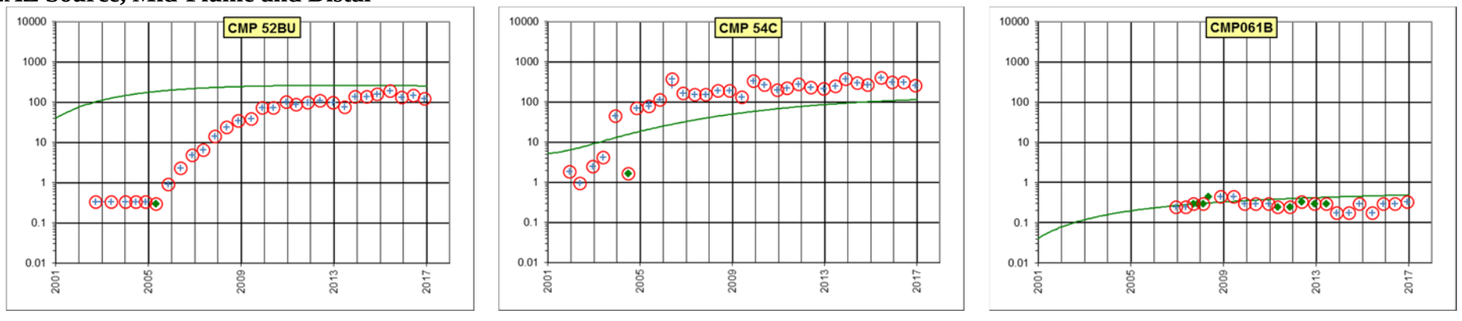

Figure 4.16 PCE Concentration vs. Time for Selected Wells

TZ Source, Distal

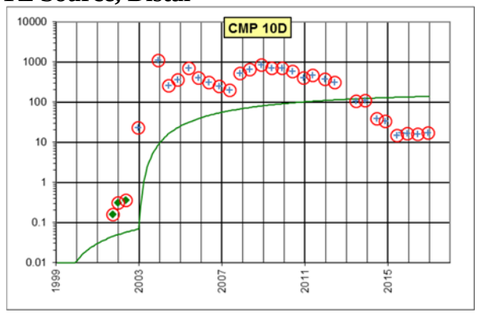

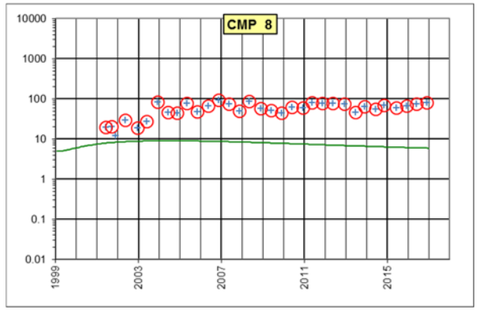

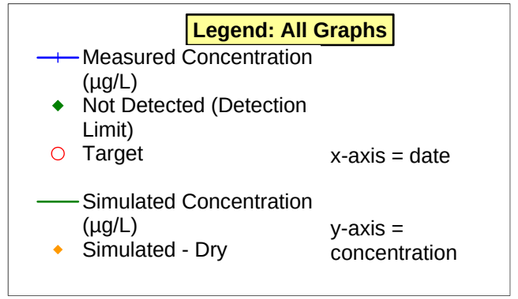

MAZ Source, Mid-Plume and Distal

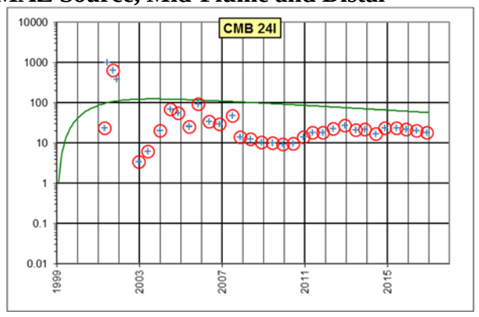

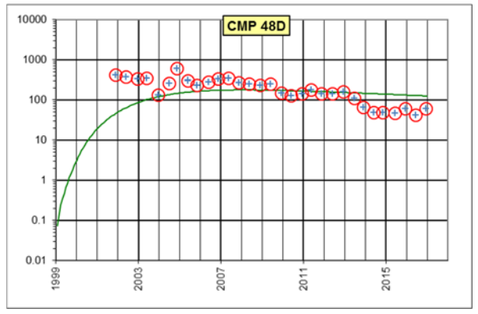

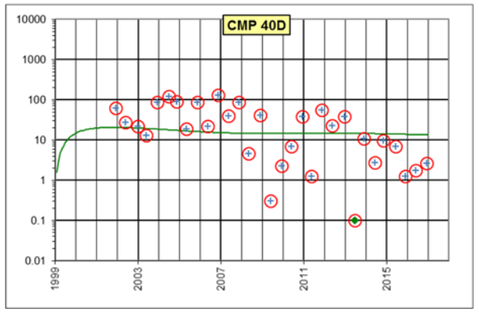

LAZ Source, Mid-Plume and Distal

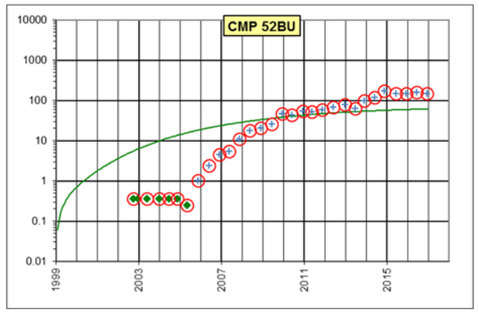

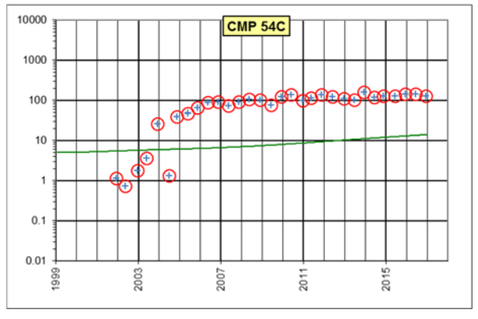

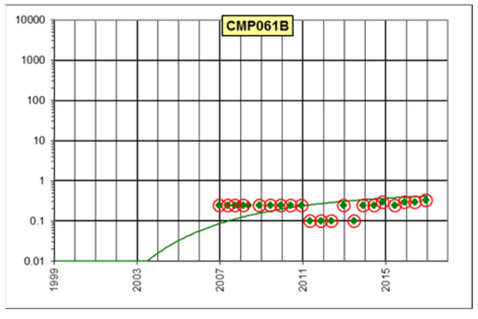

Figure 4.17 TCE Concentration vs. Time for Selected Wells

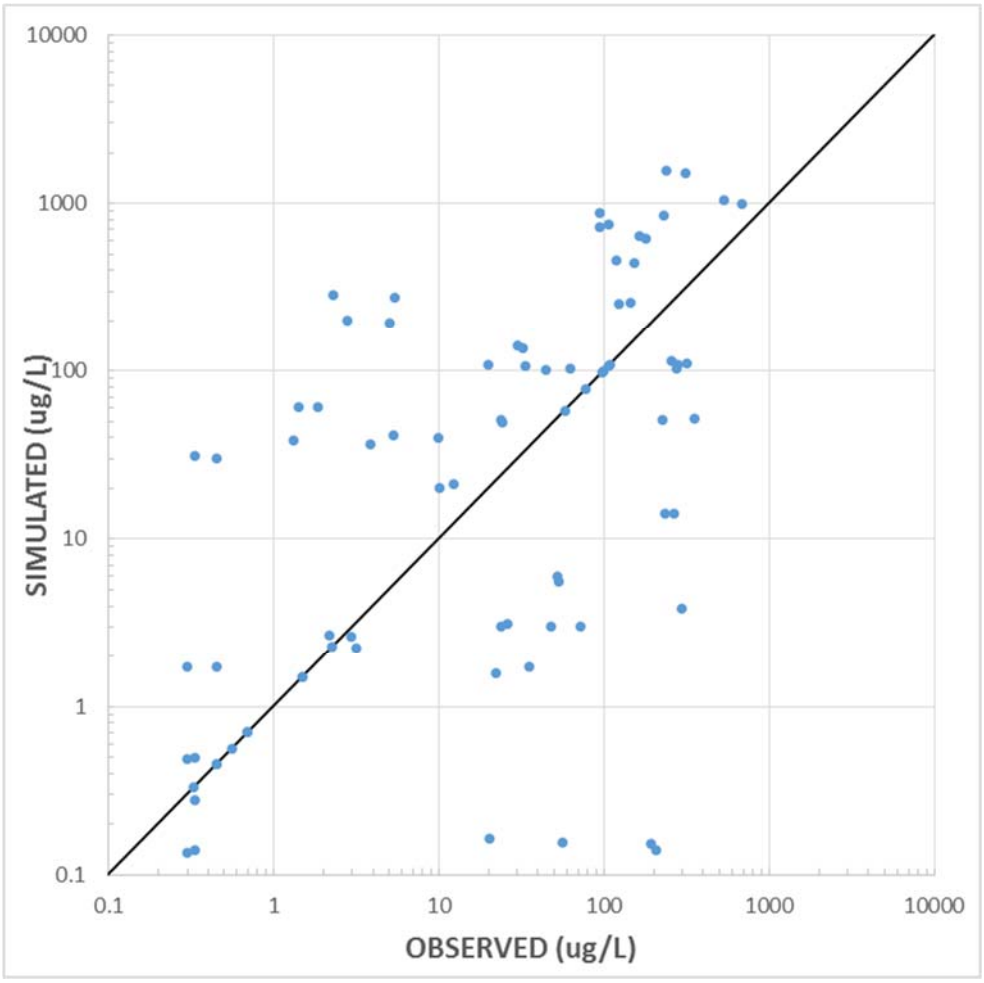

Figure 4.18 Modeled vs Observed PCE Concentrations in 2016

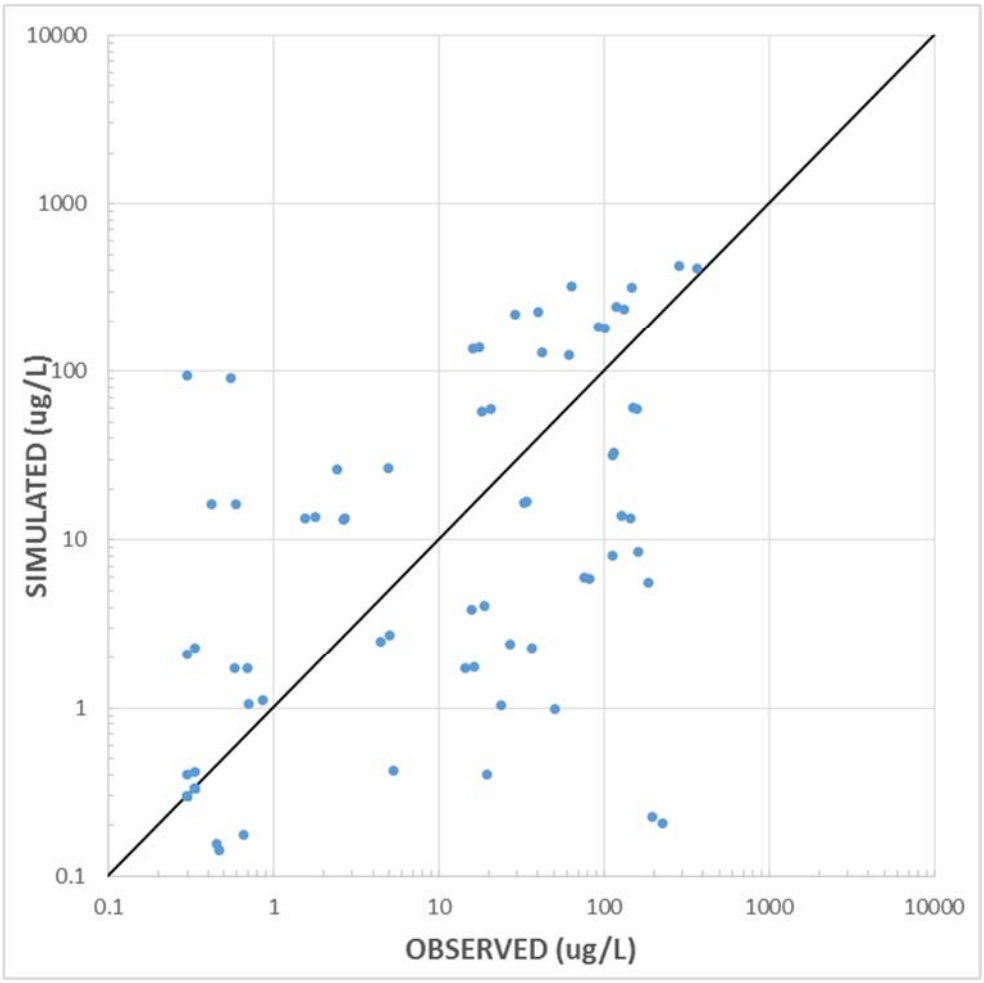

Figure 4.19 Modeled vs Observed TCE Concentrations in 2016

5.0 MODEL PREDICTIONS

In this section, the results of the predictive transport (MT3DMS) simulations are presented. These simulations show the expected future development of the COI plumes. Two source scenarios are considered for each COI (except lindane and 1,4-dioxane): continuing 2016 source (0.28 kg/yr and 0.17 kg/yr for PCE and TCE, respectively) and hypothetical complete source removal (i.e. no source). The sensitivity of model results to sorption (retardation) and porosity is also discussed.

In each simulation, initial plume conditions are applied in year 2017 and 100 years are simulated (1 stress period of 100 yr duration with 50 time steps). Note that the applied initial plume conditions are based on 2016 plume configurations (SRNS 2017). This specification ensures that the initial condition (mass, concentrations, plume extent) are consistent with the current data and conceptual model. In this sense, the calibration is used as a means of verifying accurate model behavior from 2002 to 2016, while actual data are used to set the initial conditions for the 100-year predictive simulations. As in the calibration, concentrations are initialized in aquifers and confining beds. The initialized contamination in the low permeability confining beds will likely migrate slower than contamination in the aquifers and may serve as sources to the aquifers in the long term.

Simulated concentrations of PCE and TCE at the Pen Branch groundwater discharge location are presented below. Wetlands adjoining these locations appear to provide significant degradation of PCE and TCE. Application to this site of a wetlands-specific degradation factor derived from observations of TCE degradation at an instrumented site within the C-area of SRS (GeoTrans 2001), suggest that the modeled PCE and TCE discharge concentrations may be reduced by two orders of magnitude.

5.1 PCE Transport

Figure 5.1 shows the initial 2017 PCE plume. After 23 years (in 2040) of transport in the full-source scenario (Figure 5.2), the PCE plume in the aquifer is due to both the initial plume and the vadose-zone source. The plume extends from the CMP Pits to Pen Branch, and is present above the MCL (5 μg/L) in all three aquifer zones. The plume distribution after 43 years (in 2060, Figure

5.3) is similar to the 2040 plume, but slightly more attenuated. At 100 years (2117, Figure 5.4) the plume is almost entirely attenuated.

Figures 5.5, 5.6 and 5.7 show PCE plume configurations at the same times as Figures 5.2, 5.3 and 5.4 for the no-source scenario. Comparison to the full-source scenario suggest that the source has a limited effect on plume migration. That is, the magnitude and extent of contamination appears to be due primarily to the pre-remediation source. Further, these results suggest that accurate quantification of source behavior beyond these bounding computations is unnecessary. Figure 5.8 shows the PCE mass in the hydrogeologic system versus time for the two scenarios. Mass declines over time from a maximum of 270 kg due to first order decay and discharge to Pen Branch. As suggested from the plume configurations, the effect of the source is minimal and its presence causes slightly more mass to remain in the system after 100 years than the no-source scenario.

Figure 5.9 shows the maximum simulated PCE concentration exiting the model near Pen Branch. This concentration is sometimes used as an exposure-point concentration in risk calculations, because it is the maximum concentration that would reach a surface water body or environmental receptor at the ground surface. The figure is generated by identifying the maximum concentration at wetland drains for each time step. The location of the maximum concentration will change with time as the plume attenuates. A maximum concentration of 61 µg/L occurs in the first few years of the simulation and declines to below the 5 µg/L MCL by year 2108 (91 years). However, note that the model does not account for degradation in the wetlands, which can be substantial, as described in the introduction to this section. An order of magnitude reduction in concentration due to degradation in the wetlands would result in discharge concentrations of PCE being below the MCL within five years. As noted for the plumes and mass computations, the effect of the source is minimal, with concentrations being slightly higher when a continuous source is simulated.

Figure 5.10 shows the mass flux (kg/yr) of PCE to discharge locations along Pen Branch. The maximum flux of slightly over 1 kg/yr occurs within the first five years of the simulation and declines to less than 0.2 kg/yr by 2107. Note that degradation in the wetlands would lower the mass flux of PCE entering Pen Branch.

Table 5.1 Predicted Impacts to Pen Branch

Model Run	MCL or RSL (µg/L)	Maximum Concentration (µg/L)	Year of Maximum	Year Concentration Drops below MCL
PCE Source	5	61	2	91
PCE No Source	5	61	2	91
TCE Source	5	47	1	48
TCE No Source	5	47	1	48
Lindane	0.2	0.06	31	1
1,4-Dioxane *	0.46	0.46	1	2
PCE No Source Kd/2	5	61	1	77
PCE No Source Porosity 0.2	5	60	2	88

* RSL, all others list MCL

5.2 TCE Transport

Figure 5.11 shows the initial 2017 TCE plume. TCE plume migration is similar to the PCE migration, as shown in Figures 5.12, 5.13, and 5.14 for years 2040, 2060, and 2117, respectively. As was the case for PCE, TCE plume migration is almost identical whether the 2016 source is included or not. For brevity, the TCE results for no source are not shown here. The plume extends from the CMP Pits to Pen Branch, and is present above the MCL (5 µg/L) in all three aquifer zones. The plume distribution after 43 years (in 2060, Figure 5.13) is similar to the 2040 plume (Figure 5.12), but slightly more attenuated. At 100 years (2117, Figure 5.14) the plume is almost entirely attenuated.

Figure 5.15 shows the TCE mass in the hydrogeologic system versus time for the two scenarios. Mass declines over time from a maximum of 130 kg due to first order decay and discharge to Pen Branch. As suggested from the plume configurations, the effect of the source is minimal and its presence causes approximately 10 kg more mass to remain in the system after 100 years than the no-source scenario.

Figure 5.16 shows the maximum TCE concentration simulated at any discharge location along Pen Branch and its tributary. Simulated discharge concentrations begin at 48 ug/L and stay above the

MCL of 5 µg/L for 48 years for both source removal scenarios. As noted above, additional degradation within the wetlands could further reduce the simulated TCE concentrations. An order of magnitude reduction results in the TCE concentration being below the MCL for the duration of the 100 year simulation period.

Figure 5.17 shows the mass flux (kg/yr) of TCE to discharge locations along Pen Branch. The maximum flux of slightly over 0.4 kg/yr occurs within the first five years of the simulation and declines to less than 0.1 kg/yr by 2107. Note that degradation in the wetlands would lower the mass flux of TCE entering Pen Branch.

5.3 Lindane Transport

Lindane is also a COI for groundwater at the CMP Pits, and is modeled in this study. However, the initial concentrations of lindane are fairly low (Figure 5.18), and no source term is simulated. In addition, the mass in the system (Figure 5.19) is very low, starting at less than 0.18 kg, and declining with time. Figure 5.20 shows that the maximum lindane concentration at the Pen Branch wetlands of 0.06 ug/L occurs at year 47. Consequently, the 0.2 µg/L MCL for lindane is never exceeded at discharge locations (Figure 5.20).

5.4 1,4-Dioxane Transport

1,4-dioxane is also a COI for groundwater at the CMP Pits, and is modeled in this study. Like lindane, the initial concentrations of 1,4-dioxane are fairly low (Figure 5.21) and no source term is simulated. In addition, the mass in the system (Figure 5.22) is very low, starting at less than 2.2 kg, and declining with time. Figure 5.23 shows that the maximum 1,4-dioxane concentration at the Pen Branch wetlands currently occurs at 0.46 ug/L. This concentration decreases with time, such that the 0.46 µg/L RSL (SRNS 2017) for 1,4-dioxane is not exceeded at discharge locations (Figure 5.23).

5.5 Sensitivity Analysis of Key Transport Parameters

This section describes an assessment of the effect on model predictions of uncertainty regarding parameters specific to the solute transport model. Key solute transport parameters were identified informally by noting the response of the model to changes in parameters during calibration and predictive simulations. These parameters are: 1) K_d, 2) porosity, and 3) source term mass flux. Sensitivity simulations are presented only for PCE because this is one of the two major COI's and the sensitivity of TCE is believed to be similar to that of PCE.

K_d is a soil-water distribution coefficient and affects the degree of sorption. Combined with other parameters (porosity and bulk density) the effect of sorption can also be represented by a retardation factor. The retardation factor (R) is conceptually easier to visualize because its numerical value is simply the factor by which the apparent plume velocity is reduced. Sensitivity to K_d is presented using variations in R. Figure 5.24 show the PCE mass in the aquifer vs time for a two-fold reduction in R. Note that the initial mass in the aquifer is about half of the original value for the reduced R because there is less mass partitioned to the soil. This proportion remains throughout the simulation. Of perhaps greater interest is the maximum PCE concentration at the Pen Branch discharge location (Figure 5.25). For the reduced R, the MCL is attained at 27 years instead of the 38 years with the original R.

Porosity primarily affects the groundwater velocity, with lower values increasing the velocity:

$$V = K\, i / \theta$$

Where:

i = hydraulic gradient

In addition, porosity affects the computation of retardation, which affects the mass in the system and velocity:

$$R = (1 + K_d\, (\rho_b / \theta))$$

In this case, decreasing porosity increases retardation, thereby decreasing velocity.

The effect of decreasing porosity from a base value of 0.3 to 0.2 was tested in the model. It was found to slightly raise (2 ug/L) the maximum concentration at the Pen Branch wetlands in late time (>50 yrs, Figure 5.25). It had no effect on the time to attain MCLs.

The sensitivity of the model to source term mass flux was discussed for the simulation of various contaminants. In general, the remaining source has little effect on concentrations because the mass flux is so small relative to the mass already in the system. Figure 5.24 shows the limited effect that the source has on PCE mass in the system. Figure 5.25 shows that maximum concentrations at Pen Branch are unaffected by source because the mass in the system determines the concentration at the creek.

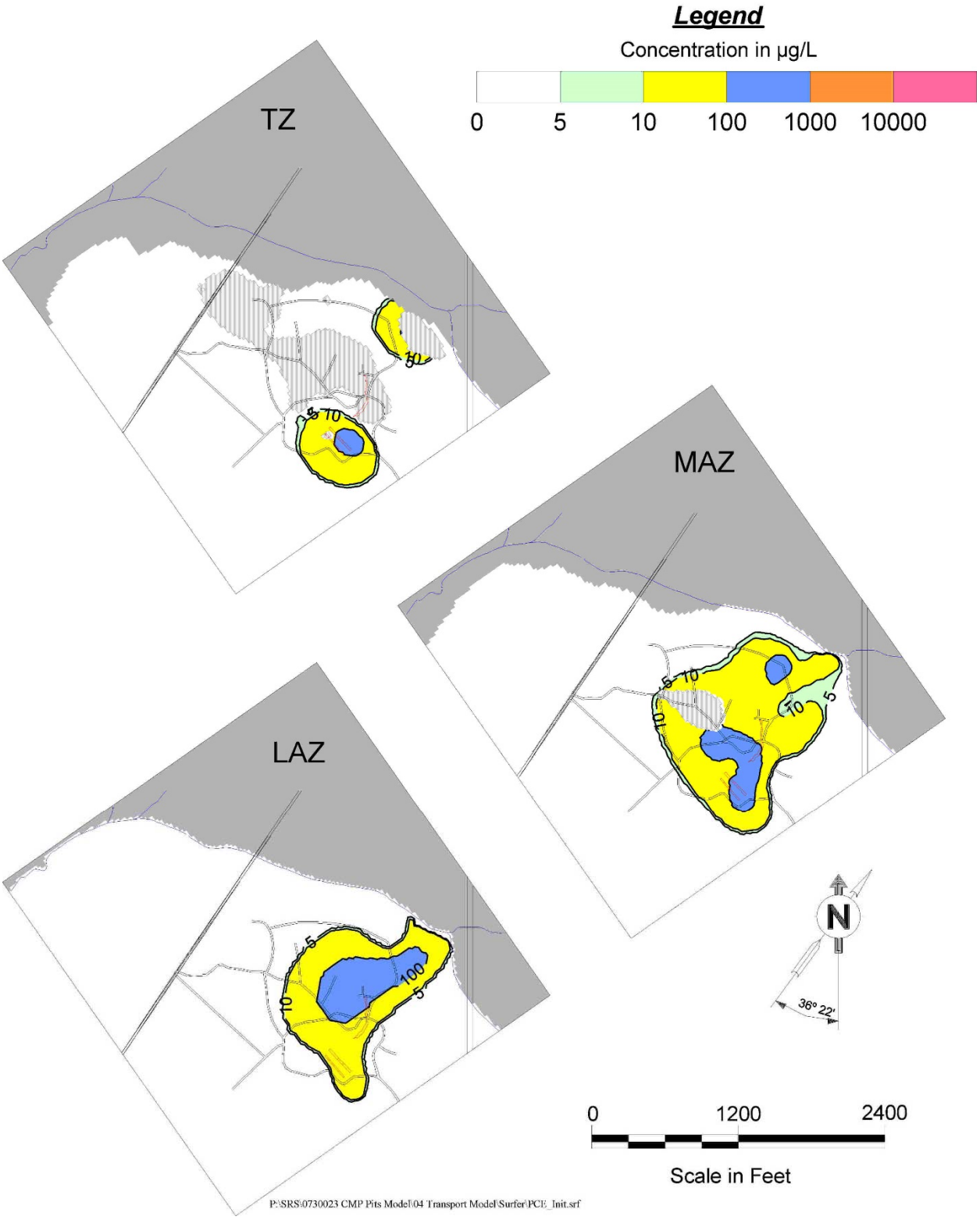

Figure 5.1 Initial 2017 PCE Plume for All Aquifers

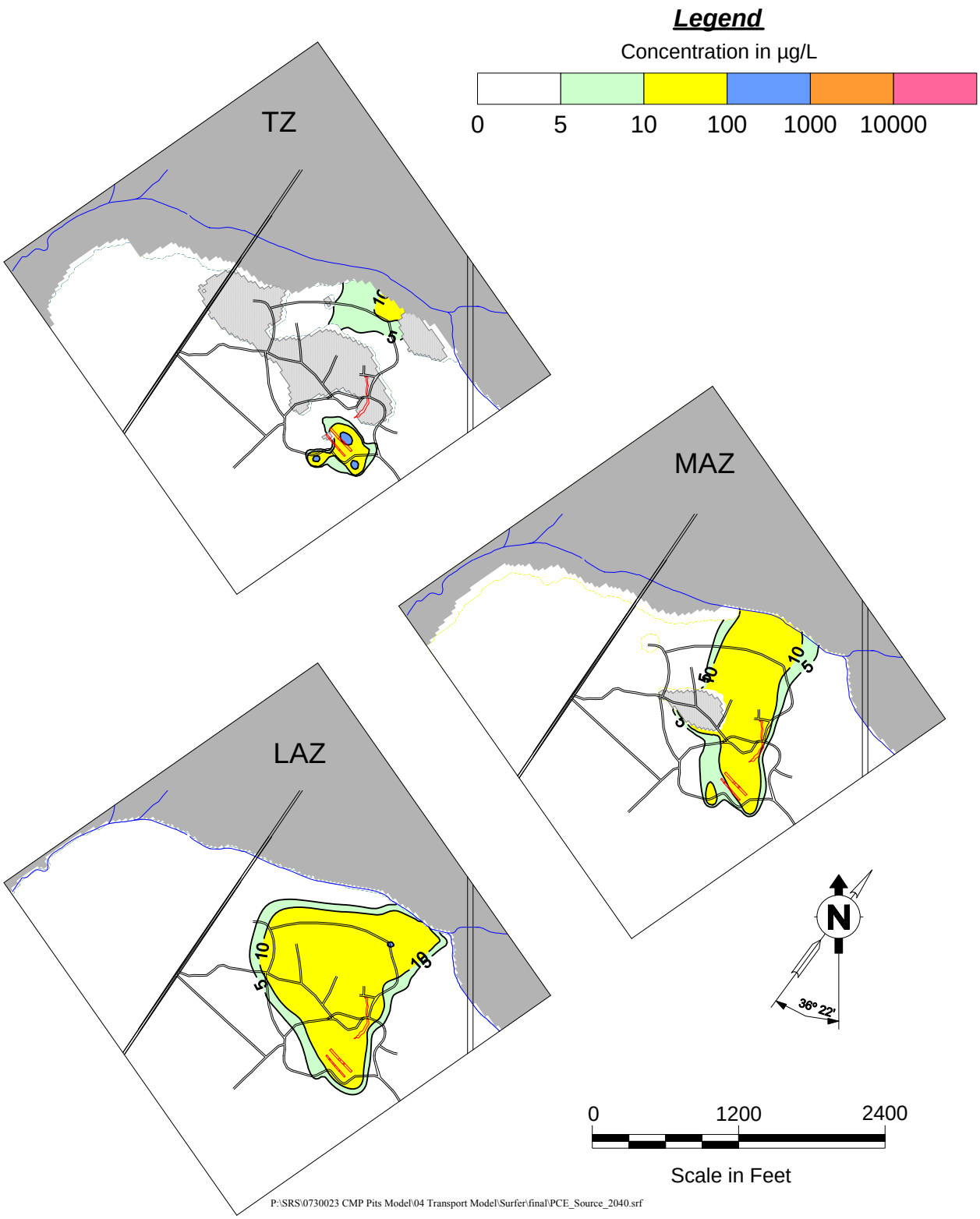

Figure 5.2 Modeled PCE Plume Configuration in 2040 with the Continuing 2016 Source

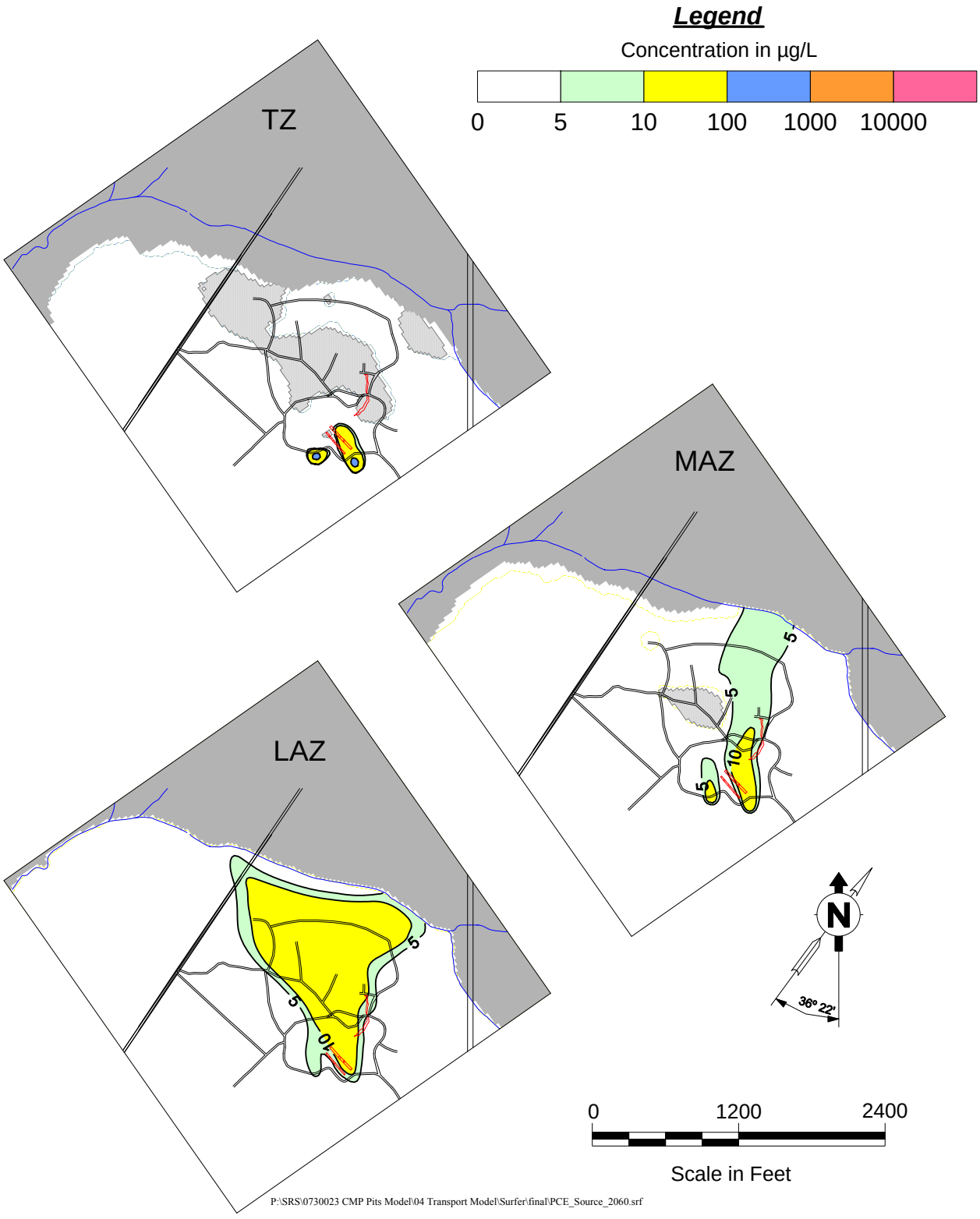

Figure 5.3 Modeled PCE Plume Configuration in 2060 with the Continuing 2016 Source

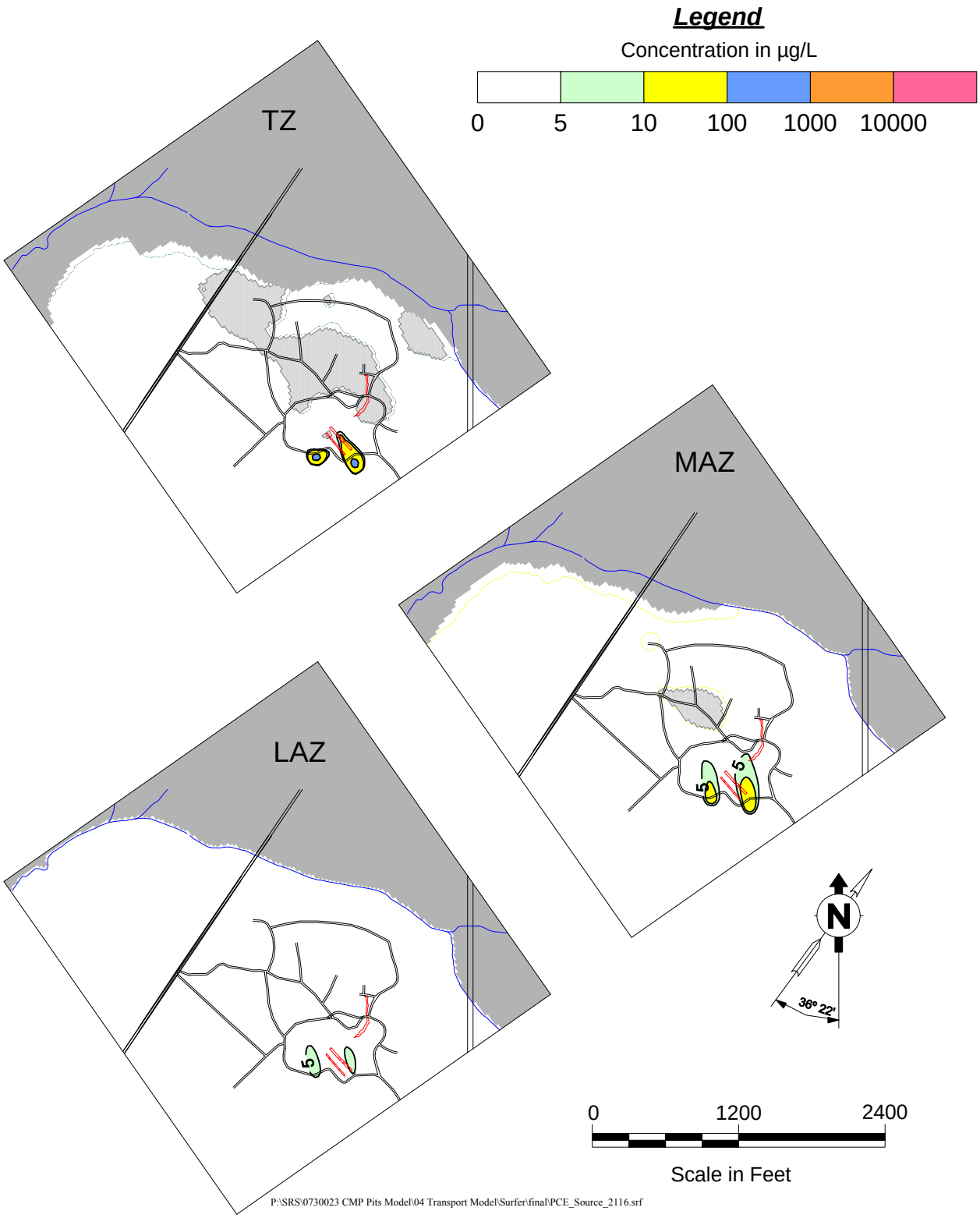

Figure 5.4 Modeled PCE Plume Configuration in 2116 with the Continuing 2016 Source

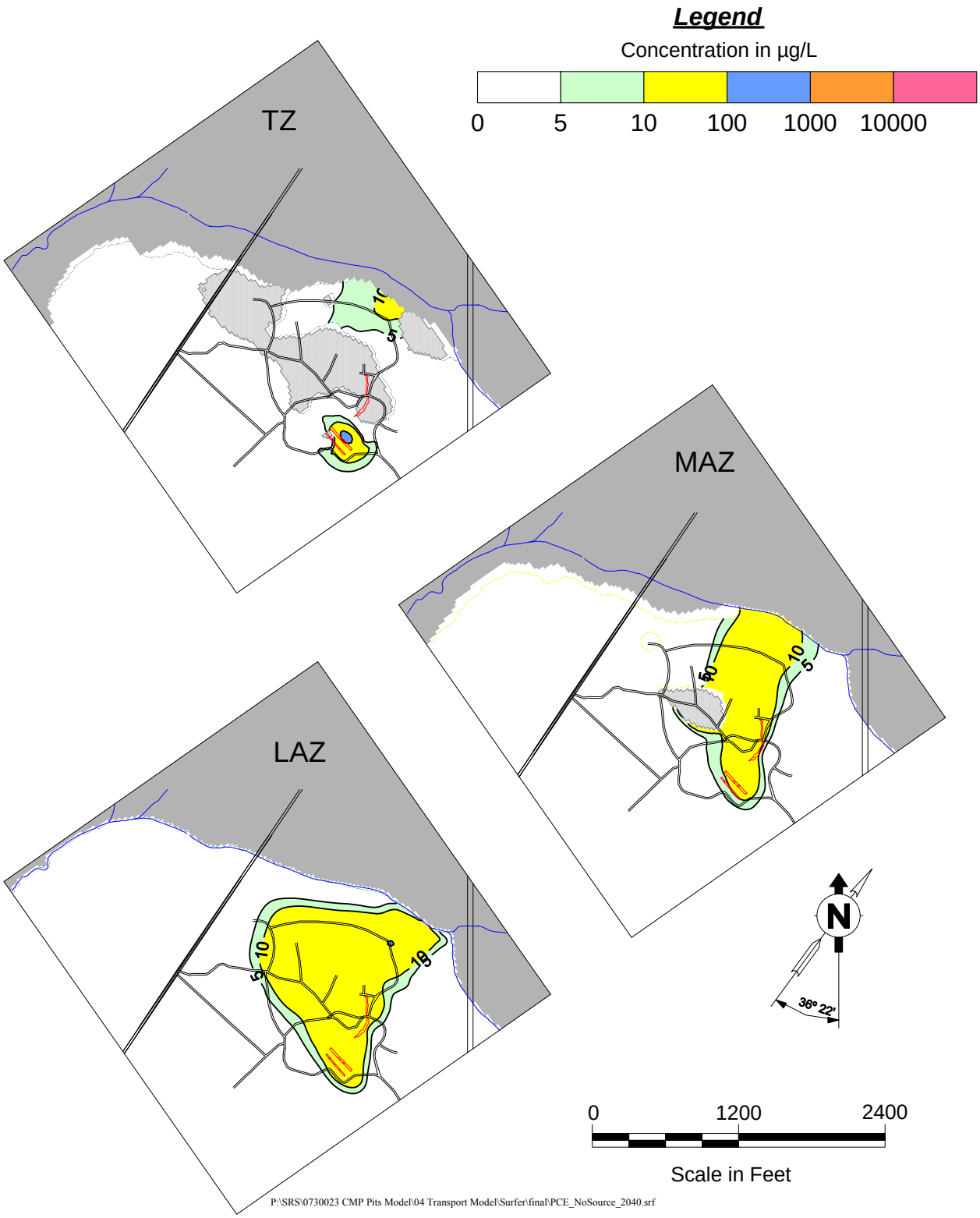

Figure 5.5 Modeled PCE Plume Configuration in 2040 with No Source

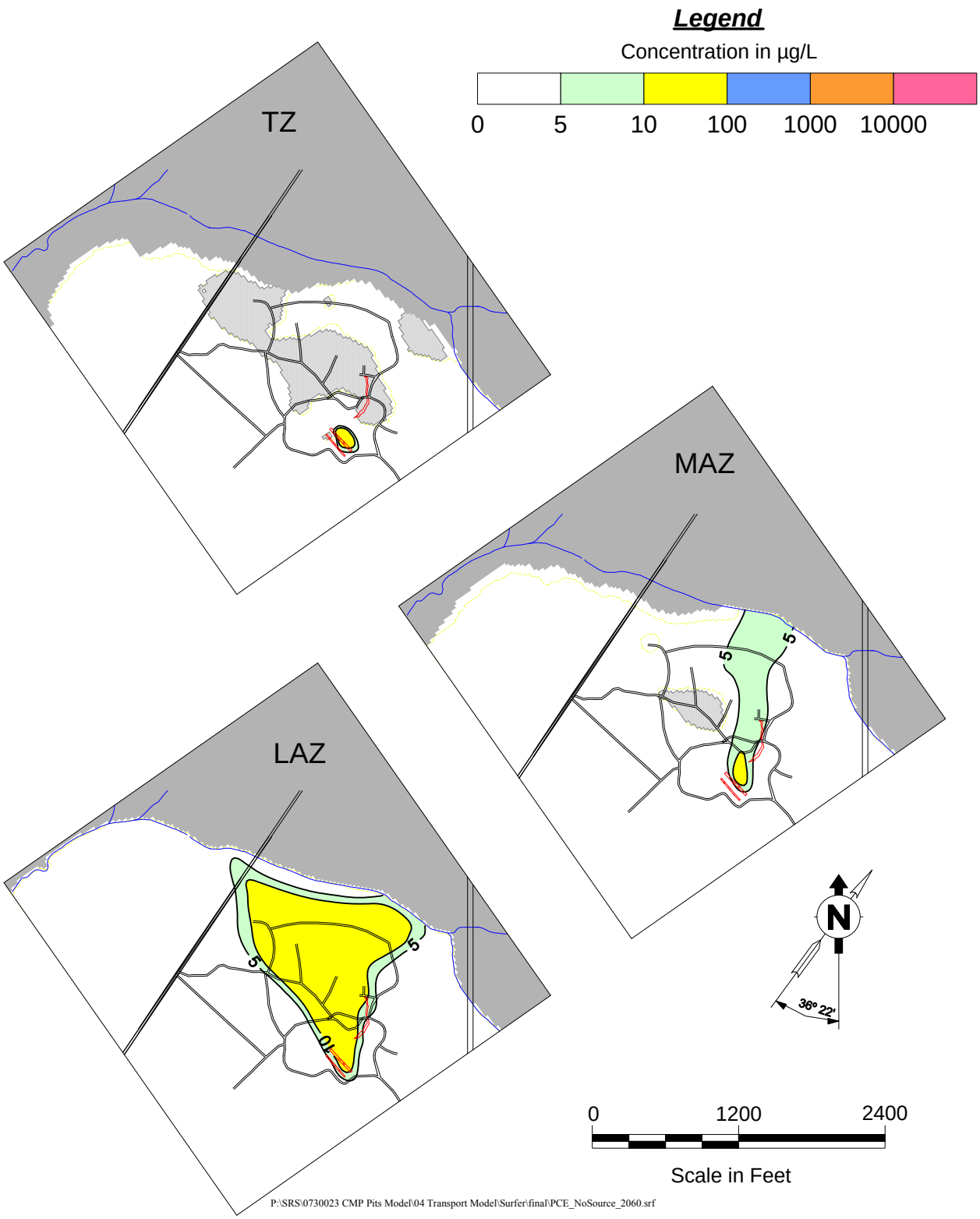

Figure 5.6 Modeled PCE Plume Configuration in 2060 with No Source

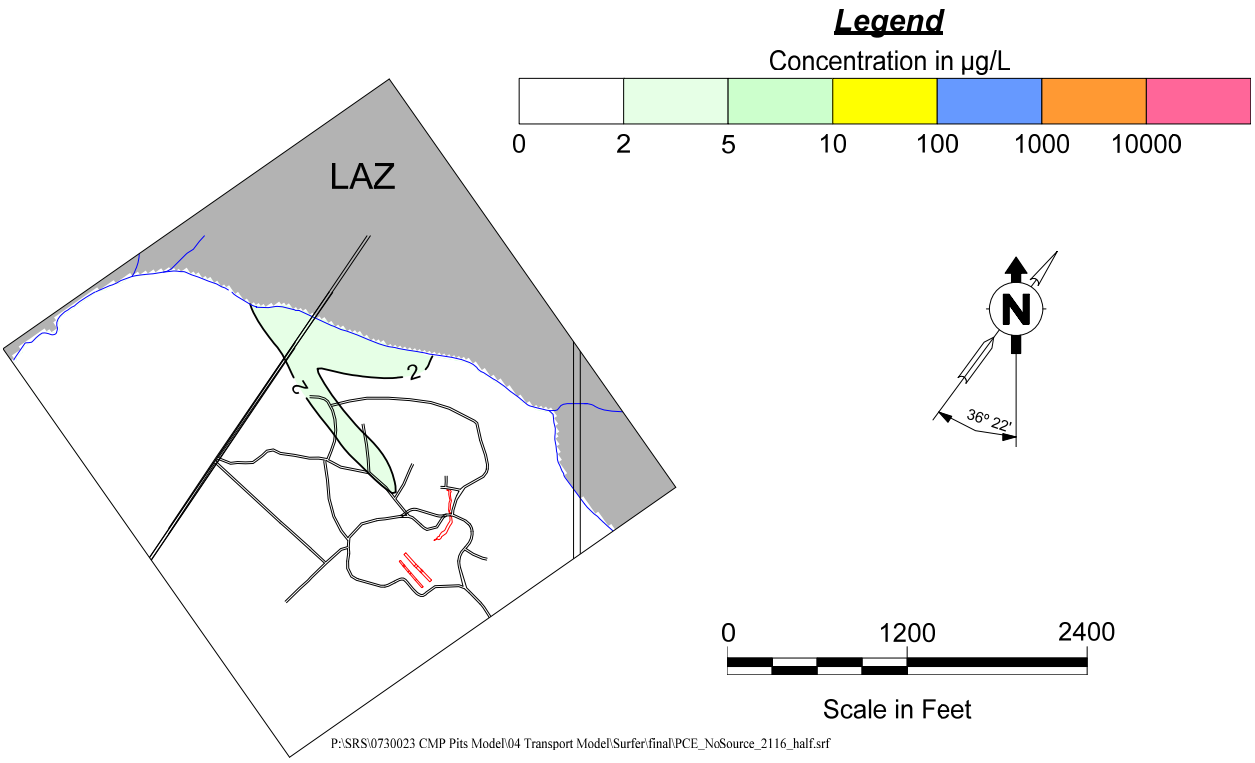

Figure 5.7 Modeled PCE Plume Configuration in 2116 with No Source (Concentrations in TZ and MAZ less than 2 µg/L)

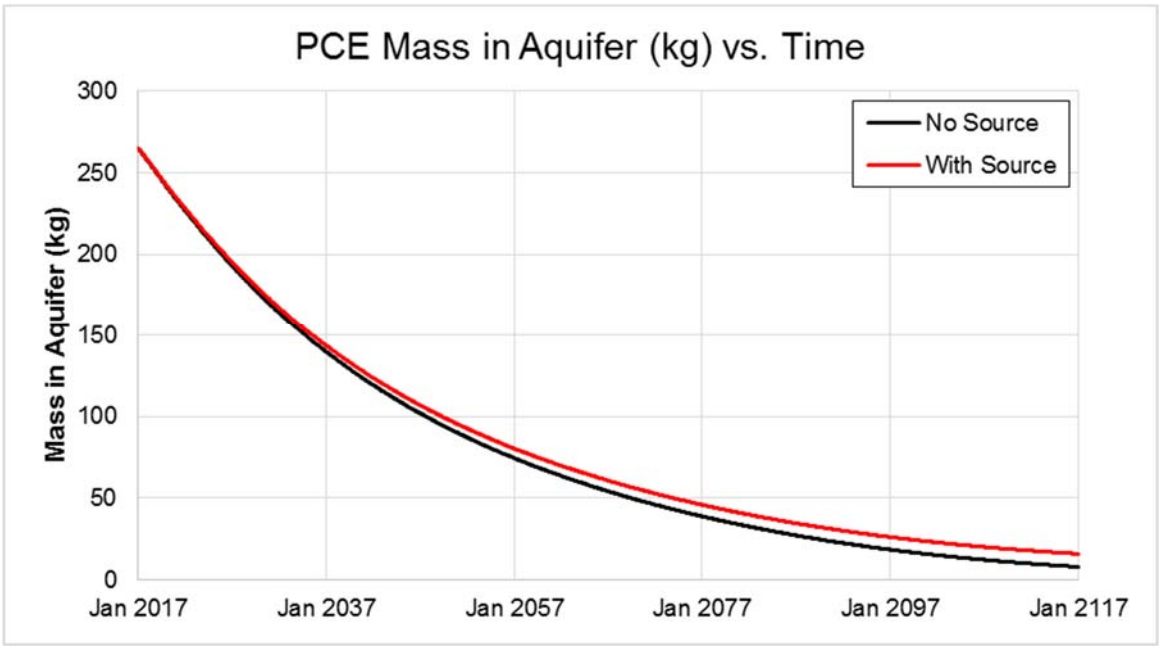

Figure 5.8 Modeled PCE Mass in System vs Time for the Two Scenarios

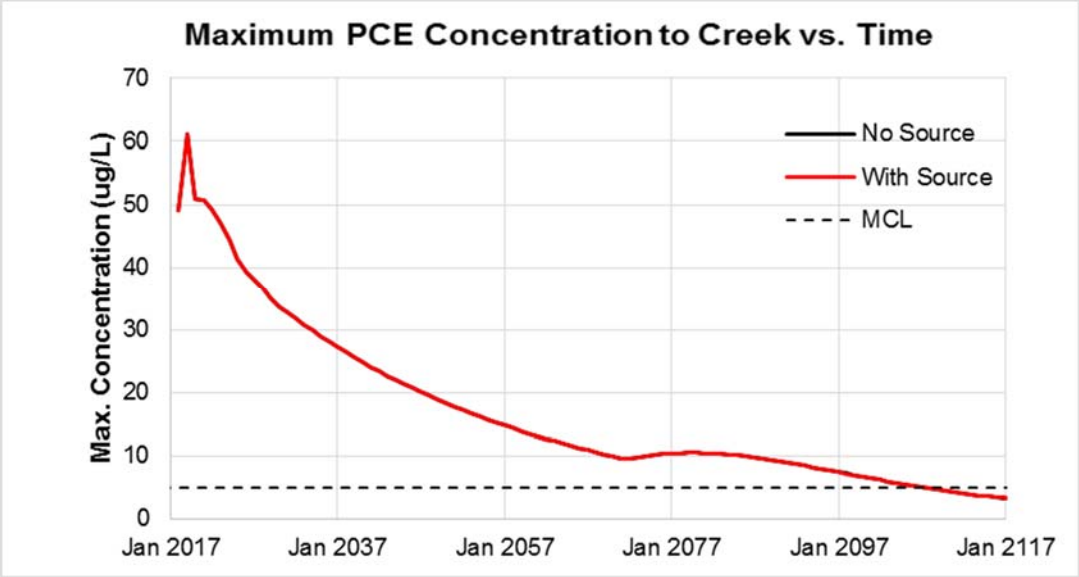

Figure 5.9 Modeled PCE Maximum Concentration vs Time to Pen Branch

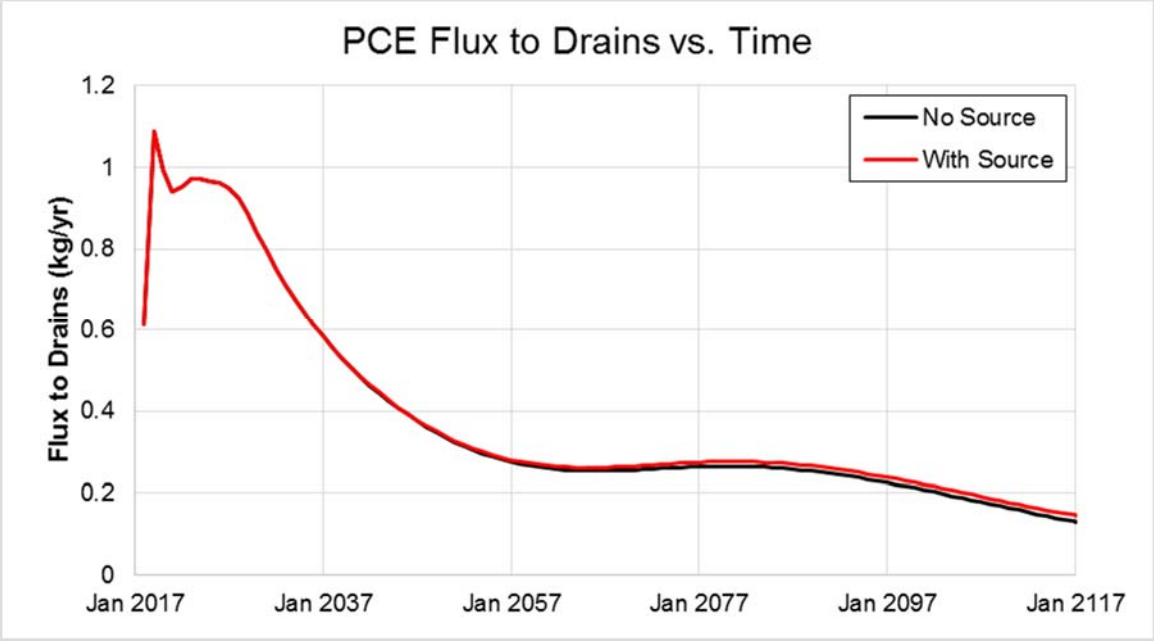

Figure 5.10 Modeled PCE Flux vs Time to Pen Branch

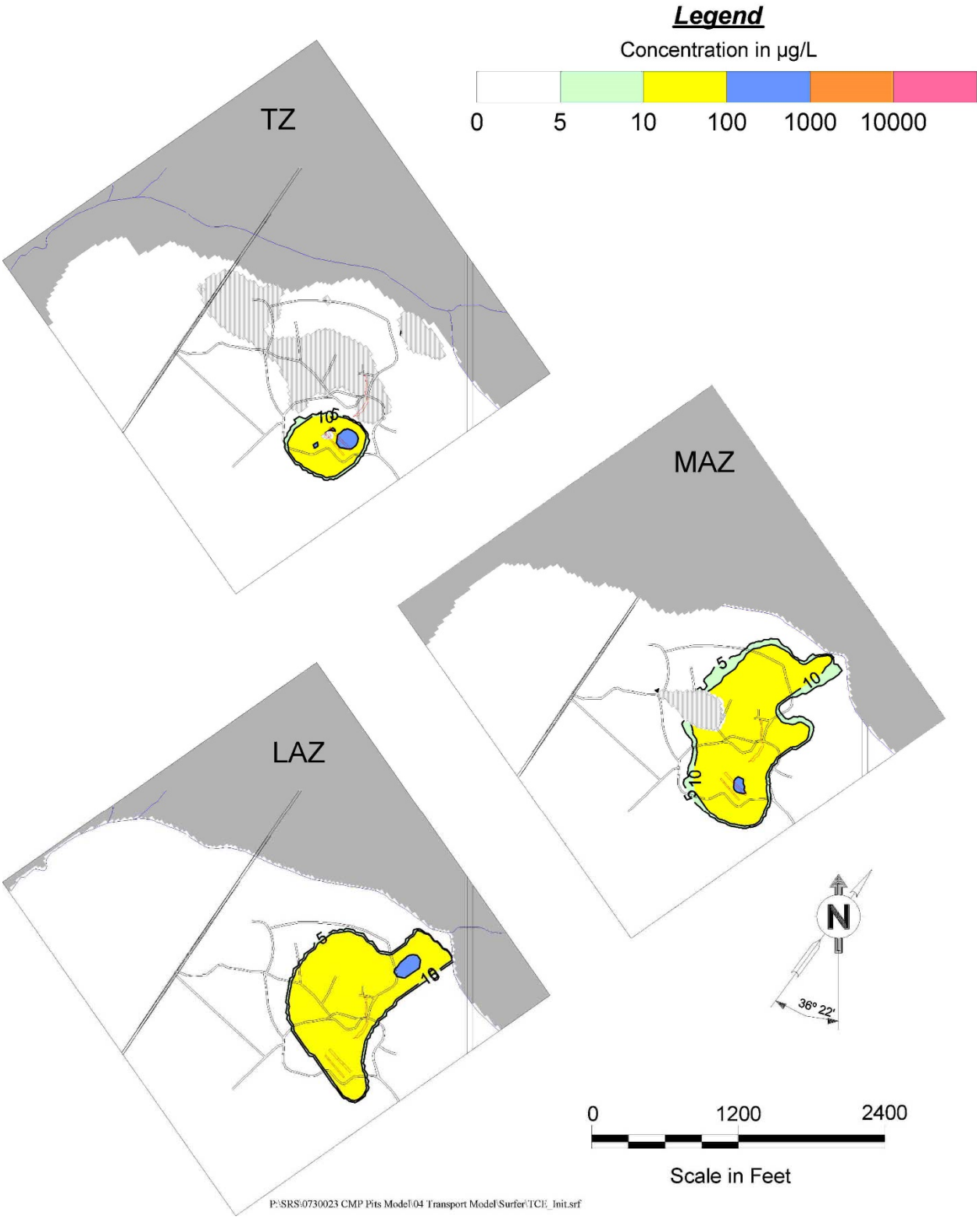

Figure 5.11 Initial 2017 TCE Plume for All Aquifers

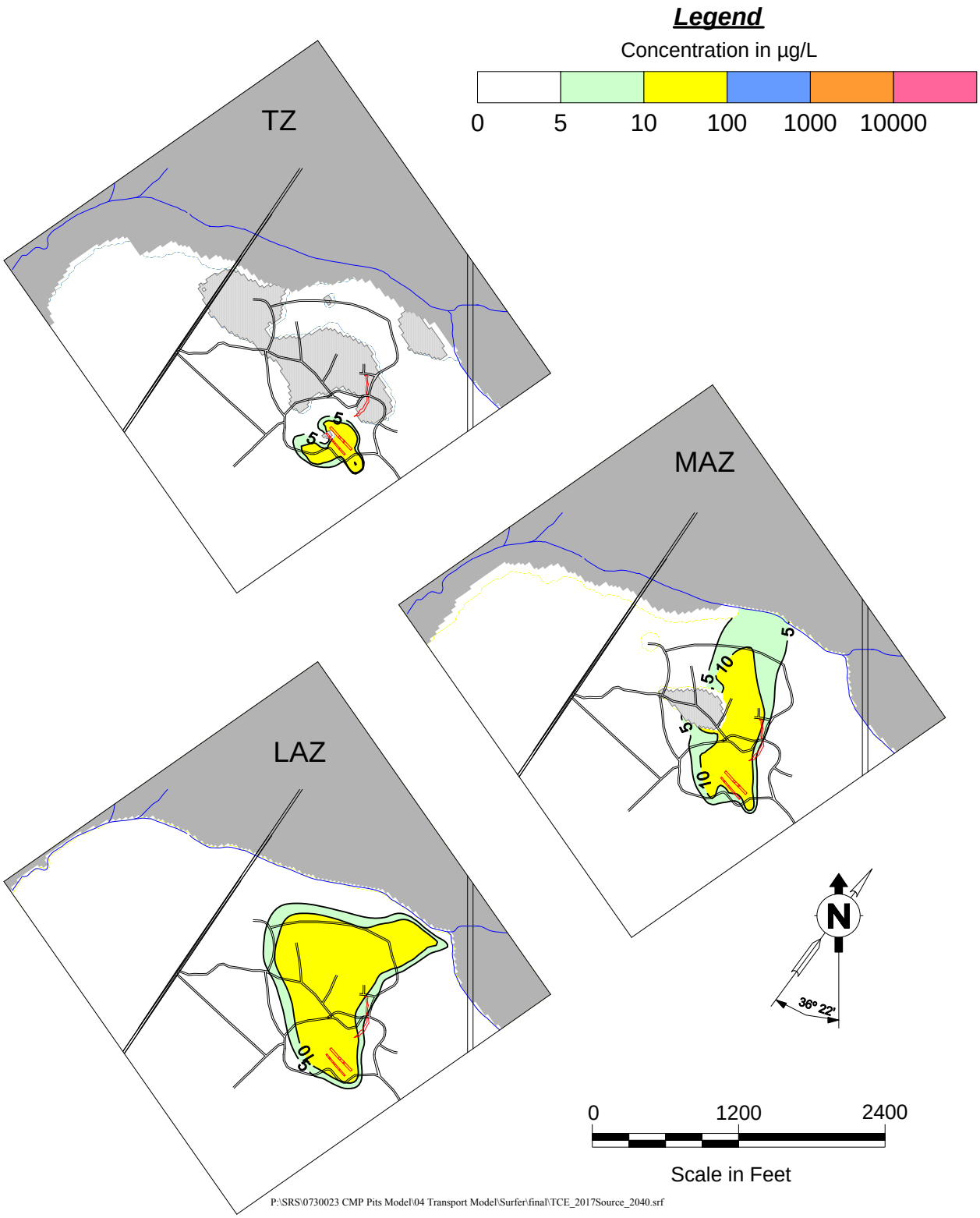

Figure 5.12 Modeled TCE Plume Configuration in 2040 with the Continuing 2016 Source

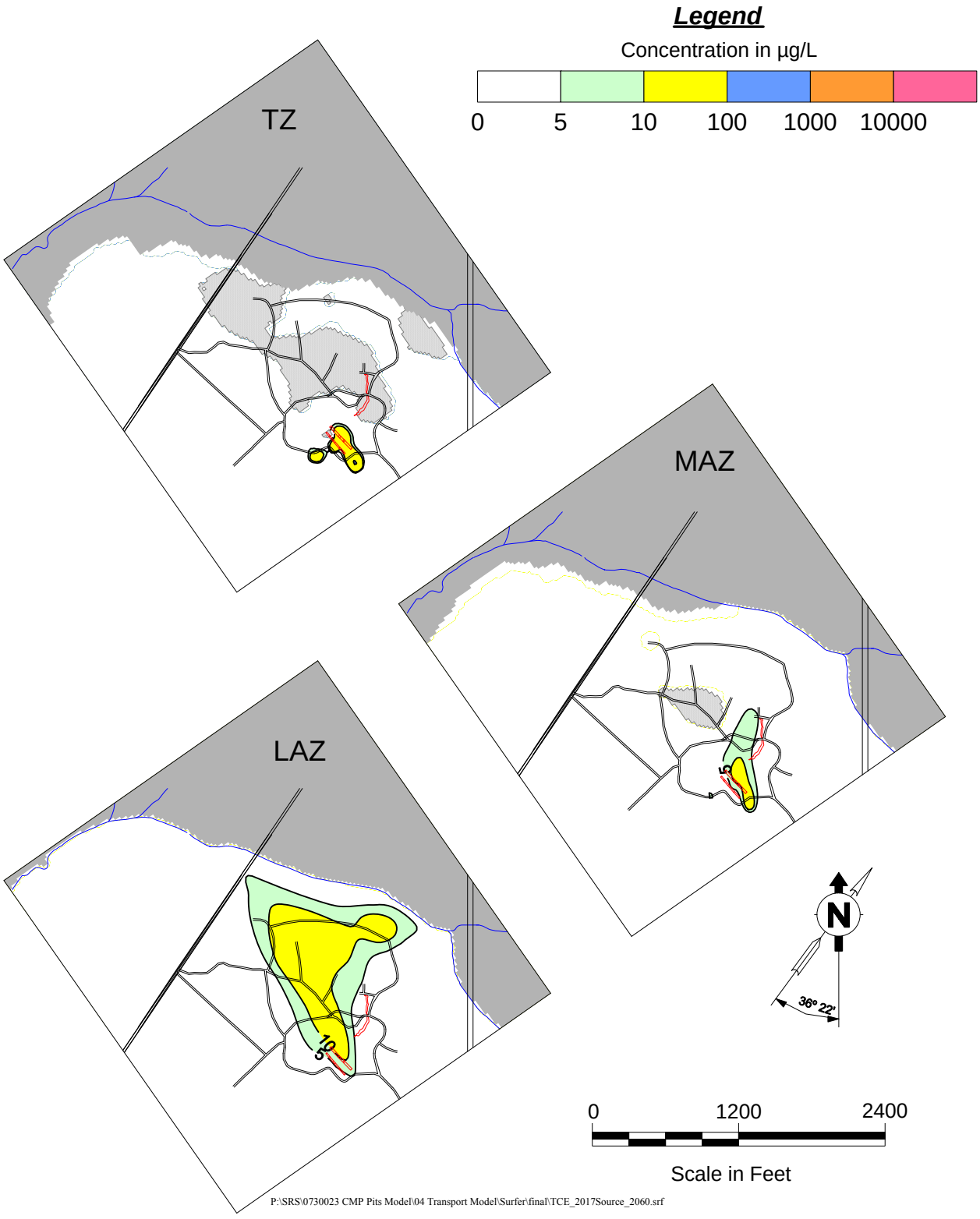

Figure 5.13 Modeled TCE Plume Configuration in 2060 with the Continuing 2016 Source

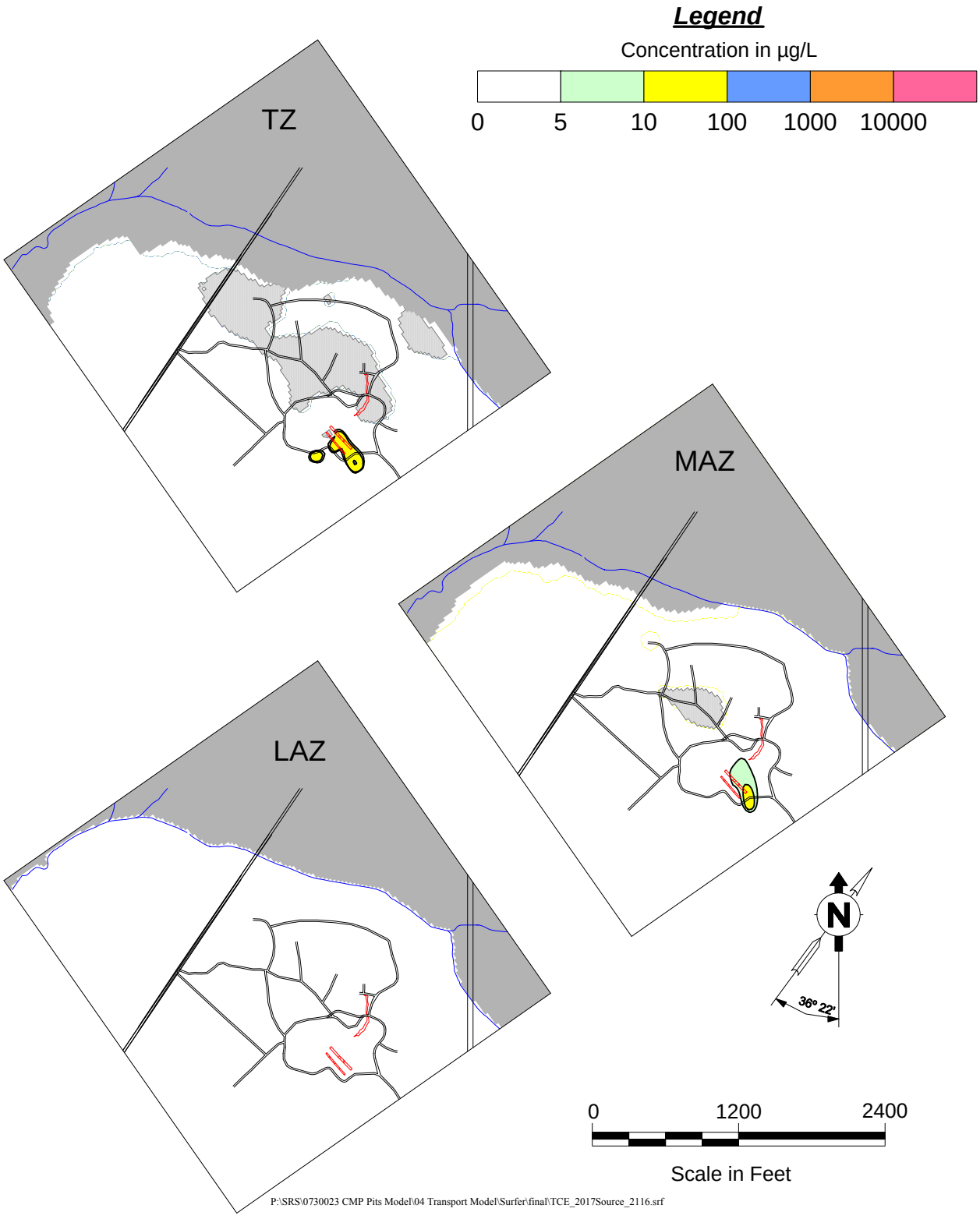

Figure 5.14 Modeled TCE Plume Configuration in 2116 with the Continuing 2016 Source

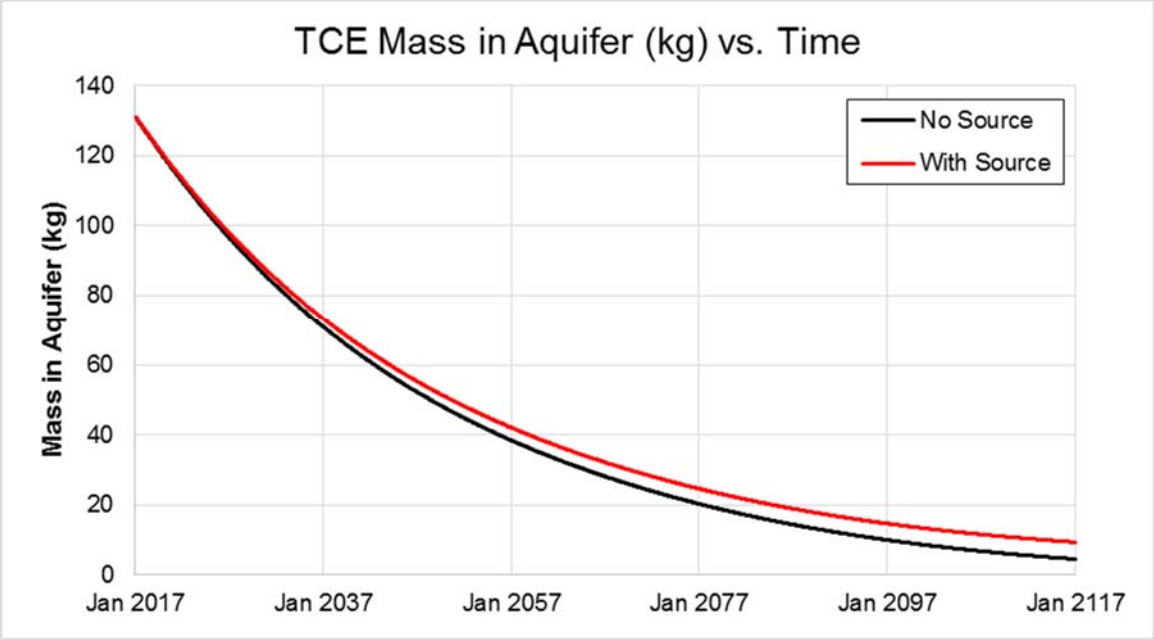

Figure 5.15 Modeled TCE Mass in System vs Time for the Two Scenarios

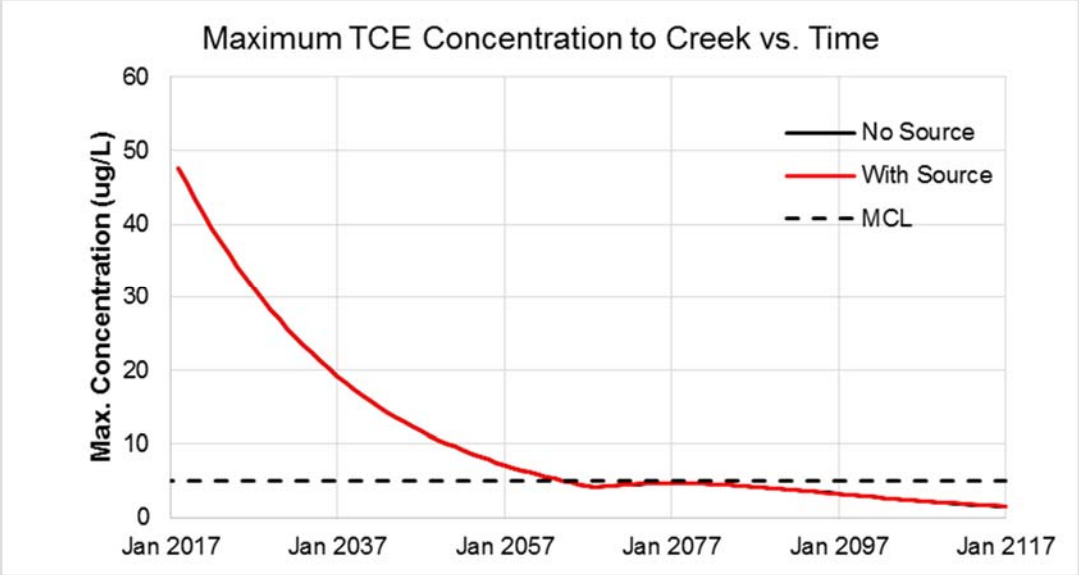

Figure 5.16 Modeled TCE Maximum Concentration vs Time to Pen Branch

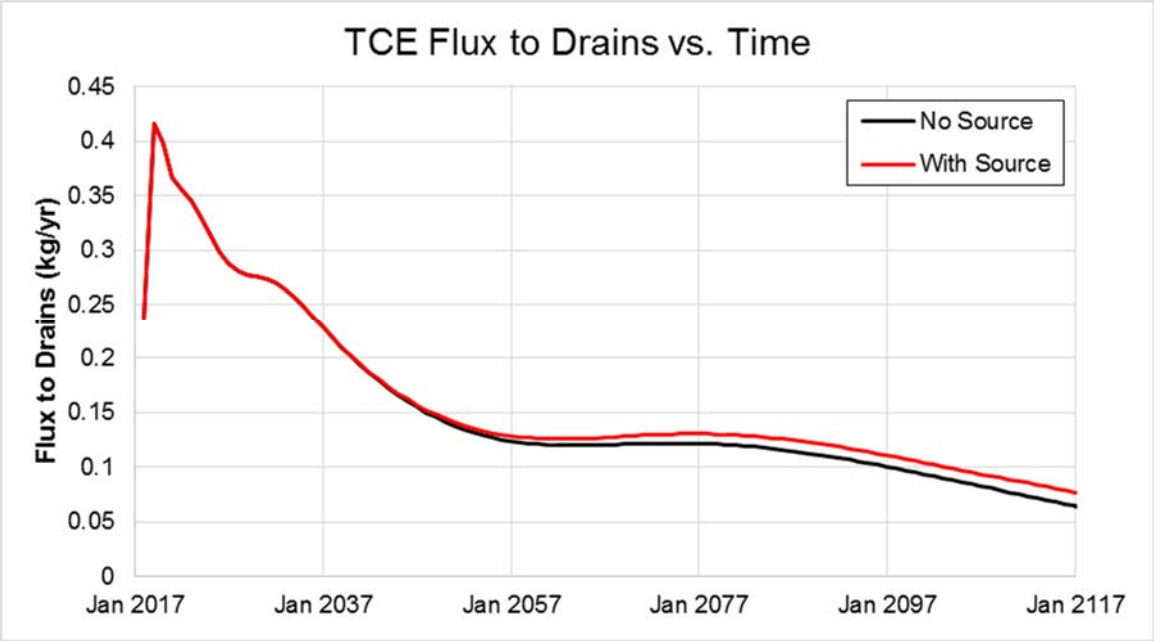

Figure 5.17 Modeled TCE Flux vs Time to Pen Branch

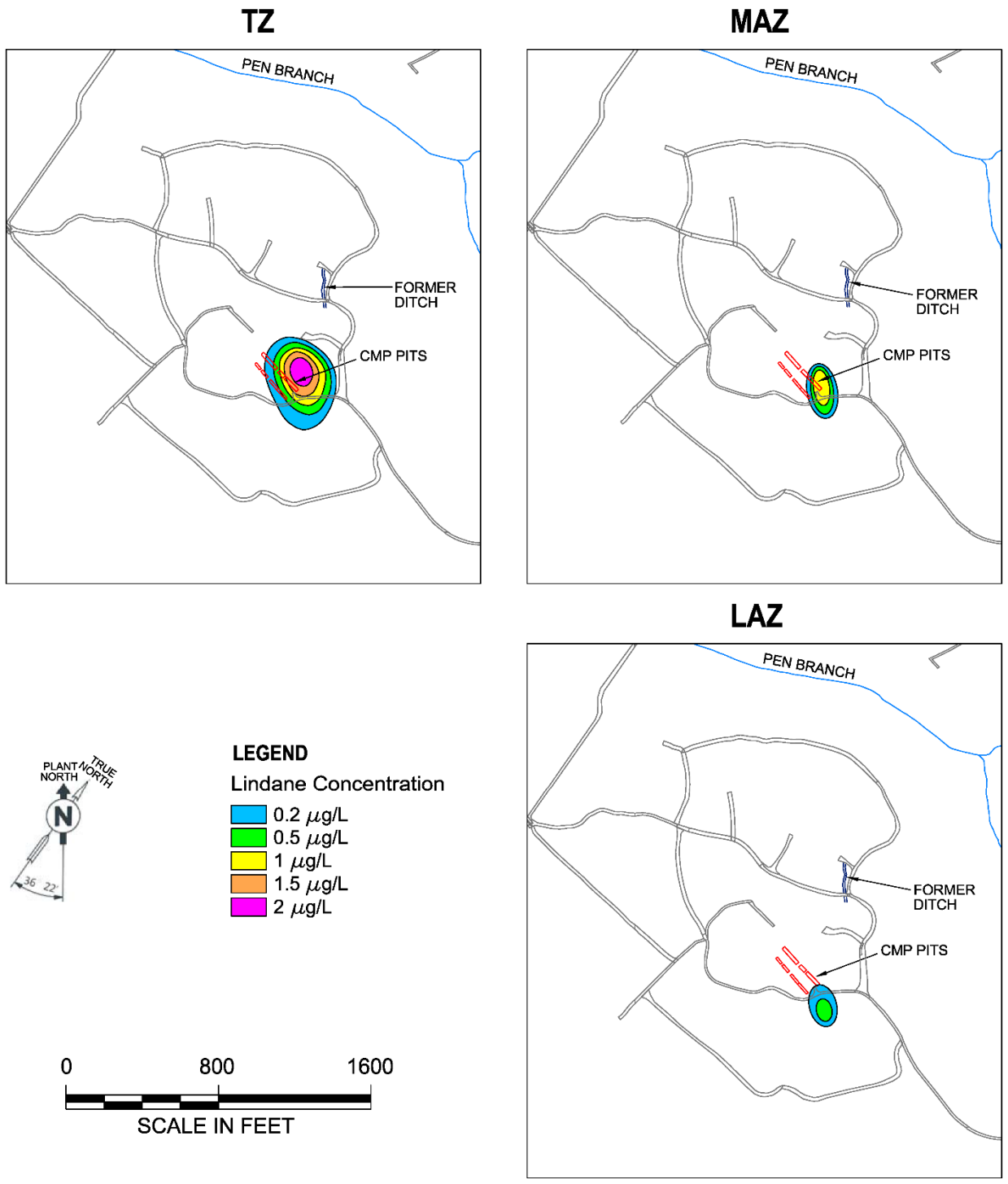

Figure 5.18 Initial 2017 Lindane Plume for All Aquifers

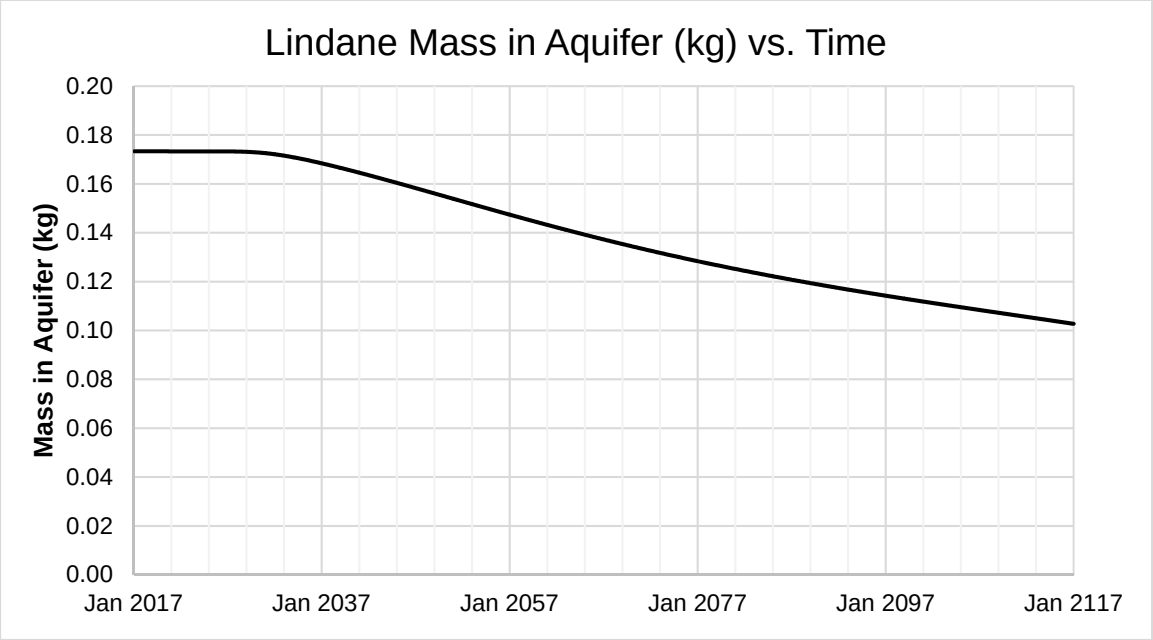

Figure 5.19 Modeled Lindane Mass in System vs Time

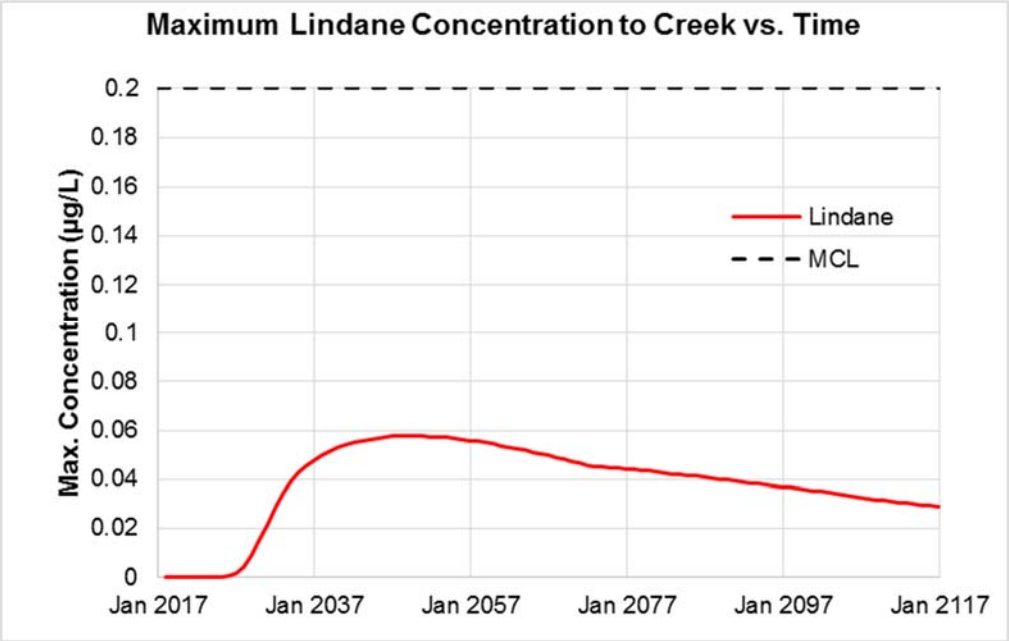

Figure 5.20 Modeled Lindane Maximum Concentration vs Time to Pen Branch

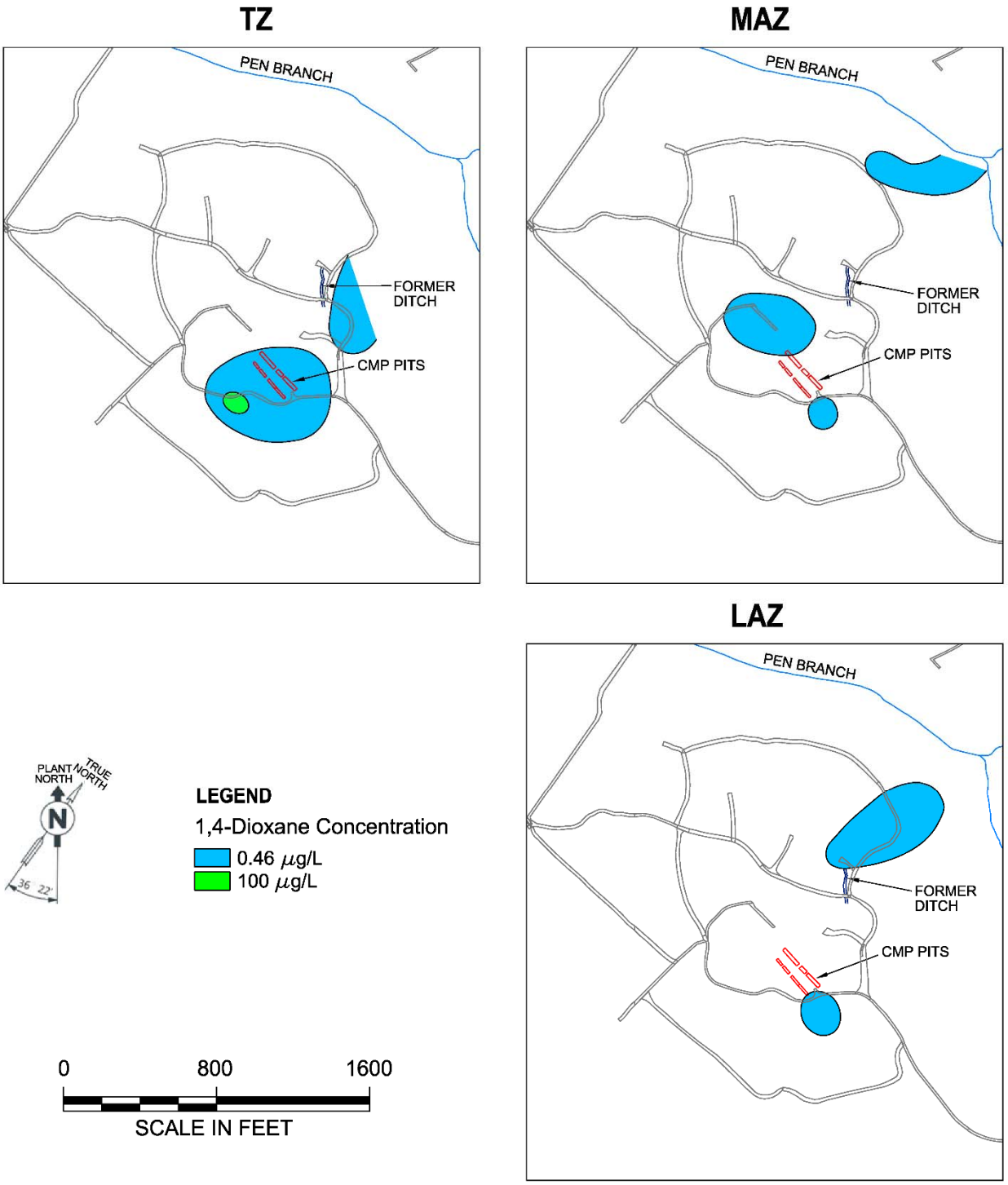

Figure 5.21 Initial 2017 1,4-Dioxane Plume for All Aquifers

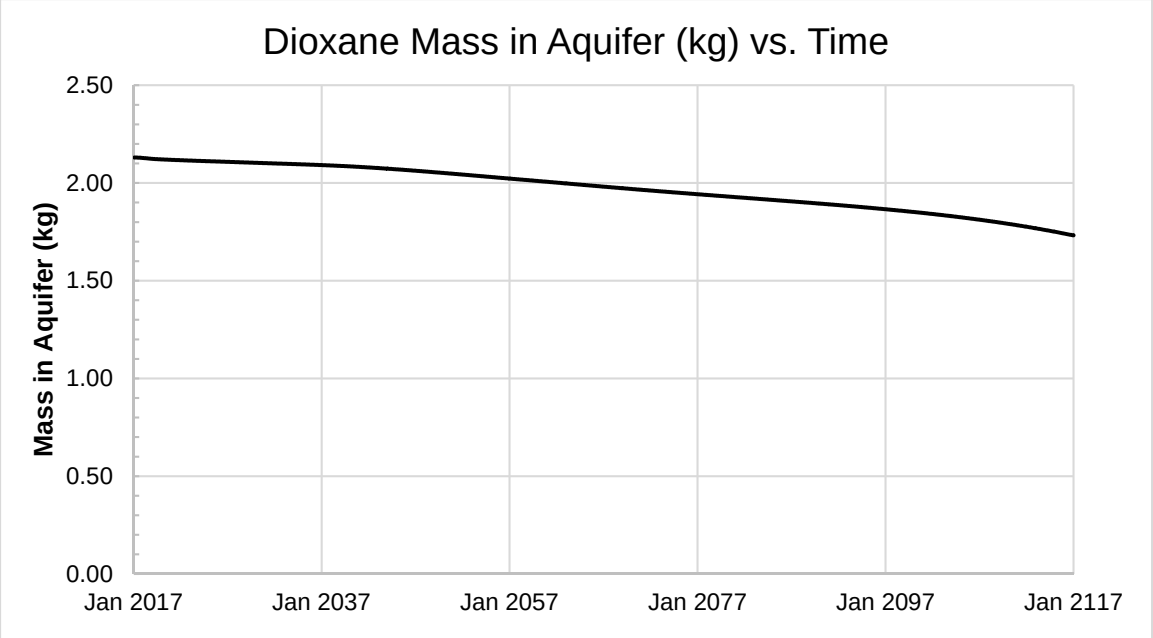

Figure 5.22 Modeled 1,4-Dioxane Mass in System vs Time

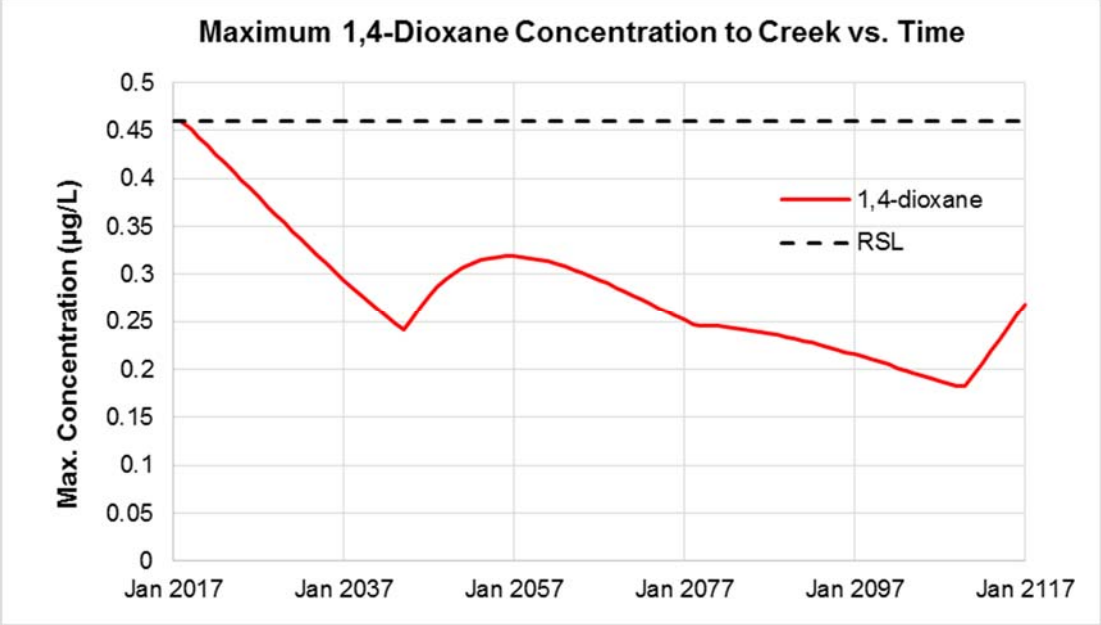

Figure 5.23 Modeled 1,4-Dioxane Maximum Concentration vs Time to Pen Branch

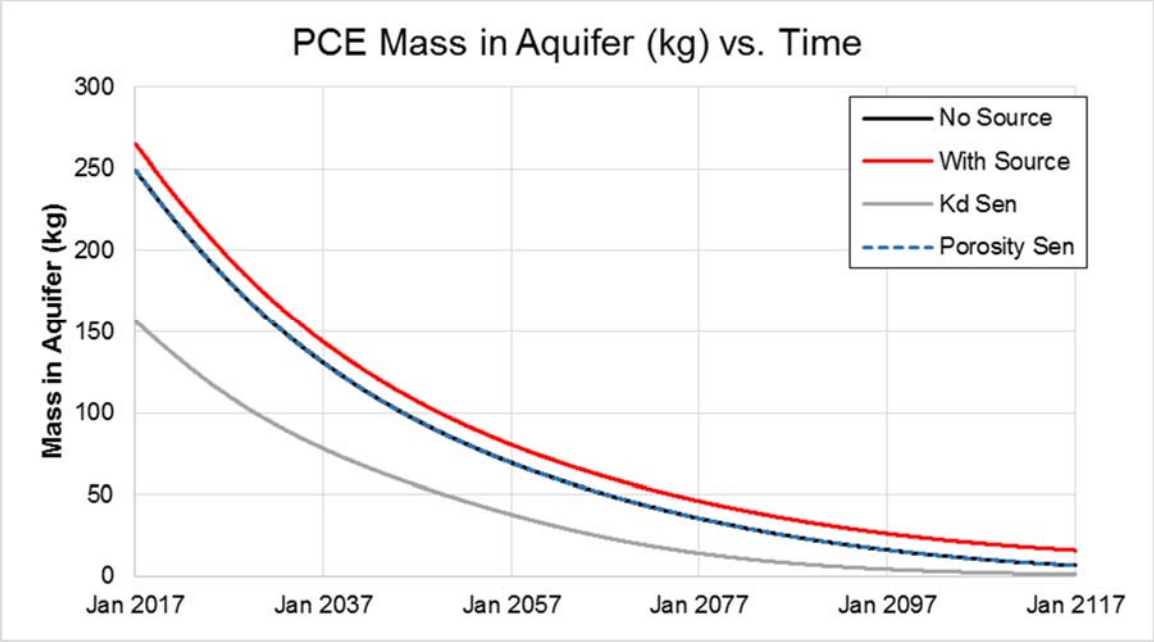

Figure 5.24 Modeled PCE Mass in System vs Time with Sensitivity to Kd and Porosity

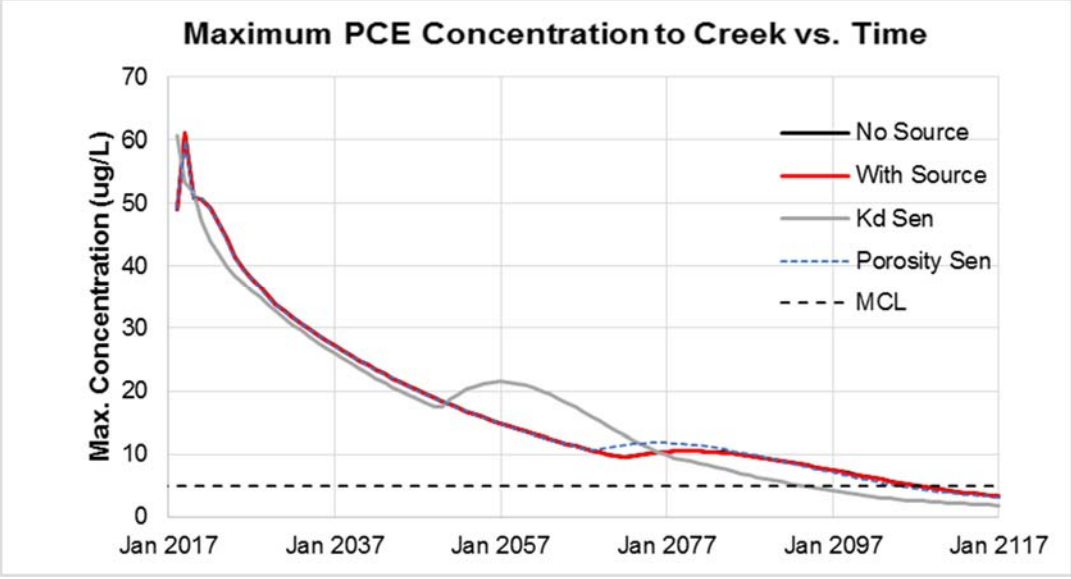

Figure 5.25 Modeled PCE Maximum Concentration vs Time to Pen Branch with Sensitivity to Kd and Porosity

6.0 SUMMARY AND CONCLUSIONS

The prior numerical model of groundwater flow and transport at the CMP Pits was updated to include new hydrologic, chemical, and stratigraphic data. An improved understanding of the effect of remedial activities, based on observed concentration responses over a multiple year period following remediation, reduces the uncertainty of this important process. The updated flow model uses reasonable assumptions and is calibrated to head measurements at monitoring wells. The transport model uses the current understanding of source behavior and current plume maps as targets. It is calibrated to plume behavior over the 2002-2016 period.

The largest degree of uncertainty in the prior model was the vadose source term behavior. The effect of the source in the current model was evaluated by comparing the future plume behavior with a continuous source based on current conditions to behavior with no source. The difference was found to be minor for both the 14 year calibration period and the 100 year predictive period. This observation suggests that accurate quantification of the source for the purpose of predicting future plume behavior is not necessary.

For PCE and TCE, predictive simulations indicate that discharge concentrations will exceed MCLs for 40 and 30 years, respectively. However, it should be noted that the wetlands adjoining the groundwater discharge locations along Pen Branch appear to provide significant degradation of PCE and TCE. Application to this site of a wetlands-specific degradation factor derived from observations of TCE degradation at an instrumented site within the C-area of SRS, suggest that the modeled PCE and TCE discharge concentrations may be reduced by two orders of magnitude, resulting in TCE discharge concentrations currently being below MCLs and PCE discharge concentrations exceeding MCLs for approximately five years. 1,4-dioxane and lindane are unlikely to discharge to surface water at concentrations in excess of MCLs or RSLs and therefore appear to be much less important COIs than PCE and TCE at the site.

In addition to uncertainties in parameter value assignments, several simplifying assumptions in the model may limit its predictive accuracy. The model assumes fairly homogeneous properties, which is a simplified representation of heterogeneous field conditions. Also, quantification of the process of sorption is uncertain and affects the longevity of the plume. Degradation of PCE and TCE are

assumed to be relatively slow (25 years). No degradation was conservatively assumed for lindane and 1,4-dioxane.

Despite the uncertainties in the model, it may be used as a tool to establish a reasonable range of future conditions, and it can be used to support the MNA remedial alternative for the CMP Pits OU. At this site, dry areas within aquifers seems to influence and alter contaminant flow paths. A better understanding of future plume behavior might be attained after 1) a focused investigation of the source of the northeastern part of the plume, 2) investigation of the source of the concentrations in the monitoring wells south of the pits (CMP10 and CMP11), and 3) a reconstruction of historical water-level and plume maps. Reasonable hypotheses and conceptual models were proposed to explain the source of concentrations to the south and northeast of the pits. These conceptual models offer an explanation of the distribution of contamination and are used in the predictive model, but could be evaluated further. The historical (pre-2008) water-level and plume maps are inconsistent with one another: plumes trajectories are not perpendicular to potentiometric contour lines. However, additional data is not expected to greatly improve model calibration or affect estimates of contaminant mass and transport.

7.0 REFERENCES

Aadland, R.K. and H.W. Bledsoe 1990, ***Classification of Hydrostratigraphic Units at the Savannah River Site, South Carolina (U)***, WSRC-RP-90-987.

Brigham Young University (BYU) 2013, ***The Department of Defense, Groundwater Modeling System (GMS)*** Version 9.0.5, Brigham Young University Environmental Modeling Research Laboratory.

Doherty, J, 2016, ***PEST: Model-independent parameter estimation, User manual, Part 1***,6th Edition. Watermark Numerical Computing, 366 p.

Fogle, T.L. and K.E. Brewer 2001. ***Groundwater Transport Modeling for Southern TCE and Tritium Plumes in the C-Area Groundwater Operable Unit (U)***, WSRC-TR-2001-00206, Rev. 0.

GeoTrans, Inc. 2001. ***Groundwater Modeling for the C-Area Burning/Rubble Pit (U)***, WSRC-TR-2001-00298, Rev. 0.

GeoTrans Inc., 2002a. ***Groundwater Modeling for the Chemicals, Metals, and Pesticides Pits (U),*** WSRC-RP-2002-4195, Rev. 0, Westinghouse Savannah River Company, Savannah River Site, Aiken, SC

GeoTrans, Inc, 2002b. ***Vadose Zone Analytical Modeling for the Chemicals, Metals, and Pesticides Pits Operable Unit (U)***. WSRC-RP-2002-4079, Revision 0.

Harbaugh, A., Banta, E., Hill, M., and M. McDonald, 2000, "MODFLOW-2000, The U.S. Geological Survey Modular Ground-Water Model – User Guide to Modularization Concepts and the Ground-Water Flow Processes", U.S. Geological Survey ***Open-File Report*** **00-92**.

Hiergesell, R. A. 1998. ***The Regional Water Table of the Savannah River Site and Related Coverages***, WSRC-TR-98-00045, Westinghouse Savannah River Company, (September 1998)

Lester, B.H. and G.W. Council, 2008. ***R-Area Groundwater Plume Transport Analysis,*** ERD-EN-2008-0061, Washington Savannah River Company, Savannah River Site, Aiken, SC

Ohio EPA (Ohio Environmental Protection Agency) 2003. ***Sampling and Analysis of Fraction of Organic Carbon (foc) in Soil***, VAP TDC Document VA30007.03.019, Division of Emergency and Remedial Response, Ohio Environmental Protection Agency

Riley, R.G., Szecsody, J.E., Mitroshkov, A.V., and C.F. Brown, 2006. ***Desorption Behavior of Trichloroethene and Tetrachloroethene in U.S. Department of Energy Savannah River Site Unconfined Aquifer Sediments***, PNNL-15884, Pacific Northwest National Laboratory, 2006.

Shukla, Sanjay, Saied Mostaghimi, Vernon O Shanholt, Michael C. Collins, and Burton B Ross, 2000. "A County-Level Assessment of Ground Water Contamination by Pesticides", ***GWMR***, Winter 2000.

SRNS 2009. ***Effectiveness Monitoring Report for the Electrical Resistance Heating (ERH)/Soil Vapor Extraction (SVE) and Monitored Natural Attenuation (MNA) at Chemicals, Metals, and Pesticides (CMP) Pits Operable Unit (OU), March 2008 through-March 2009***, SRNS-RP-2009-00573, Revision 0, June 2009. CERCLIS Number 24.

SRNS 2010. ***Effectiveness Monitoring Report for the Electrical Resistance Heating (ERH)/Soil Vapor Extraction (SVE) and Monitored Natural Attenuation (MNA) at Chemicals, Metals, and Pesticides (CMP) Pits Operable Unit (OU), March 2009 through-March 2010***, SRNS-RP-2010-00896, Revision 0, June 2010. CERCLIS Number 24.

SRNS 2015. **Baseline Groundwater Model Update for P-Area Groundwater Operable Unit, NBN, P-Area Reactor Groundwater Operable Unit**, SRNS RP-2015-00768, Revision 0, September 2015.SRNS 2017. ***Effectiveness Monitoring Report for the MNA at CMP Pits OU, March 2016-March 2017***, SRNS-RP-2017-00163, Revision 0, June 2017. CERCLIS Number 24.

U.S. Environmental Protection Agency 2014. ***Technical Fact Sheet – 1,4-Dioxane***. EPA 505-F-14-011, January 2014.

WSRC 1996. ***RCRA Facility Investigation/Remedial Investigation/Baseline Risk Asessment for the CBRP OU***. WSRC-96-170, Rev. 1.2.

WSRC 2001. ***Meteorological Monthly Monitoring for the Savannah River Site***, WSRC-TR-2001-00009-012, Westinghouse Savannah River Company, Savannah River Site, Aiken, South Carolina.

WSRC 2003. ***RCRA Facility Investigation/Remedial Investigation Addendum with Baseline Risk Assessment for the CMP Pits (U),*** WSRC-RP-2002-4049, Rev. 1.1, August, Westinghouse Savannah River Company, Savannah River Site, Aiken, SC

Zheng, C. and P.P. Wang 1998. ***MT3DMS: A Modular Three-Dimensional Multispecies Transport Model.*** User's Manual